

# AGC24



## International Campaign of Airborne Emergency Radiation Monitoring Teams

Přerov, 3-7 June 2024

[DOI:10.20348/STOREDB/1233](https://doi.org/10.20348/STOREDB/1233)

This work is distributed under the Creative Commons Attribution-NoDerivatives 4.0 International License



SÚRO, v.v.i.  
Report No. 19/2025  
October 2025  
ISBN 978-80-11-07424-1



Státní ústav  
radiační ochrany, v. v. i.



## Authors:

**Ohera Marcel<sup>1)</sup>, Gryc Lubomír<sup>1)</sup>, Helebrant Jan<sup>1)</sup>, Češpírová Irena<sup>1)</sup>,  
Nováková Martina<sup>1)</sup>, Poretti Cristina<sup>2)</sup>, Hess Adrian<sup>2)</sup>, Scharding  
Gerald<sup>2)</sup>, Stabilini Alberto<sup>3)</sup>, Chevreuil Martial<sup>4)</sup>, Couvez Céline<sup>4)</sup>,  
Manach Erwan<sup>4)</sup>, Vidal Romain<sup>4)</sup>**

<sup>1)</sup> National Radiation Protection Institute (SÚRO), 140 00 Prague, Czech Republic

<sup>2)</sup> Swiss National Emergency Operations Center (NEOC), 3003 Bern, Switzerland

<sup>3)</sup> Paul Scherrer Institute (PSI), 5232 Villigen PSI, Switzerland

<sup>4)</sup> Institut de Radioprotection et de Sûreté Nucléaire (IRSN) (now Autorité de Sûreté  
Nucléaire et de Radioprotection (ASN) 31 rue de l'Ecluse, 78116 Le Vésinet, France



Státní ústav  
radiační ochrany, v. v. i.



## Table of Contents

1	Introduction .....	7
2	Airborne Gamma-spectrometry Campaign Preparation .....	9
2.1	General information.....	9
2.2	AGC24 Preparation.....	9
2.3	IT infrastructure and data sharing.....	10
2.4	Communication and location tracking .....	11
2.5	Media .....	12
3	Measuring systems of AGC24 participants .....	13
3.1	Czech team (CZ).....	13
3.1.1	IRIS airborne gamma-spectrometer .....	13
3.2	Swiss team (CH).....	16
3.2.1	Measuring system RLL .....	16
3.3	French team (FR) .....	19
3.3.1	Measuring systems.....	19
4	Data processing .....	23
4.1	ERS 2.0 format.....	23
4.2	Common colour scale for map display.....	26
4.3	Data post-processing.....	26
4.3.1	Czech team (CZ).....	26
4.3.2	Swiss team (CH) .....	28
4.3.3	French team (FR).....	28
5	AGC24 Timetable .....	29
6	AGC24 Tasks Overview .....	30
6.1	Introduction .....	30
6.2	Range distance from Přerov Airport by helicopters.....	30
6.3	TASK I - VYSKOV.....	32
6.3.1	Location.....	32
6.3.2	TASK I : VYSKOV - Reference area mapping .....	35

6.4	TASK II - VYSOCINA.....	36
6.4.1	Location.....	36
6.4.2	TASK II : VYSOCINA .....	38
6.5	TASK III - OPAVA.....	39
6.5.1	Location.....	39
6.5.2	TASK III : OPAVSKO .....	40
6.6	TASK - IV LIBAVA.....	41
6.6.1	Location.....	41
6.6.2	TASK IV : LIBAVA .....	42
7	PRESENTATION OF RESULTS.....	43
7.1	TASK I - A: Polygon (70 m and 140 m).....	44
7.1.1	Czech team – polygon (70 m and 140 m).....	44
7.1.2	Swiss team – polygon (70 m and 140 m).....	48
7.1.3	French team – polygon (70 m and 140 m).....	53
7.2	TASK I - B: HOVERING .....	57
7.3	TASK II - VYSOCINA.....	60
7.3.1	Czech team.....	60
7.3.2	Swiss team.....	64
7.3.3	French team.....	67
7.4	TASK III - OPAVA REGION .....	70
7.4.1	Composite maps .....	72
7.5	TASK IV - LIBAVA.....	78
7.5.1	Czech team.....	79
7.5.2	Swiss team.....	81
7.5.3	French team.....	83
7.5.4	Overview of activities of point sources .....	84
8	Conclusions from AGC24 international campaign.....	85
	References .....	88

## 1 Introduction

The International Campaign of Airborne Emergency Radiation Monitoring Teams was organized by the National Radiation Protection Institute in cooperation with the Czech Army and the Malešice Air Repair Works LOM Praha, s.p. The campaign follows similar exercises from previous years, the last three exercises were in Germany in 2015, Switzerland in 2017 [1], and France in 2019. The Czech airborne radiation monitoring team participated in all three mentioned exercises.

The aim of these exercises is to continue the mutual cooperation between national airborne monitoring teams in the European Union. If an accident occurs at a nuclear power facility on EU territory, there is a high possibility that mutual assistance will be required in the territory of a neighbouring state. The national airborne monitoring teams use different monitoring systems, different evaluation programmes and different equipment calibration procedures. For this reason, it is necessary to ensure the interoperability of the airborne teams, the validation of the monitoring methodologies and the reproducibility of the results. Among other things, the exercise aims at mutual data transfer. For this purpose an ERS 2.0 data set was created to be verified in practice during the exercises. Such an activity requires regular training and comparative measurements under normal radiation situation. It is also necessary to practice the logistics in the cooperation of several teams and helicopter pilots. In the case of participation of foreign airborne monitoring teams, it is necessary to train common logistics for the radiation situation monitoring while ensuring perfect flight safety of all participants.

The next exercise had been planned to take place in the Czech Republic in 2021, but this was disrupted by the Covid19 pandemic. Preparation for this exercise started in 2022 and took almost 2 years. Finally, the airport in Přerov was chosen for the airborne campaign, due to its accessibility to interesting sites in terms of airborne radiation monitoring (reference area, area with uranium mining remains, area with  $^{137}\text{Cs}$  contamination), as well as the area sufficient for such a large number of participants and the provision of airborne equipment and, above all, in terms of air traffic control. The exercise which was called the Airborne Gammaspectrometry Campaign 2024 (abbreviated to AGC24) was scheduled from 3<sup>rd</sup> to 7<sup>th</sup> June 2024 at Přerov Airport. Originally, the exercise was to be attended by two aviation teams from Germany, one team from Switzerland, one team from France and one team from the Czech Republic represented by the specialists from the National Radiation Protection Institute (SÚRO) and the specialists from the 314<sup>th</sup> CBRN Monitoring Centre of the Czech Army. In the end, three teams took part in the exercise - a team from France, Switzerland and the Czech Republic.

The International Airborne Monitoring Campaign was scheduled for a total of 6 days including the arrivals of the teams. On Monday, 3<sup>rd</sup> June 2024 in the morning a meeting with the mayors of the surrounding towns and villages took place, also the representatives of the press and media were invited to this meeting. After this meeting, the airborne radiation monitoring exercise started. In total, each team had to complete four tasks over the four days according to the schedule, evaluate the data and present the preliminary data processing on the last day on Friday 7<sup>th</sup> June 2024. The exercise was completed at noon on Friday 7<sup>th</sup> June 2024. All teams were allowed to further evaluate the data in detail and present the results by the deadline for processing in this report.

This report presents the individual tasks and the final results of each team.

## 2 Airborne Gamma-spectrometry Campaign Preparation

### 2.1 General information

The Airborne Gamma-spectrometry Campaign (hereinafter referred to as AGC24) is an international exercise in which helicopters provided by the foreign teams, are an indispensable tool in addition to measuring instruments. This, however, entails a great deal of preparation, especially timely preparation. A fundamental element is the definition of the objectives of the exercise. To successfully meet them, the following tasks are required:

- Ensure appropriate diplomatic clearance and cross-border permissions for individual helicopters and related logistics,
- Air space delimitation and its timely reservation,
- Provision of an airbase with logistical support
- Provision of helicopter hangars
- Providing access to restricted areas or territories
- Provision of facilities for individual teams during the exercise and their transport
- Providing support for individual teams
- IT infrastructure
- Providing an environment for domestic and foreign media and others.

### 2.2 AGC24 Preparation

Preparation for the exercise at the airport began a year in advance. The Přerov Airport was chosen for many reasons. The owner, LOM Praha, s.p. (retrieved from Letecké Opravny Malešice Praha), is a company providing maintenance services for Mi family helicopters in NATO and EU countries certified by Russian companies MVZ Mil and OAO Klimov, the Interstate Aviation Committee MAK and domestic aviation authorities. The Přerov Airport is a domestic public and international non-public airport, which was established on 1<sup>st</sup> October 2013 from the original military airport Přerov-Bochoř. After agreement with the owner of LOM Praha, we were given permission to take over the airbase for AGC24. A significant factor in the choice of the airport was the relative proximity of the sites where the measurements could take place.

Another important step was to secure permission for all helicopters to cross the borders of the country and operate for a week on the territory of the Czech Republic. Obtaining permission was complicated by the fact that each team uses a helicopter from a different "organization" - military, police and civilian helicopter - which affects where permission must

be sought (Ministry of Defence, Ministry of Interior and Ministry of Foreign Affairs). A hangar was also provided for the French and German helicopters. Their helicopters were small and could be all time in hangar. The Swiss helicopter Super Puma and the Czech helicopter Mi-17 had a secured area near the hangars. Fuel for the helicopters was prepared near the hangars.

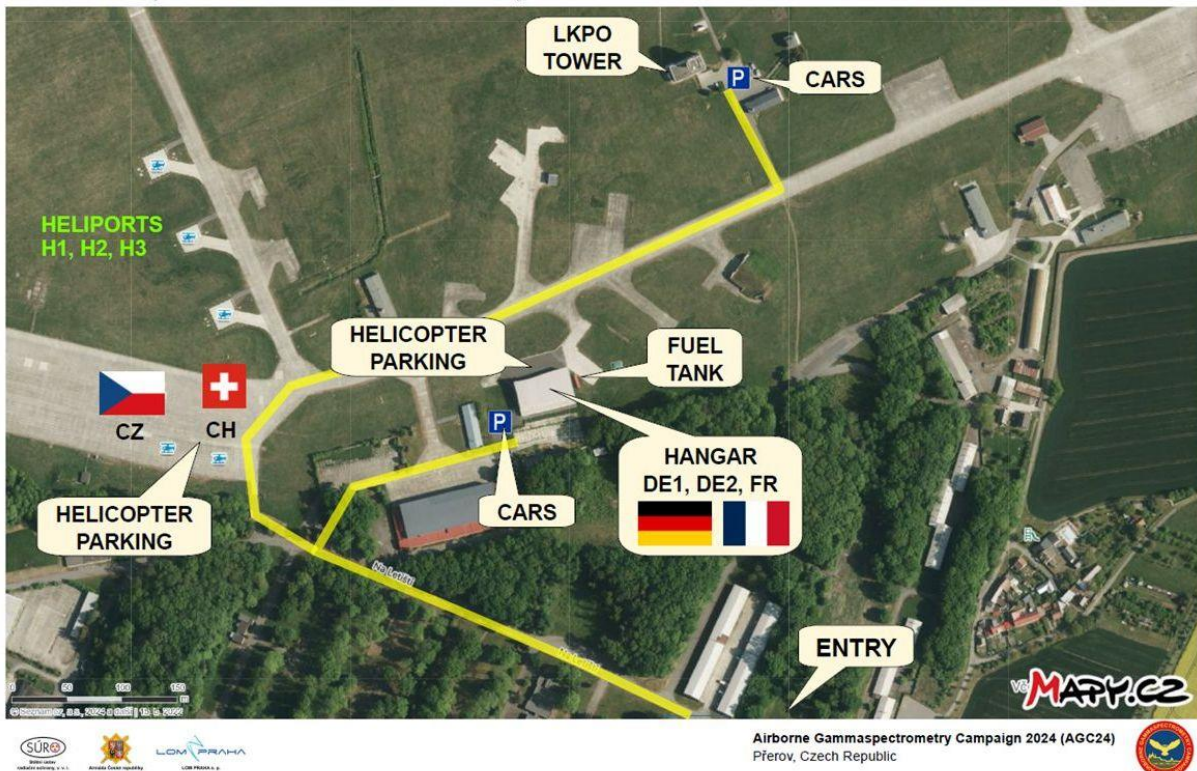


Fig. 1 Přerov Airport – orientation map

Accommodation for all participants was provided in nearby Přerov, with meals and transport from the hotel to the airport arranged by each team. A day room was provided for each team at the airport, and a hangar was prepared for joint meetings.

The representatives of the Czech Air Forces secured air space in the required locations for all AGC24 flight missions and the Czech Army secured the entry permissions into military areas.

### 2.3 IT infrastructure and data sharing

There was no internet connection available at Přerov Airport. As part of AGC24, it was therefore necessary to solve most of the data communication using locally running services. Synology NAS and WiFi routers were used, which provided password-protected shared folders

to individual teams. Synology offers a web interface, there is no need to install anything, and everything can be controlled from a standard internet browser using a web interface similar.

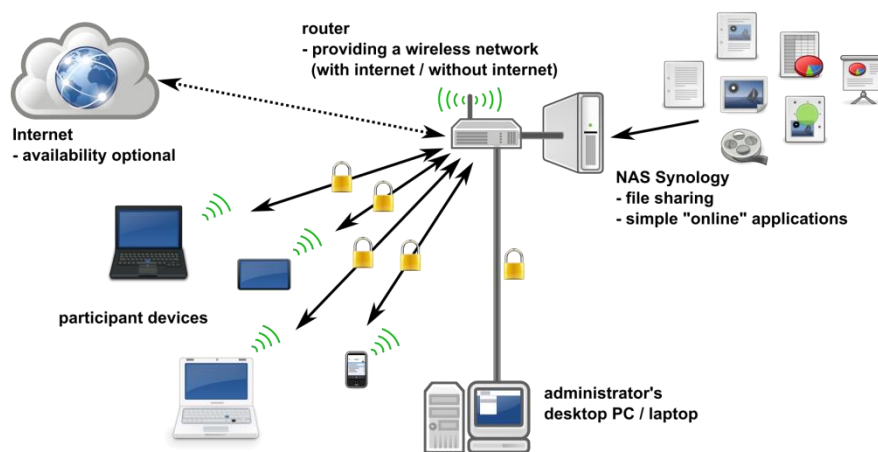


Fig. 2 IT infrastructure deployed within the AGC24 exercise

All participants had read-only access to a common shared folder where all the assignments for individual monitoring tasks, organizational information, GIS (Geographic Information System) files such as background maps, etc. were available.

Each team had its own "Home" folder with full permissions, where measured and evaluated data, maps, etc. were uploaded.

Synology also allows the NAS to be accessed via the Synology QuickConnect service after connecting to the internet. This allowed participants to access their folders in the same way again after the exercise - this time remotely, via the internet.

## 2.4 Communication and location tracking

License-free PMR446 (Private Mobile Radio, 446 MHz) handheld radios („walkie-talkies“) were used for organizational needs. This type of communication is not encrypted and can be received by anyone within range, so no potentially confidential or sensitive information was transmitted this way.

For sharing information and communication between participants the open-source, encrypted messaging service Signal (by Signal Technology Foundation) was used.

All participants were invited in advance to the AGC24 Signal group chat, within which communication took place, including information directly from individual helicopters, organizational information, etc.

Publicly available ADS-B Exchange map (<https://globe.adsbexchange.com>) was used both for live tracking of the participating aircrafts and for social media posts.



Fig. 3 Czech team performing measurements in Libava area (source: ADS-B Exchange map)

## 2.5 Media

As part of the exercise, the measured data is processed and then shared. For this purpose, a type of data file [2] called ERS - European Radiometric and Spectrometric format has been developed in the past. For a smooth data transfer, it is advisable to send a test file in advance to verify mutual compatibility. It is also advisable to define the so-called Map colour scale beforehand, for the sake of uniformity of the values displayed in the maps.

Different countries use different coordinate systems. This has to be taken into account before the exercise so that the coordinates given are understandable for all teams and refer to the same location in all coordinate systems. The most commonly used coordinate system was WGS84 (EPSG:4326), which is used for example in GPS navigation.

### 3 Measuring systems of AGC24 participants

Firstly, this chapter describes to which national institution each airborne monitoring team is assigned. Secondly, the chapter describes the measuring systems, their installation in helicopters including the short description of helicopters currently used during AGC24 campaign. The descriptions are listed in the following order of teams: 1) Czech team (CZ), 2) Swiss team (CH), 3) French team (FR).

#### 3.1 Czech team (CZ)

The Czech airborne team is classified under the National Radiation Protection Institute organization. The National Radiation Protection Institute (hereinafter referred to as SÚRO) is a public research institution engaged in professional activities in the field of population protection against ionizing radiation and it was established by the decision of the chairman of the State Office for Nuclear Safety (hereinafter referred to as SÚJB). For details see about the organization <https://www.suro.cz/cz>.

The activities of the Czech aerial team are carried out in the framework of the Czech radiation monitoring network in cooperation with the specialists of the Czech Armed Forces (hereinafter referred to as AČR) who operate their own Army Radiation Monitoring Network (ARMS). Both teams conduct joint exercises both within the Czech Republic and international exercises and use Mi-17 army transport helicopter.

The helicopter at the AGC24 was provided by the AČR on the basis of a long-term contract between SÚJB (the founder of the SÚRO) and the AČR.

##### 3.1.1 IRIS airborne gamma-spectrometer

The Czech team used so-called IRIS airborne gamma-ray spectrometric system during AGC24 which was developed by Pico Envirotec Inc. Company in Toronto, Canada. Two boxes (Master and Slave), each box with 2 NaI(Tl) crystals with dimensions 4" x 4" x 10" were used (Fig. 4). The gamma-ray spectrometer is provided with all electronics and additional accessories, i.e. GPS receiver, radar altimeter, newly developed pilot guidance unit (Fig. 5) and AGAMA software package for the project (survey) preparation, data browsing and the data post-processing and data presentation on the georeferenced maps. The spectrometer is fully independent on all on-board systems and it can be easily installed in all airplanes or helicopters

as cargo. The IRIS airborne gamma-ray spectrometric system and additional measuring instruments were installed during AGC24 on military Mi-17 helicopter (Figs. 6 and 7).

The energy range of the gamma-ray spectrometer is always set from approximately 35 keV to 3 MeV, usually in 512 channels. The last channel (channel 512, respectively) is used as a cosmic window and it collects all cosmic photons with energies higher than 3 MeV. After starting, the system is tuned to the photopeak of  $^{40}\text{K}$  and afterwards also to the photon emission of  $^{208}\text{TI}$  at 2614 keV. The gain of the individual photo-multipliers is adjusted automatically to maintain the peaks at pre-defined channels. The gain adjustment is performed in real time together with a procedure for linearization of the energy calibration. Thus, the system does not require any radioactive calibration sources before and during flight. Spectra, GPS positions, altitude and other parameters measured and important for data processing are saved in one-second intervals into a PEI binary file for later data browsing and post-processing, now in AGAMA software package developed by SÚRO and NUVIA, a.s. in the framework of the project [3]. The IRIS operator has available three different types of screens on the monitor during the flight: navigation, spectrum and data. All information about positions relative to the polygon and survey or tie lines including ground speed, altitude, survey lines, etc. are displayed on-line during flight independently on a board instrument (Pilot Guidance Unit) in the cockpit (Fig. 5).



Fig. 4 Airborne Gamma Spectrometer IRIS



Fig. 5 Newly developed Pilot Guidance Unit



Fig. 6 Mi-17 helicopter used during AGC24 by the Czech team

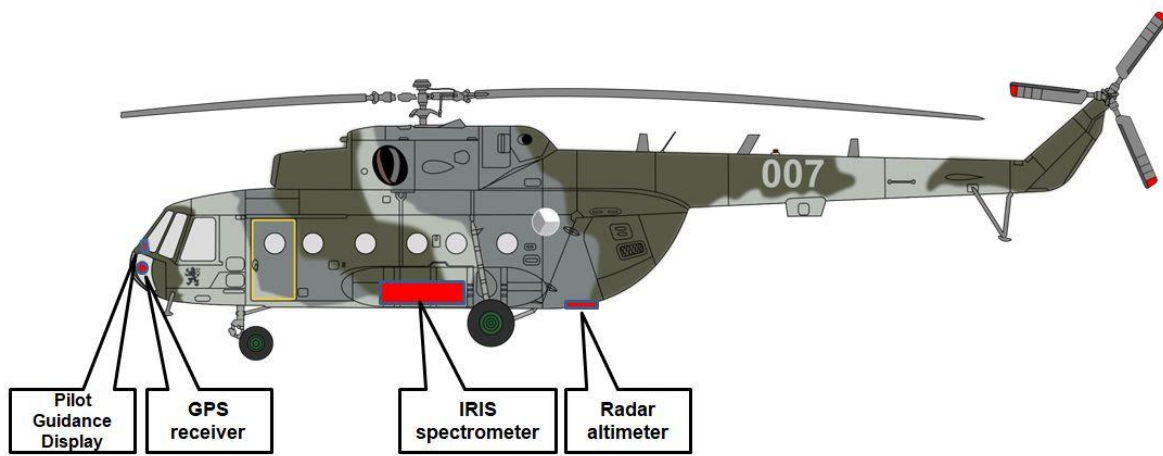


Fig. 7 Position of important instruments in Mi-17 helicopter

### 3.2 Swiss team (CH)

Information about the Swiss team is detailed in [1] and [4] and taken up throughout the whole chapter 3.2.

The deployment of the airborne gamma-spectrometric system is organized by the National Emergency Operations Centre (NEOC). NEOC is also responsible for the recruitment and instruction of the measurement team and the operational readiness of the system. Airborne operations are coordinated and performed by the Swiss Air Force. The gamma-spectrometric equipment is stationed at the military airfield of Dübendorf. Responsibility for scientific support, development and maintenance of the aeroradiometric measurement equipment passed from ETHZ to the Radiation Metrology Section of the Paul Scherrer Institute (PSI) in 2003 in cooperation with ENSI. General scientific coordination and planning of the annual measuring flights are provided by the Expert Team for Aeroradiometrics (FAR). FAR was a working group of the Swiss Federal Commission for NBC-protection (ComNBC) and consists of experts from all Swiss institutions concerned with aeroradiometry. FAR was reorganized as an expert group of the NEOC in 2008. For more information see <http://www.far.ensi.ch/>.

#### 3.2.1 Measuring system RLL

The measuring system RLL (Radiometrie Land-Luft) used both for civil and military measurements consists of a radiation detector featuring four NaI(Tl) scintillation crystals

having a total volume of 16.8 litres with their associated photo-multipliers and multichannel analysers (MCA) for low level measurements, and one Geiger-Müller tube and associated electronics for high dose-rate measurements. The spectroscopic measuring chain provides a linear energy calibration of the MCA up to 3 MeV divided into 1024 channels. NaI detectors, Geiger-Müller tube and associated electronics are installed in an aluminium case with thermal insulation foam. The detection container is mounted in the cargo bay below the centre of the helicopter. The RLL system uses position, air pressure, air temperature and radar altitude data provided by the helicopter via the internal ARINC bus. Fig. 8 shows the complete system packaged for storage. The equipment control, data acquisition and storage are performed with a rugged computer working as a data server. Two further rugged redundant client computers are used as operator interface for real-time evaluation, data mapping and communication. All computers are installed in an equipment rack, including an additional battery as power supply back-up. Both operators can operate the system with their associated client computer, display, keyboard and trackball. The additional third central display of the operator's console is mirrored on a screen in the cockpit located between both pilots and is used for information exchange with the pilots and general radiological situation awareness (Fig. 9). The measuring system RLL is mounted in an Aerospatiale AS 332 Super Puma helicopter (TH 06) of the Swiss Air Forces (Fig. 10). This helicopter has excellent navigation properties and allows emergency operations during bad weather conditions and night time.



Fig. 8 Components of the RLL system. 1. Lifting platform for the installation of the detection container. 2. Floor plates and accessories case. 3. Monitors and operator console. 4. Detection container. 5. Operator seats and equipment rack.

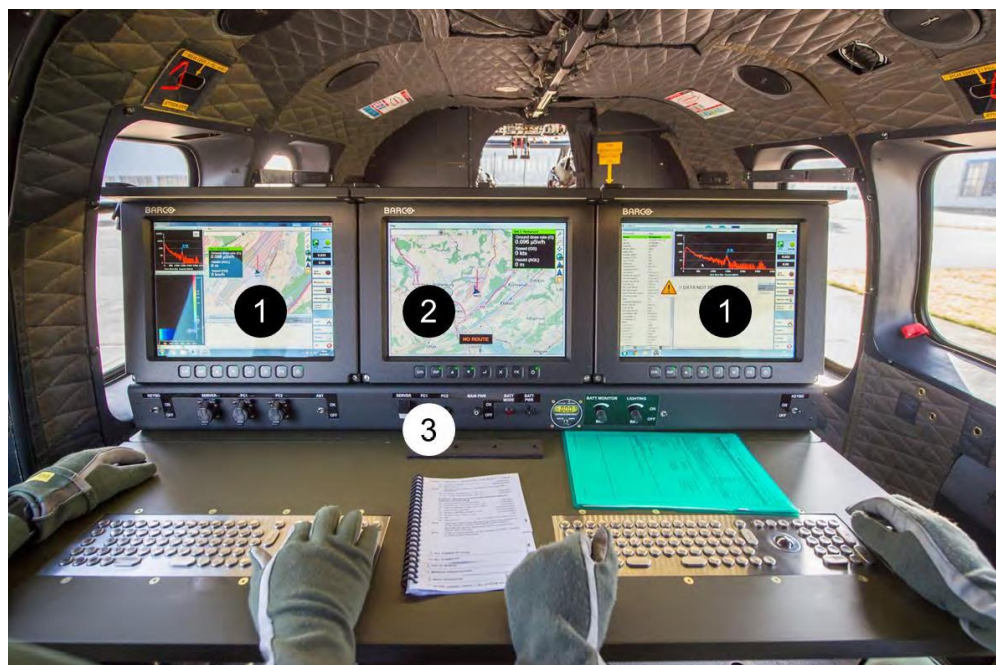


Fig. 9 Operator console of the RLL system. 1. Displays of the client computers. 2. Common display (mirrored in the cockpit). 3. Control panel with switches for power, lighting and communication and USB ports for file exchange.

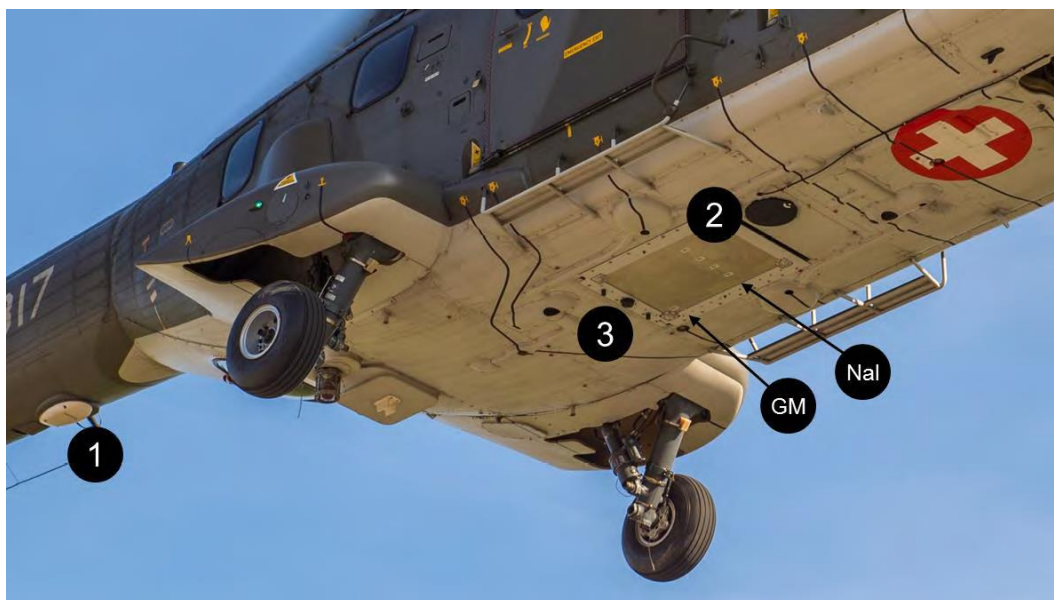


Fig. 10 RLL detector mounted in the cargo bay of a Super Puma helicopter. 1. Radar altimeter. 2. Detection container marked with detector reference points. 3. UMTS antenna for data upload.

### 3.3 French team (FR)

The Radioprotection and Nuclear Safety Institute (IRSN) is the French public expert on nuclear and radiological risks. Among IRSN's missions is the participation of the regular radiological monitoring of the territory's environment. As a technical expert on radiological and nuclear risks, IRSN also participates in the French emergency management system. In order to complete existing static monitoring capabilities, such as the Teleray remote sensing network, IRSN acquired mobile in-situ measurement systems, introduced in the global monitoring toolbox from 2010.

The IRSN mobile in situ measurements systems are based on gamma-rays detectors of various sizes and provide geolocated measurements every second. These systems can be deployed in backpacks, vehicles or aircrafts.

The mobile measurement systems are deployed for environmental surveys in peace time and are part of the IRSN's mobile unit dedicated to the characterization of the environmental contamination in the event of a nuclear accident. They are regularly deployed in the framework of national nuclear emergency exercises by trained people.

#### 3.3.1 Measuring systems

##### Measuring system ULYSSE

The IRSN aerial measuring system, known as "ULYSSE", is composed of different parts that can be easily set into various carriers, in a very modular way. It is based on devices and the SpirMobile suite, provided by Miron, a Franco-American company specialized in radiation detection, protection and measurement.

The elementary detection device is an individual hardened IP65 box containing a thallium doped sodium iodide NaI(Tl) crystal, a photomultiplier tube and multi-channel analyzer, and a Geiger-Müller tube. The dimensions of the crystal and the box are 4" × 4" × 16" (4 liters) and 24 cm × 24 cm × 84 cm, respectively. The standard configuration for AMS employed 4 detectors, for a total detection volume of 16 liters.

The detection units are connected to an acquisition laptop and powered through USB ruggedized cables. A fast digital analyzer is associated with each detector, 1024 channels elementary spectra are continuously acquired and processed by the acquisition server every second. The elementary spectrum is first stabilized by fitting the energy-channel dependence, operation realized by a dedicated algorithm looking for NORM peaks ( $^{40}\text{K}$ ,  $^{238}\text{U}$ ,  $^{232}\text{Th}$ ). The

spectrum is then scaled and linearized in order to provide spectrum with:  $E$  (keV) =  $3 \times$  channel. Various channels can be set, for instance, left, right or total channels.



Fig. 11 IRSN Nal 4 liters unit box.

Measurement positioning is performed using an external GPS device connected to the laptop's acquisition server, typically via Bluetooth, at a refresh rate of 10 Hz. Height above ground is calculated from the GPS altitude above sea level, from which the terrain elevation, provided by an embedded digital elevation model, is subtracted. The standard embedded DEM for AMS is the 90-meters resolution SRTM.

On-board real time mapping visualization and analysis are realized using the dedicated Mirion software, installed on acquisition laptop. Two IRSN specialists aboard the aircraft share the tasks of monitoring, verifications, controls and communication with ground team. One laptop serves as the main acquisition server while another one serves as a client. The software panels of both operators can be configured in various ways. The flight plan is provided to the pilot in the form of gpx or kml files for integration into his own navigation device.

IRSN has developed specific scripts that transmit acquired measurement data to IRSN databases, in real time via a 4G connection. This allows back-office operators to monitor the mission and perform analysis during the flight or at the end of it, without delay.

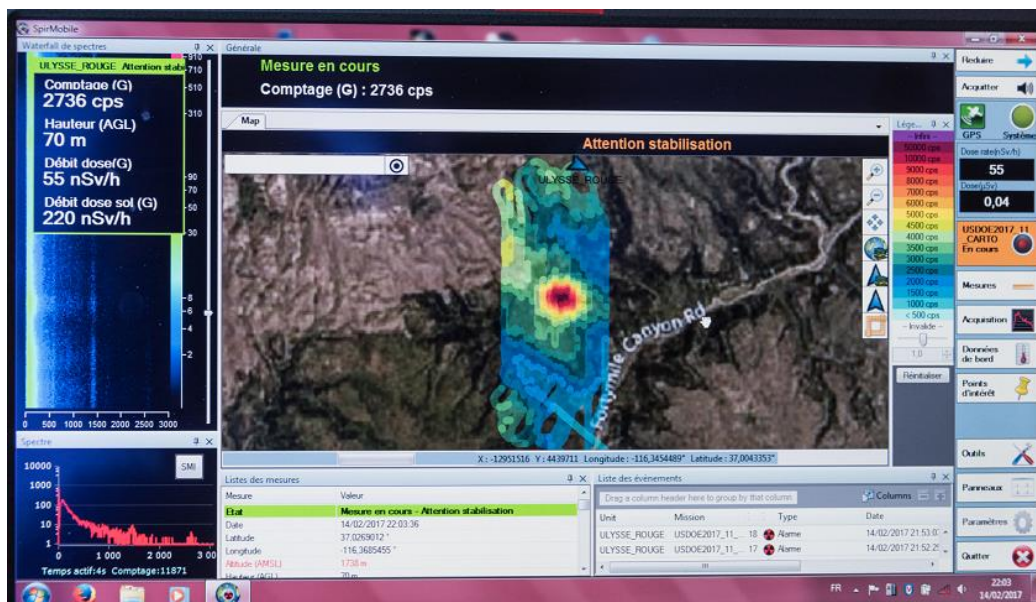


Fig. 12 IRSN Mirion IHM.

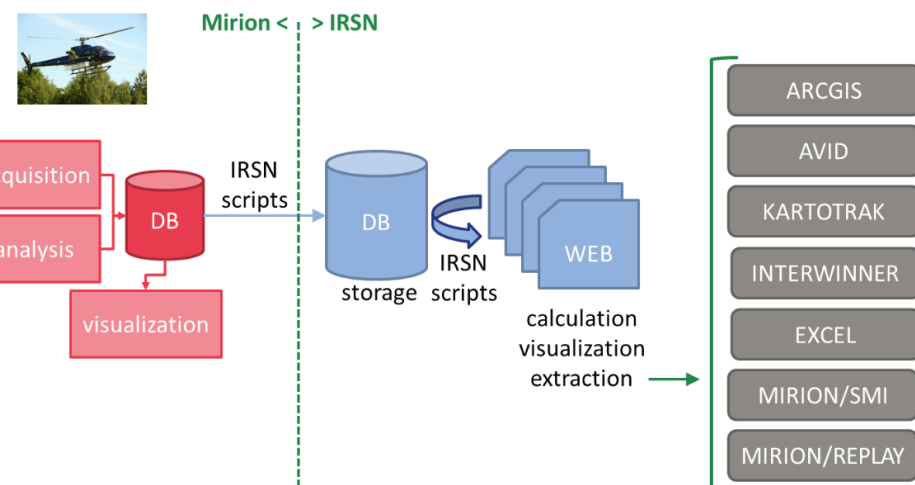


Fig. 13 IRSN processing suite

For the standard helicopter surveys, IRSN uses a chartered AS350 helicopter, equipped with 2 lateral externally mounted metallic gridded baskets, two individual units being arranged in each basket. A 4-years contract with a private helicopter company offers IRSN the possibility to get helicopter ready for surveys. The contracting company for the AGC2024, Hélicoptères de France, is a company whose activities cover a broad spectrum, including aerial work in the Alps and scientific flights such as LiDAR measurements campaigns.



Fig. 14 AS350 for the AGC24, equipped with lateral basket containing 2 x 4 liters Nal units

## 4 Data processing

Each of the participating teams evaluates the data using generally rather different methods. The objective of this exercise is to verify that the individual data evaluation approaches used provide similar estimates of nuclide activities and ambient dose equivalent rates within acceptable uncertainties. To this end, two specific tasks were used in the AGC24 exercises the monitoring over a reference area with well-known values of natural nuclide activities and ambient dose equivalent rates, and generating composite maps based on data provided by each teams from different interconnected areas that were designated for the survey of individual teams.

However, the data are stored in different data formats by the individual teams and a common platform for sharing and transferring data has been required to work together with the evaluated data. This platform, called ERS 2.0 - European Radiometric and Spectrometric format, has been developed over the last few years and the ERS 2.0 version was used in full for the first time in this exercise. In addition, for displaying the data on the maps, the same colour scale must be used for comparison.

Regarding the data processing procedures, this chapter should also be devoted to short descriptions of the data processing of each monitoring team.

### 4.1 ERS 2.0 format

The data exchange between the participants utilised the European Radiometric and Spectrometry (ERS) format described already in detail in [1] and [2].

The following table contains the selection of the most important variables, parameters and units used by the ERS 2.0 format during this campaign. For other abbreviations and description see [2].

Tab. 1 ERS 2.0 format

Identifier	Abbreviation	Description	Value format or unit
A	AP_	Activity of a point source Bq	Bq
A	AA_	Activity per unit area of a source distributed over an area	Bq m <sup>-2</sup>
A	AD_	Activity per unit dry weight of a source distributed in volume	Bq kg <sup>-1</sup>
A	AW_	Activity per unit wet weight of a source distributed in volume	Bq kg <sup>-1</sup>
D	DHS	Ambient dose equivalent H*(10)	µSv
D	DHSR	Ambient dose equivalent rate dH*(10)/dt	µSv h <sup>-1</sup>



Státní ústav  
radiační ochrany, v. v. i.



Armáda České republiky



LOM PRAHA s. p.

Identifier	Abbreviation	Description	Value format or unit
T	TL	Acquisition live time	ms
T	TR	Acquisition real time	ms

Identifier	Abbreviation	Description	Value format or unit
	CD	Date;YYYY-MM-DD; date_UTC	
	CT	Time;hh:mm:ss;time_UTC	
	CDT	Date and time;YYYY-MM- hh: DD mm:ss;datetime_UTC	
P	PN	Measurement or sample point coordinate N-S (latitude) Negative values are allowed, when appropriate	Numeric
P	PE	Measurement or sample point coordinate E-W (longitude) Negative values are allowed, when appropriate	Numeric
P	PZ	Altitude above sea level	m
P	PH	Ground clearance	m
P	PA	Name or code for the measurement or sample point	
P	PP	Position precision	
#	#C_winname	Counts in window or ROI winname	Numeric
#	#R_winname	Count rate in window or ROI name	s <sup>-1</sup>
#	#S	Full raw spectrum. The number of channels is given by ISC	Numeric
#	#SC	Checksum of the spectral data. Equals the total counts in spectrum	Numeric

Identifier tail	Abbreviation	Description	Value format or unit
Type_2	_ANT	Anthropogenic radionuclides can be used for activity, dose, dose rate, fluence, fluence rate, source descriptions and source coordinates	As identifier
Type_2	_GND	Contribution of ground (_ANT + _NAT) Can be used for activity, dose, dose rate, fluence, fluence rate, source descriptions and source coordinates	As identifier
Type_2	_COS	Cosmic contribution. Example: DHSR_COS includes contributions of photons, neutrons and charged particles produced by cosmic radiation	As identifier
Type 1	_LC	Decision limit. Example for activity per unit area AA_LC	As identifier
Type 1	_LD	Detection limit	As identifier
Type 1	_LQ	Determination limit	As identifier
Type 1	_UR	Random uncertainty	As identifier
Type 1	_US	Systematic uncertainty	As identifier
Type 1	_UT	Combined total uncertainty	As identifier
Type 1	_URP	Relative random uncertainty	%

Identifier tail	Abbreviation	Description	Value format or unit
Type 1	_USP	Relative systematic uncertainty	%
Type 1	_UTP	Relative combined total uncertainty	%

## 4.2 Common colour scale for map display

In order to achieve an optical comparison in the maps, it is necessary to keep the same colour scale for the measured values. The colour scale shown in the following table has already been used in previous exercises, for example [1]. The colour scales for each nuclide are based on realistic values that can be determined by airborne measurements during normal radiation situation in Europe.

Tab. 2 Map color codes

	Color code (RGB)	ambient dose rate (DHSR) ( $\mu\text{Sv h}^{-1}$ )	Cs-137 (AA_Cs-137) ( $\text{Bq m}^{-2}$ )	K-40 (AD_K-40) ( $\text{Bq kg}^{-1}$ )	U-238 (AD_U-238) ( $\text{Bq kg}^{-1}$ )	Th-232 (AD_Th-232) ( $\text{Bq kg}^{-1}$ )	Flight Height (PH) Altitude above ground (m)
	#3366B3	< 0.04	< 2500	< 50	< 12.5	< 12.5	< 70
	#4D94FF	0.04 - 0.06	2 500 - 5 000	50 - 100	12.5 - 25	12.5 - 25	70 - 80
	#66FFFF	0.06 - 0.08	5 000 - 7 500	100 - 150	25 - 50	25 - 50	80 - 90
	#66FFA3	0.08 - 0.10	7 500 - 10 000	150 - 200	50 - 100	50 - 75	90 - 110
	#ADFF99	0.10 - 0.15	10 000 - 12 500	200 - 300	100 - 200	75 - 100	110 - 120
	#E6FF80	0.15 - 0.20	12 500 - 15 000	300 - 400	200 - 300	100 - 150	120 - 130
	#FFEB33	0.20 - 0.30	15 000 - 20 000	400 - 500	300 - 400	150 - 200	130 - 140
	#FFB033	0.30 - 0.50	20 000 - 30 000	500 - 600	400 - 500	200 - 250	140 - 150
	#FF0000	> 0.50	> 30 000	> 600	> 500	> 250	> 150

## 4.3 Data post-processing

As the descriptions and methods of data post-processing of all three teams participating in AGC24 were detailed in the 2018 report [1], there will be mentioned only to the important information and the changes to the data post-processing procedures, which differ from the description given in [1].

### 4.3.1 Czech team (CZ)

Probably the most important change in the Czech team is the evaluation of the data of the airborne measurements. Between 2017 and 2020, a new evaluation program called AGAMA was developed in cooperation with NUVIA, a.s. Company. This program, in addition

to using a sophisticated environment, has a number of new features compared to the older PRAGA4 program used in past during the ARM17 and AGC19 campaigns. We list below the most important features of this software package:

- a) **Project preparation** - It allows the creation of any polygon, survey and tie lines and their continuous change on georeferenced on-line or off-line maps. AGAMA also allows creating a project of spiral shapes with different distances between spiral lines.
- b) **Helicopter background and cosmic spectra calculation** – AGAMA software package involves the calculation of helicopter background and gamma cosmic contribution based on experimental measurement at three altitudes from 1900 m to 2900 above sea level. The mathematical procedure is described in detail in [5].
- c) **Input/output data formats – PEI binary, ASCII, ERS 1.0, ERS 2.0, KML/KMZ**
- d) **LSQ – Least square method** based on response functions calculated by the Monte Carlo code (for K, U, Th homogeneously distributed,  $^{137}\text{Cs}$  and  $^{134}\text{Cs}$  (both exponential and surface distribution) and  $^{103}\text{Ru}$ ,  $^{131}\text{I}$  only surface distribution), see [6].
- e) **Non-negative least square method** based on response functions calculated by the Monte Carlo code – same as LSQ, but all negative values are mathematically corrected to zeros, see [6].
- f) **Extended window (ROI) method** based on IAEA recommendations – Standard window method was extended to four elements (K, U, Th, and  $^{137}\text{Cs}$ ) using a combination of Monte Carlo simulation and the experimental calibration. Other six stripping parameters and three sensitivities were defined and calculated for  $^{137}\text{Cs}$ , see [6].
- g) **Air dose rate in nGy h<sup>-1</sup>**
  - DHSR calculated from powerspectrum (full spectrum from 30 keV to 3 MeV) and recalculated to 1 m above the ground. The method for small symmetric detectors is described in [8], large-volume NaI(Tl) detectors used in airborne gamma-spectrometers are partly described in [6].
  - DHSR calculated from activities in extended window method [7].
- h) **Cosmic dose rate calculation** (depending on altitude above sea level)
- i) **MDA calculation – Currie and ISO IEC 11929-2010** - calculation based on [9], [10]
- j) **Data browsing and copying for other data processing** (other mapping software, e.g. MapInfo, free available QGIS, etc. )
- k) **Heat maps in AGAMA software for quick overview**, see [6]

The basic principles used in the calculations in the AGAMA software package are presented in the internal report of SÚRO [6].

#### 4.3.2 Swiss team (CH)

The method of data processing and evaluation of activities and ambient dose equivalent rates has not changed in principle since the procedures described in the report [1]. A very detailed description of the procedures is given in report [1], to which reference is hereby made.

#### 4.3.3 French team (FR)

Different French AMS data processing can be highlighted hereby, following the status described in [1].

An algorithm has been developed to better determine the location and activity of lost radioactive sources. Using 3D Monte-Carlo simulation of the full-absorption peak of individual detecting unit, the algorithm tries to optimize the source location that reproduces the observed measured signals.

IAEA windows method, already available for K-U-Th, has been extended to  $^{137}\text{Cs}$ , based on experimental measurements done in Sweden with SSM on Borlange pads (2018). Used for the AGC24 intercomparison, the method still needs to be validated.

A new method for the calculation of the gamma dose rate at 1m above ground, initially using manufacturer coefficients, has been determined. It is simply based on the total counts and uses experimental results obtained during the DOE-IRSN joint survey (2017). This alternative method provides similar results but with better statistical variability, in particular for environmental surveys.

Studies have been done for the determination of background counts for the calculation of the dose rate and the K, U, Th concentrations. A relationship table is now available that provides sets of counts for various background (radon) conditions. Associated with the table, a new calibration strategy has been set, based on measurements at different heights above a reference area and, if possible, on ground measurements.

## 5 AGC24 Timetable

Although the absence of the German teams gave the possibility of greater time flexibility, the exercise lost very experienced teams that had the opportunity to make airborne measurements of the entire Chernobyl exclusion zone. Their participation in the exercise was sorely missed, but at least the German representatives participated in the campaign as observers.

Tab. 3 AGC24 schedule

AGC24 timetable							
2.6. - 7.6. 2024		Přerov	Libavá	Vyškov	Opavsko	Vysocina	
SUN, 2nd	- 17:00	Arrival					
	17:00 - 18:00	Welcome, Preparatory Meeting					
MON, 3rd	08:00 - 12:00	Public and Sponsor Presentation					
	12:00 - 12:30	Briefing					
	12:30 - 14:30	Data Evaluation		CH			
	14:30 - 16:30			FR			
	16:30 - 18:30			CZ			
TUE, 4th	08:30 - 09:00	Briefing					
	09:00 - 11:00	Data Evaluation			CZ		
	11:00 - 13:00				CH		
	13:00 - 15:00				FR		
	15:00 - 16:00						
WED, 5th	08:30 - 09:00	Briefing					
	09:00 - 11:00	Data Evaluation		FR			
	11:00 - 13:00			CH			
	13:00 - 15:00			CZ			
	20:00 -	Social Event					
THU, 6th	08:30 - 09:00	Briefing					
	09:00 - 12:00	Data Evaluation			CH		
	13:00 - 16:00				FR	CZ	
FRI, 7th	09:00 - 09:30	Briefing					
	09:30 - 12:00	Presentation and Closure					
	12:00 -	Departure					

German 1	DE1	legend	France	FR
German 2	DE2		Swiss	CH
Host	CZ		DE1, DE2	no helicopter

## 6 AGC24 Tasks Overview

This chapter describes the individual tasks to be performed by the airborne monitoring teams. It describes why such tasks (including description of locations) were selected and it includes the forms given to each team to perform individual tasks. The teams followed the time schedule outlined in Chapter 5.

### 6.1 Introduction

The Czech Republic offers interesting locations in terms of airborne gamma-spectrometry. It is a country with rich remains of uranium ore mining and uranium processing areas. Also in 1986, the territory of the former Czechoslovakia was affected by radioactive fallout from the Chernobyl nuclear power plant accident. Traces of both uranium mining and the Chernobyl nuclear accident are still evident and measurable in the territory.

### 6.2 Range distance from Přerov Airport by helicopters

The selection of the Přerov Airport was explained earlier in Chapter 2. Additionally to other aspects, the airport has a good position to interesting locations in view of the airborne monitoring. This airport offers flight distances without refueling to reach each TASK locations. The following figure shows the range distances for individual selected tasks from Přerov Airport. Descriptions of individual tasks are given in the following subchapters.

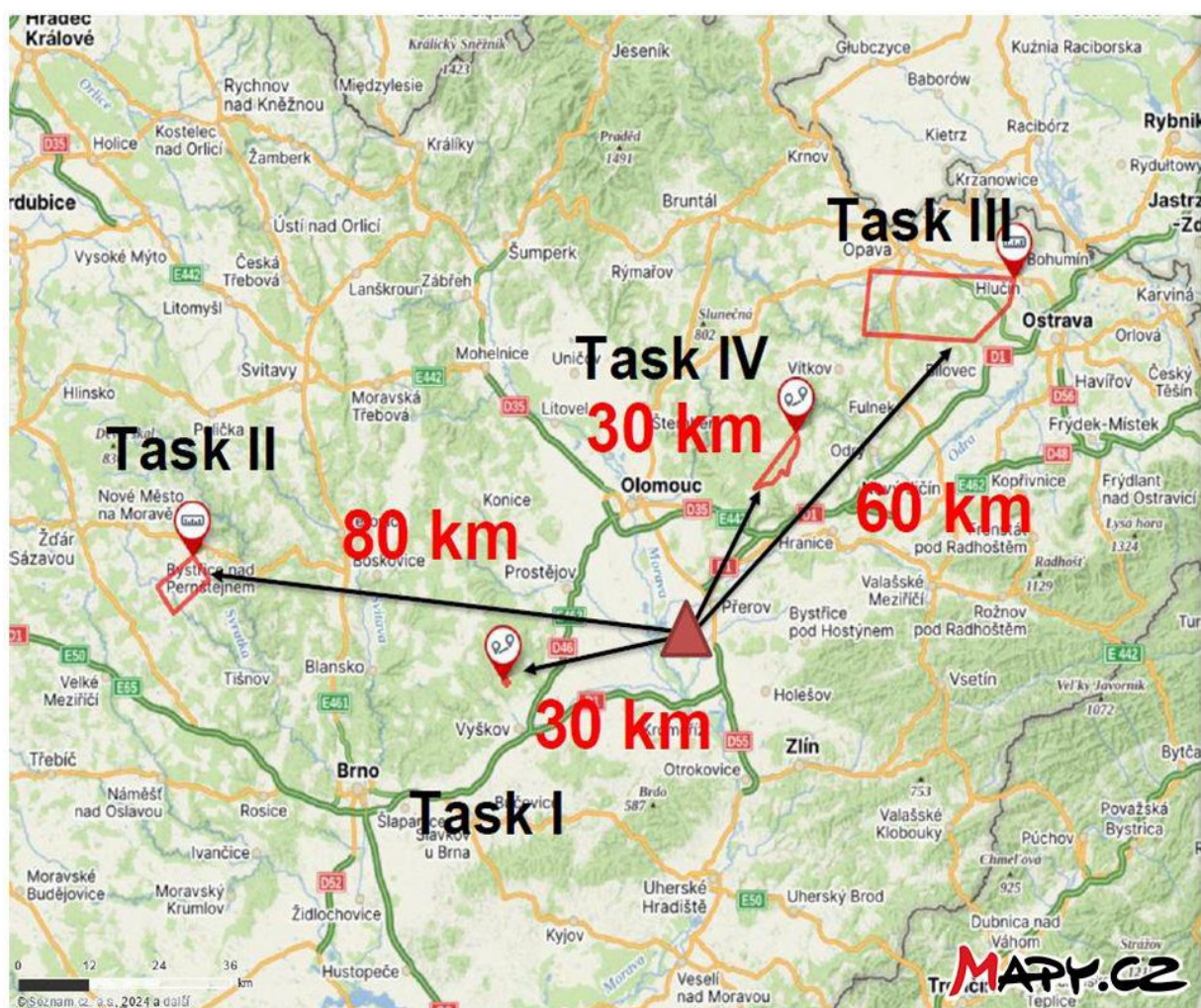


Fig. 15 Range distances from Přerov Airport to individual areas

## 6.3 TASK I - VYSKOV

### 6.3.1 Location

There are available detailed measurements on three reference areas for the airborne monitoring in the Czech Republic. One is located near Vyškov city in Březina Military Training Area. The area has never been cultivated, the activity concentrations of natural radionuclides are steady and nearly homogeneously distributed in soil. Surface activities of  $^{137}\text{Cs}$  are still low, less than  $3 \text{ kBq m}^{-2}$ . The reference area were measured twice, in 2008 at 16 points and in 2018 at 32 points by *in-situ* HPGe gamma-spectrometry [11], approximately a 60 m grid was applied, and the HPGe detector was always placed 1 m above the ground, the spectra were measured 1800 seconds. Activity concentrations of natural radionuclides ( $^{40}\text{K}$ , U-series, Th-series), surface activities of  $^{137}\text{Cs}$  and ambient dose equivalent rates at 1 m above the ground in  $\mu\text{Sv.h}^{-1}$  were determined.

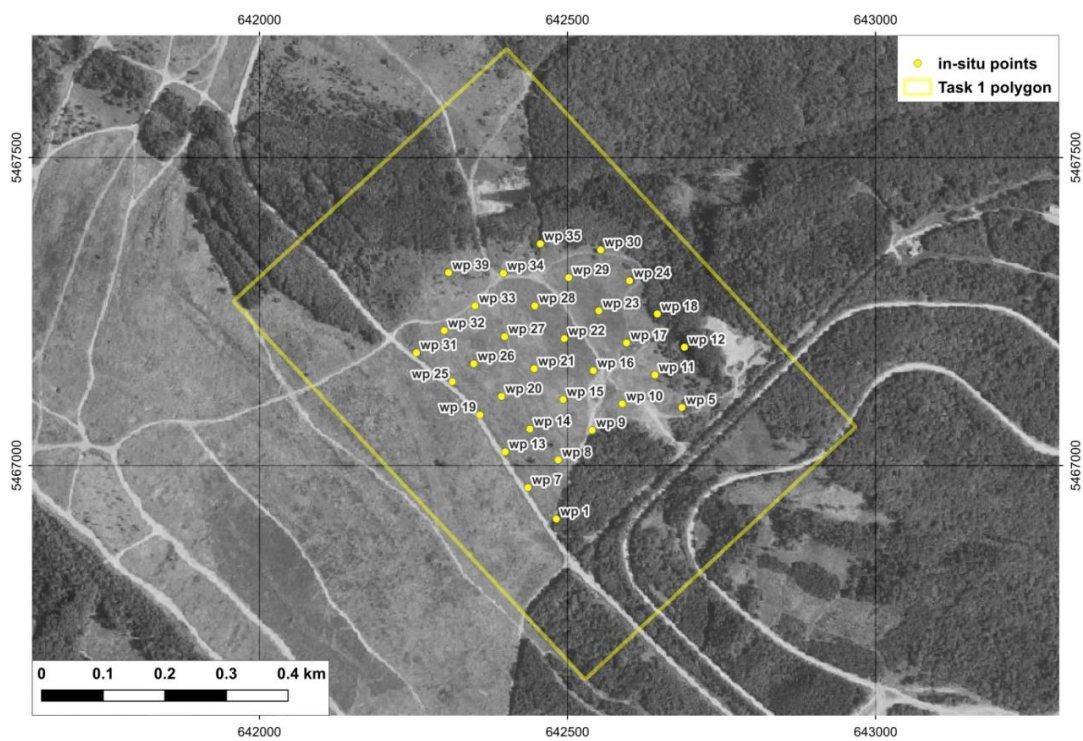
Tab. 4 Activity concentrations of  $^{40}\text{K}$ , U-series and Th-series in  $\text{Bq kg}^{-1}$  and surface activities with exponential distribution of  $^{137}\text{Cs}$  in  $\text{kBq m}^{-2}$  at reference area (Vyškov) in 32 measuring points in 2018

Waypoint	Longitude	Latitude	$\text{K} [\text{Bq kg}^{-1}]$	$\text{U} [\text{Bq kg}^{-1}]$	$\text{Th} [\text{Bq kg}^{-1}]$	$\text{Cs} [\text{kBq m}^{-2}]$
wp 1	49.33828741N	16.96137959E	552 $\pm$ 90	37 $\pm$ 7	41 $\pm$ 7	2.1 $\pm$ 0.5
wp 5	49.33986689N	16.96425087E	612 $\pm$ 100	40 $\pm$ 7	45 $\pm$ 8	0.6 $\pm$ 0.1
wp 7	49.33875663N	16.96076498E	543 $\pm$ 89	37 $\pm$ 7	42 $\pm$ 7	2.1 $\pm$ 0.6
wp 8	49.33914973N	16.96145518E	534 $\pm$ 87	38 $\pm$ 7	43 $\pm$ 7	1.7 $\pm$ 0.4
wp 9	49.3395684N	16.96222901E	589 $\pm$ 96	41 $\pm$ 7	45 $\pm$ 8	0.8 $\pm$ 0.2
wp 10	49.33994351N	16.96291851E	619 $\pm$ 101	40 $\pm$ 7	42 $\pm$ 7	2.0 $\pm$ 0.5
wp 11	49.34035364N	16.96366449E	571 $\pm$ 93	40 $\pm$ 7	39 $\pm$ 7	1.6 $\pm$ 0.4
wp 12	49.34074695N	16.96434098E	686 $\pm$ 112	42 $\pm$ 8	44 $\pm$ 8	2.2 $\pm$ 0.6
wp 13	49.33928668N	16.96027667E	529 $\pm$ 86	36 $\pm$ 7	39 $\pm$ 7	2.4 $\pm$ 0.6
wp 14	49.33960996N	16.96084019E	608 $\pm$ 99	40 $\pm$ 7	44 $\pm$ 8	0.9 $\pm$ 0.2
wp 15	49.34002886N	16.96160027E	567 $\pm$ 93	41 $\pm$ 7	43 $\pm$ 8	2.6 $\pm$ 0.7
wp 16	49.34043994N	16.9622912E	607 $\pm$ 99	42 $\pm$ 8	39 $\pm$ 7	2.5 $\pm$ 0.6
wp 17	49.34083186N	16.96305023E	726 $\pm$ 119	44 $\pm$ 8	45 $\pm$ 8	2.2 $\pm$ 0.6
wp 18	49.34124269N	16.96375495E	613 $\pm$ 100	41 $\pm$ 7	44 $\pm$ 8	2.1 $\pm$ 0.5
wp 19	49.33983564N	16.95973403E	703 $\pm$ 115	41 $\pm$ 8	45 $\pm$ 8	0.6 $\pm$ 0.2
wp 20	49.34009716N	16.96022627E	514 $\pm$ 84	43 $\pm$ 8	48 $\pm$ 8	2.5 $\pm$ 0.6
wp 21	49.34048933N	16.96097152E	571 $\pm$ 93	38 $\pm$ 7	39 $\pm$ 7	3.2 $\pm$ 0.8
wp 22	49.34091839N	16.96166317E	584 $\pm$ 96	36 $\pm$ 7	42 $\pm$ 7	2.5 $\pm$ 0.7
wp 23	49.34130985N	16.96244971E	583 $\pm$ 95	38 $\pm$ 7	41 $\pm$ 7	1.7 $\pm$ 0.4
wp 24	49.34173866N	16.96315515E	621 $\pm$ 102	36 $\pm$ 7	41 $\pm$ 7	2.2 $\pm$ 0.6
wp 25	49.34033159N	16.95913421E	600 $\pm$ 98	40 $\pm$ 7	43 $\pm$ 8	0.7 $\pm$ 0.2
wp 26	49.34058412N	16.95962609E	423 $\pm$ 69	32 $\pm$ 6	39 $\pm$ 7	2.3 $\pm$ 0.6
wp 27	49.34096801N	16.96032971E	549 $\pm$ 90	36 $\pm$ 7	40 $\pm$ 7	3.0 $\pm$ 0.8

Waypoint	Longitude	Latitude	K [Bq kg <sup>-1</sup> ]	U [Bq kg <sup>-1</sup> ]	Th [Bq kg <sup>-1</sup> ]	Cs [kBq m <sup>-2</sup> ]
wp 28	49.34140606N	16.96102172E	566 $\pm$ 93	36 $\pm$ 7	38 $\pm$ 7	2.9 $\pm$ 0.7
wp 29	49.34180674N	16.96179487E	672 $\pm$ 110	37 $\pm$ 7	44 $\pm$ 8	1.7 $\pm$ 0.4
wp 30	49.34219914N	16.9625264E	630 $\pm$ 103	40 $\pm$ 7	48 $\pm$ 8	1.3 $\pm$ 0.3
wp 31	49.34076763N	16.95835302E	629 $\pm$ 103	41 $\pm$ 8	43 $\pm$ 8	0.7 $\pm$ 0.2
wp 32	49.34108077N	16.95898499E	629 $\pm$ 103	41 $\pm$ 7	45 $\pm$ 8	1.2 $\pm$ 0.3
wp 33	49.3414287N	16.95968718E	572 $\pm$ 93	41 $\pm$ 7	40 $\pm$ 7	2.7 $\pm$ 0.7
wp 34	49.34189442N	16.96033899E	718 $\pm$ 117	43 $\pm$ 8	47 $\pm$ 8	0.4 $\pm$ 0.1
wp 35	49.34231193N	16.96118164E	742 $\pm$ 121	46 $\pm$ 8	46 $\pm$ 7	1.9 $\pm$ 0.5
wp 39	49.34192418N	16.95911485E	502 $\pm$ 82	35 $\pm$ 6	43 $\pm$ 7	1.1 $\pm$ 0.3
<b>AVERAGE</b>			<b>599 <math>\pm</math> 98</b>	<b>39 <math>\pm</math> 7</b>	<b>43 <math>\pm</math> 7</b>	<b>1.8 <math>\pm</math> 0.5</b>

The following Fig. 16 shows a reference area of 530 m x 450 m and Tab. 5 shows the measured average values both from 2008 and 2018. It can be seen that the values have not changed on this uncultivated reference area and the results are nearly the same in 2008 and 2018.

The task of the airborne teams was to collect data for 5 minutes at the centre of the reference area at two flight altitudes of 70 m and 140 m and to measure a polygon above the reference area defined by WGS84 coordinates (EPSG:4326).



created in QGIS, background map: Orthophoto of the Czech Republic, Czech Office for Surveying, Mapping and Cadastre - ČÚZK, (CC BY)

Fig. 16 View on the reference area in Březina Military Training Area including polygon for TASK I (including UTM coordinates - EPSG:32633)

Tab. 5 Average activities and average ambient dose equivalent rates (including cosmic ray contribution) at the Vyškov reference area in 2008 and 2018

Quantity (in-situ with HPGe)	2008	2018
Ambient dose equivalent rate [ $\mu\text{Sv h}^{-1}$ ] (terrestrial plus cosmic contribution)	$119 \pm 12$	$124 \pm 8$
Activity concentration $^{40}\text{K}$ [ $\text{Bq kg}^{-1}$ ]	$606 \pm 91$	$599 \pm 98$
Activity concentration U-series [ $\text{Bq kg}^{-1}$ ]	$36 \pm 5$	$39 \pm 7$
Activity concentration Th-series [ $\text{Bq kg}^{-1}$ ]	$38 \pm 6$	$43 \pm 7$
Surface activity $^{137}\text{Cs}$ (exponen.distr.) [ $\text{kBq m}^{-2}$ ]	$2.2 \pm 0.8$	$1.8 \pm 0.5$

In compliance with the procedure described in [7] using the constant  $a_K$ ,  $a_U$ ,  $a_{Th}$ , [nGy kg Bq $^{-1}$  h $^{-1}$ ] and  $a_{Cs137}$  [nGy kBq $^{-1}$  h $^{-1}$  m $^2$ ], the air kerma rate was calculated:

$$\text{AKR} [\text{nGy h}^{-1}] = a_K \times A_K + a_U \times A_U + a_{Th} \times A_{Th} + a_{Cs137} \times A_{Cs137}$$

where AKR is Air Kerma Rate in nGy h $^{-1}$ ,  $a_K = 0.0417$ ,  $a_U = 0.462$ ,  $a_{Th} = 0.604$  and  $a_{Cs137} = 1.05 \times 10^{-3}$  are the constant of individual elements taken from [7] and  $A_K$ ,  $A_U$ ,  $A_{Th}$  are the activity concentrations of  $^{40}\text{K}$ , U-series, Th-series in Bq.kg $^{-1}$  and  $A_{Cs137}$  is the surface activity of  $^{137}\text{Cs}$  in kBq m $^{-2}$ .

The ambient dose equivalent rate of  $\text{DHSR}_{\text{TOT}}$  is the sum of the ambient dose equivalent rate of the anthropogenic component of  $\text{DHSR}_{\text{GND}}$  plus the ambient dose equivalent rate of cosmic radiation including all secondary cosmic particles  $\text{DHSR}_{\text{cos}}$ . The resulting value is given in  $\mu\text{Sv h}^{-1}$ .

The anthropogenic component  $\text{DHSR}_{\text{GND}}$  is given by:

$$\text{DHSR}_{\text{GND}} [\mu\text{Sv h}^{-1}] = \text{AKR} \times 1.2 \times 0.001$$

where the cosmic radiation is calculated from a simple formula:

$$\text{DHSR}_{\text{cos}} [\mu\text{Sv h}^{-1}] = 32 \times 2^{(0.001 \times h)/1.5}$$

where  $h$  is the height above sea level in metres

$$\text{DHSR}_{\text{TOT}} [\mu\text{Sv h}^{-1}] = \text{DHSR} [\mu\text{Sv h}^{-1}] = \text{DHSR}_{\text{GND}} + \text{DHSR}_{\text{cos}}$$

The instruction sheets for the implementation of TASK I were forwarded to all teams in the form of the following sheet.

### 6.3.2 TASK I: VYSKOV - Reference area mapping

Task name :	VYSKOV
Objective:	Measurement over the reference area. Activity concentration of AW_K-40, AW_U-238, AW_Th-232, AA_Cs-137, ambient dose equivalent rate DHSR
Flight area:	
Geographical coordinates: (WGS-84)	Centre of reference area: 49.340559N 16.961147E Polygon: 49.341586N 16.954292E 49.339517N 16.968121E 49.345172N 16.960546E 49.335931N 16.961931E
Flight parameters	<i>Task A)</i> Altitude: 1st flight: 70 m (230 ft) AGL 2nd flight: 140 m (460 ft) AGL Speed: individual Spacing: individual  <i>Task B)</i> If possible hovering over the centre of the area in 70 m and 140 m AGL for 5 min each
Special demands:	<b>NO FLY ZONE in military area beyond latitude: 49.3658233N</b>
Remarks:	Air distance Airport-Flight area about 30 km
Presentation on Friday	AW_K-40, AW_U-238, AW_Th-232, AA_Cs-137, ambient dose equivalent rate DHSR
Flight time in the region of interest	Maximum: 60 minutes

## 6.4 TASK II - VYSOCINA

### 6.4.1 Location

This location is interesting for two reasons. Firstly, the area of the Bohemian-Moravian Highlands (VYSOCINA) in the vicinity of Dolní Rožínka village is an area of already terminated uranium ore mining. This area is currently being reclaimed, there is a uranium ore reprocessing plant in the area defined by the polygon and the plant area is still characterised by an elevated dose rate and a higher content of uranium series elements. In the opposite part of the polygon along the Bobrůvka River there are remains of the Chernobyl caesium (Fig. 17). Ground measurements were carried out at the locations in 2008 by the NBC Department, University of Defence in Vyškov. In 2018, the SÚRO airborne monitoring team carried out a survey over this area and  $^{137}\text{Cs}$  was indeed detected by the airborne spectrometer. The results of the 2018 airborne monitoring of  $^{137}\text{Cs}$  are shown in the map (Fig. 18). At this time, the surface activities with an exponential distribution should be within the range up to 6 - 10 kBq  $\text{m}^{-2}$ .

The objective of the airborne teams was to measure the area, detect any anomalies to estimate activities and determine the ambient dose equivalent rates.

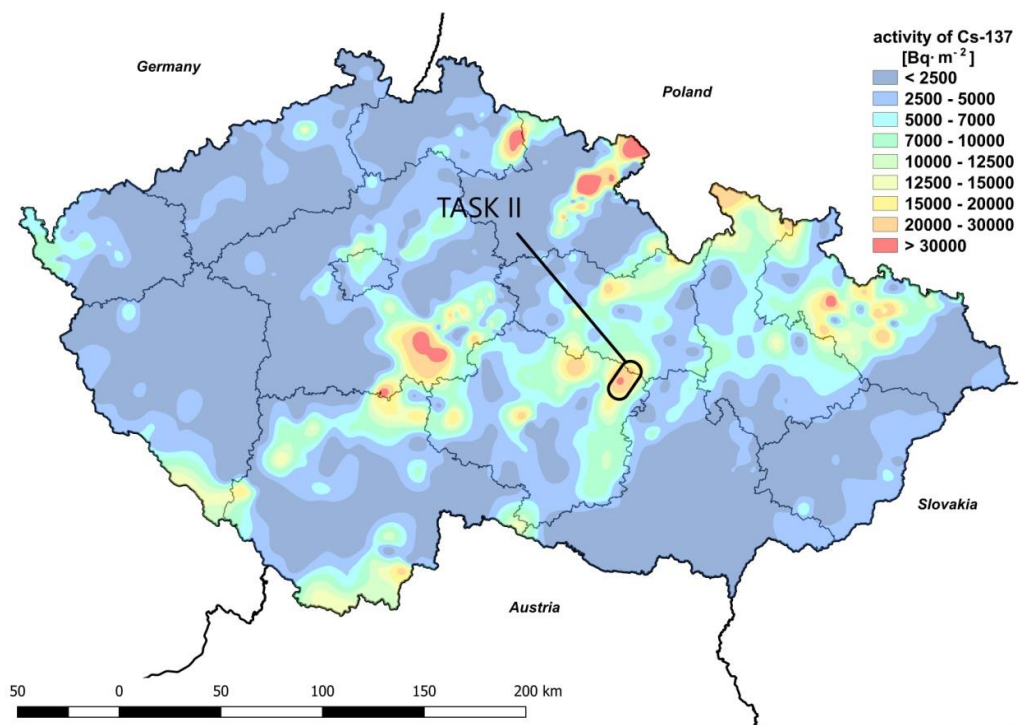


Fig. 17 Map of  $^{137}\text{Cs}$  contamination in  $\text{Bq m}^{-2}$  in 1986 [12]

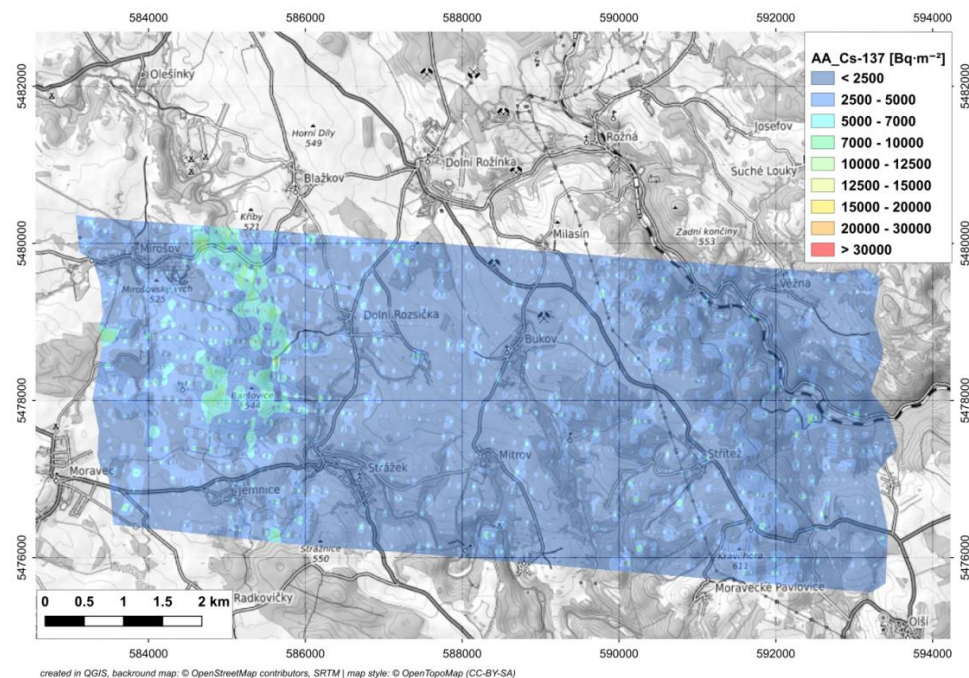


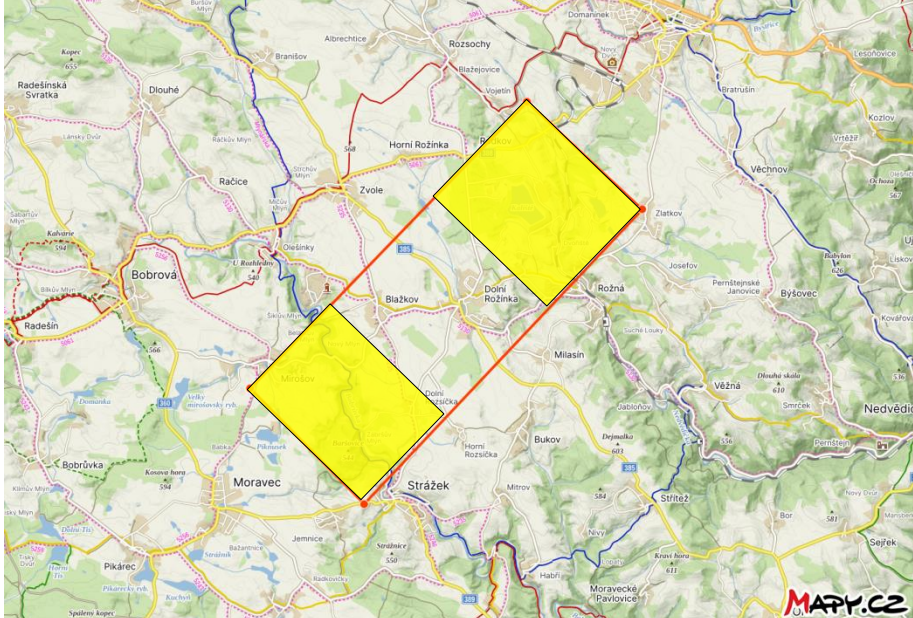
Fig. 18 SÚRO airborne monitoring of the  $^{137}\text{Cs}$  surface activity in 2018

Fig. 18 shows the  $^{137}\text{Cs}$  Chernobyl contamination in  $\text{Bq m}^{-2}$  around the Bobrůvka River monitored during the SÚRO airborne survey in 2018. The western part of this survey and the area around Dolní Rožínka with the operating uranium mine reprocessing plant was involved in TASK II. The instruction sheet for TASK II follows on the next site.



Fig. 19 Locations with (now all inactive) uranium processing plants and mines in the Czech Republic

#### 6.4.2 TASK II : VYSOCINA

Task name :	VYSOCINA (BOHEMIAN –MORAVIAN UPLANDS)	
Objective:	Activity concentrations of AW_K-40, AW_U-238, AW_Th-232, AA_Cs-137, ambient dose equivalent rate DHSR	
Flight area:		
Geographical coordinates: (WGS-84)	<p>Polygon:          49.509617N 16.224568E          49.491222N 16.254952E          49.440746N 16.181644E          49.460526N 16.151612E</p>	
Flight parameters	Speed: 100 km/h	Altitude: 100 m AGL
Special demands:	Individual flight sections for teams will be specified during AGC24	
Remarks:	Air distance Airport-Flight area about 85 km, Polygon area: 23 km <sup>2</sup> The level of interest in the yellow area is HIGH, the yellow area has no specific boundaries	
Presentation on Friday	AW_K-40, AW_U-238, AW_Th-232, AA_Cs-137, ambient dose equivalent rate DHSR Also specify interesting locations, if present	
Flight time in the region of interest	Maximum: 90 minutes	

## 6.5 TASK III - OPAVA

### 6.5.1 Location

The location was chosen because it is an area where spots of  $^{137}\text{Cs}$  can be still found. Ground measurements detected surface activities of  $^{137}\text{Cs}$  in the late 1980s about more than  $20 \text{ kBq m}^{-2}$ . In addition, this area does not contain any higher mountain ranges and is suitable for convenient airborne survey. However, due to the absence of two German teams, the survey area had to be reduced so that three teams could carry out an effective airborne survey, flying to and from the polygon without refueling.

The goal was to prepare flight logistics of three teams, allocate individual areas, specify ground speeds, flight altitude and spacing between flight lines to cover the complete polygon without refueling, and finally, create a common composite map. To create the composite map, the same colour scale was used for all teams for each range for each variable, see chapter 4.2. The map should properly create if the border crossings of individual teams in the map are smooth and continuous.

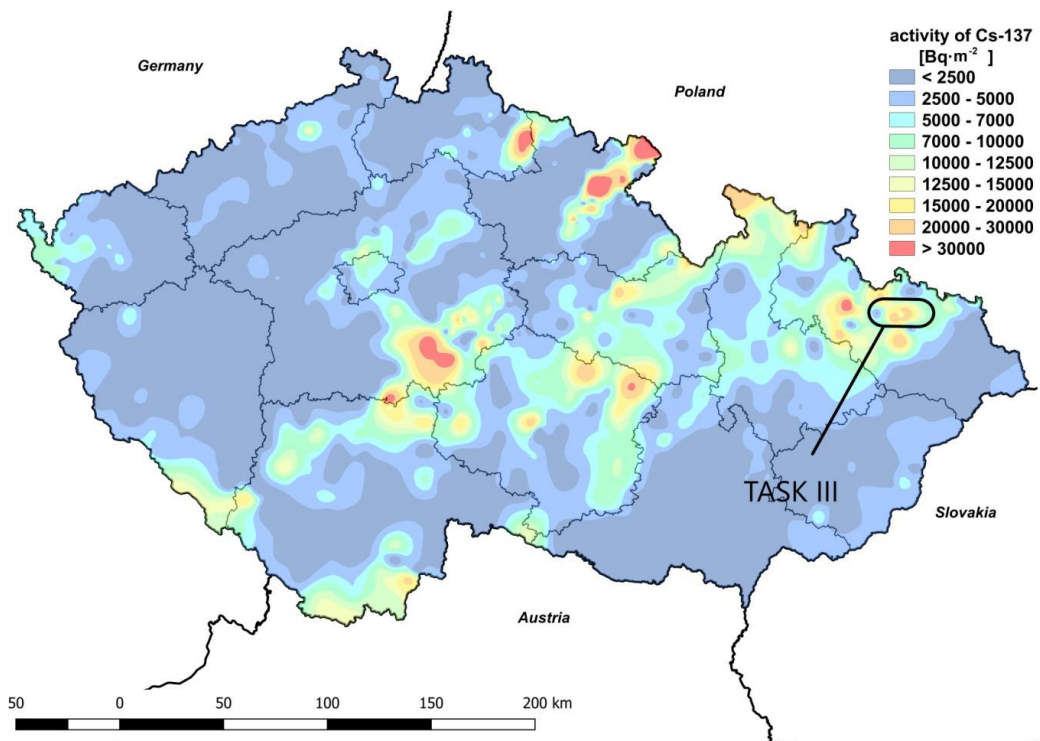
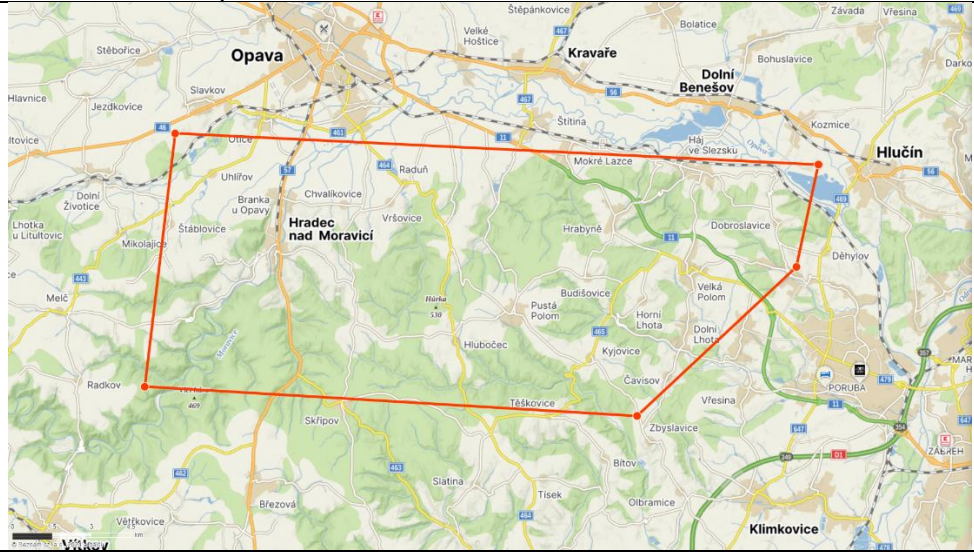


Fig. 20 Map of  $^{137}\text{Cs}$  contamination in  $\text{Bq m}^{-2}$  in 1986 [12]

The instruction sheet for TASK III is on the next site.

### 6.5.2 TASK III : OPAVSKO

Task name :	OPAVSKO
Objective:	Composite mapping Activity concentration of AW_K-40, AW_U-238, AW_Th-232, AA_Cs-137, ambient dose equivalent rate DHSR
Flight area:	
Geographical coordinates: (WGS-84)	Polygon: 49.900242N 18.162839E 49.910966N 17.822091E 49.824441N 17.805955E 49.814362N 18.066708E 49.865288N 18.151166E
Flight parameters	Speed: Individual Spacing: Individual Altitude: Max 150 m AGL
Special demands:	Individual flight sections for teams will be specified during AGC24
Remarks:	Air distance Airport-Flight area about 50-60 km
Presentation on Friday	AW_K-40, AW_U-238, AW_Th-232, AA_Cs-137, ambient dose rate DHSR
Flight time in the region of interest	According to the maximum flight capability of the helicopter.

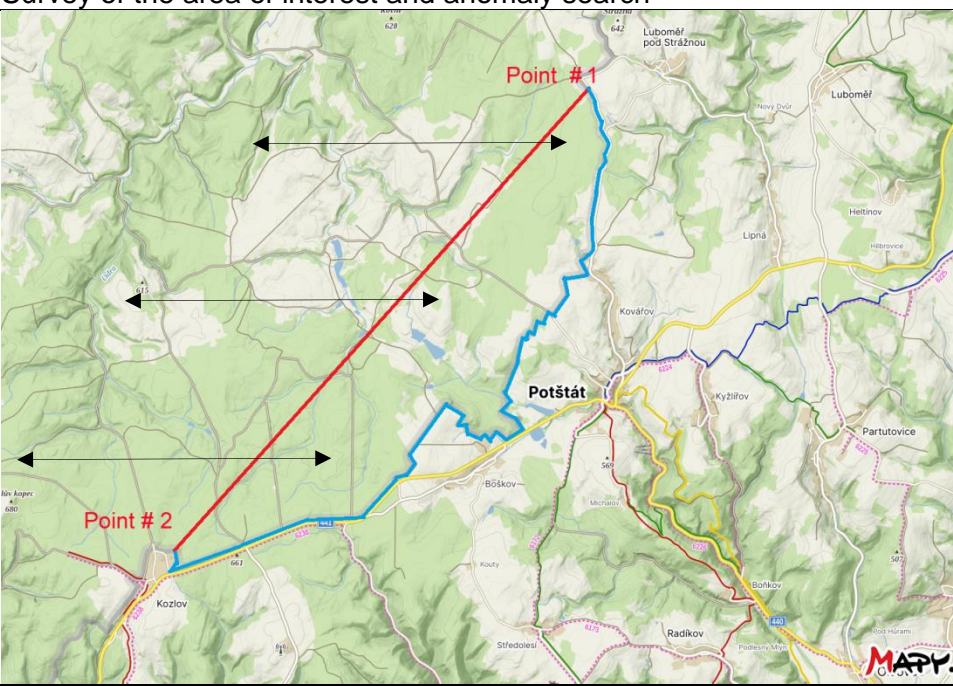
## 6.6 TASK - IV LIBAVA

### 6.6.1 Location

The objective of this task was to localize strong point sources of ionizing radiation, determine their geographical locations, and estimate their activities. For this task, we chose the area in the Libava Military Training Area. This area was in the south-eastern part in the Libava military area, directly adjacent to the military area boundary (see map on the next page).

The task was made even more difficult for the operators and pilots by the fact that they had to conduct the survey up to the boundary of the military area. For the operators, they had to design the survey as close to the border as possible, and for the pilots, the military area boundary must not be crossed (blue line in TASK IV instruction sheet). This south-eastern area in particular was extremely challenging for pilots.

## 6.6.2 TASK IV : LIBAVA

Task name :	LIBAVA
Objective:	Survey of the area of interest and anomaly search
Flight area:	
Geographical coordinates: (WGS-84)	<p>Point #1 49.6865575N 17.6463925E</p> <p>Point #2 49.6123686N 17.5453269E</p> <p>Blue line is the border of military area. Detailed WGS-84 coordinates available on the AGC24 headquarter</p>
Flight parameters	<p><b>Entry and exit to the area of interest only through the military area – see arrows</b></p> <p>Recommendation: Altitude: 100 m AGL; spacing max 250 m; speed 100-120 km per hour</p>
Special demands:	Blue line, i.e. border of military area, <b>MUST NOT BE CROSSED !!!</b>
Remarks:	Air distance Airport-Flight area about 30 km
Presentation on Friday	If found specify types of radioactive sources and estimate their activities
Flight time in the region of interest	Maximum: 90 minutes

## 7 PRESENTATION OF RESULTS

In this chapter, all available results of individual teams from each TASK I - IV are presented.

The foreign teams had delivered their output files in the form of ERS 2.0. Unified template maps in free QGIS software to retain uniform map appearance were created. The maps of TASKS I, II and IV produced in the QGIS mapping software package were created from the original data supplied by the Swiss, Czech and French teams. It means that the results and maps of TASK I, II and IV are presented without any corrections and modifications, while the data in the composite map (TASK III) were modified in order to achieve continuity and to match the data to the same conditions. The model distribution of  $^{137}\text{Cs}$  was converted to the commonly used one in the Czech Republic since the Chernobyl nuclear disaster [13]. Activity concentrations of natural radionuclides were recalculated to wet weight (AW\_ in compliance with ERS notification). In case of TASK III, the Swiss and French data were converted from AD\_ (dry weight) to AW\_ (wet weight) and such data were displayed in the composite maps.

The conversion was especially needed for the presentation of the  $^{137}\text{Cs}$  results, the Swiss and French teams were using a model distribution by [7] while the Czech team used a distribution according to [13]. Of course, in such case the results may differ significantly and a conversion had to be used for a unique composite map.

In the case of DHSR, the contributions of the terrestrial component of natural nuclides,  $^{137}\text{Cs}$  (if present) and the total cosmic contributions to the ambient dose equivalent rates were included. All teams had the similar approaches for calculating this quantity and hence no conversions had been carried out. Results are presented in  $\mu\text{Sv h}^{-1}$ .

The meaning and interpretation are discussed in detail in the framework of TASK III for the composite map.

Conclusions from all individual TASKS are presented in chapter 8.

## 7.1 TASK I - A: Polygon (70 m and 140 m)

### 7.1.1 Czech team – polygon (70 m and 140 m)

The enhanced window method (WND) in AGAMA software package was used to calculate DHSR and activities of natural nuclides. The results of WND method was used for presentation in figures. The survey was conducted over a defined polygon with 8 lines at altitudes of 70 m (and 140 m with a ground speed of about  $100 \text{ km h}^{-1}$ ). Further processing - including spline interpolation and creation of final map outputs - was performed in the open-source programs QGIS and SAGA-GIS. The original post-processed data were cropped to the polygon area.

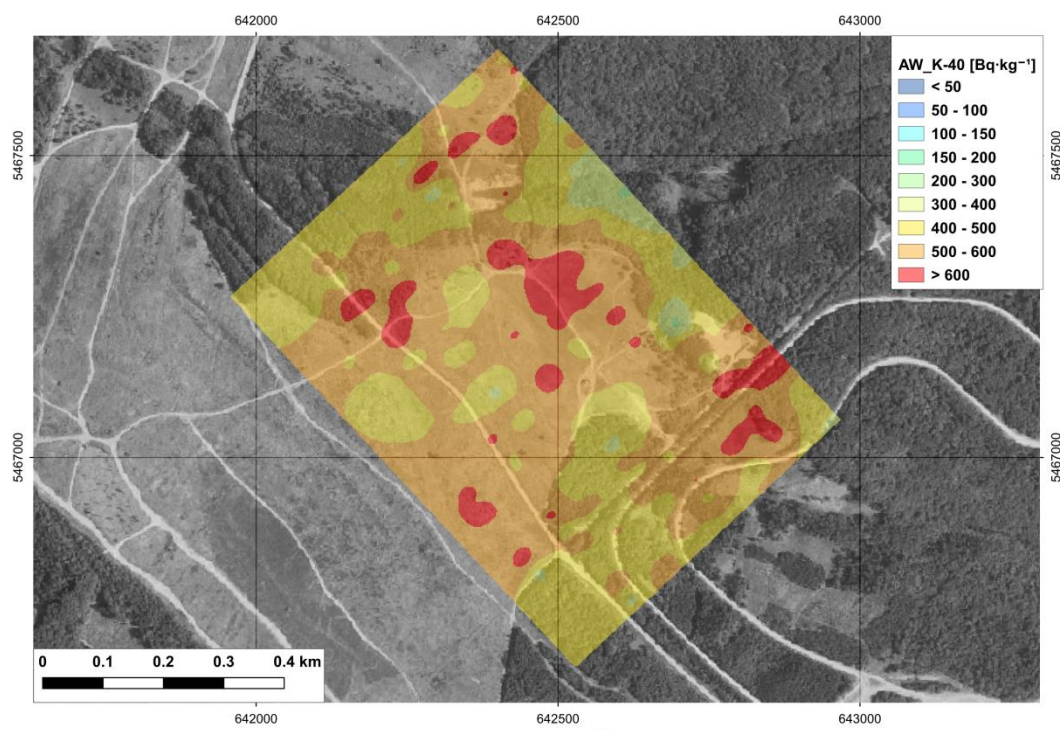


Fig. 21 Activity concentrations of  $^{40}\text{K}$  in  $\text{Bq kg}^{-1}$  from polygon survey (70 m) (Czech)

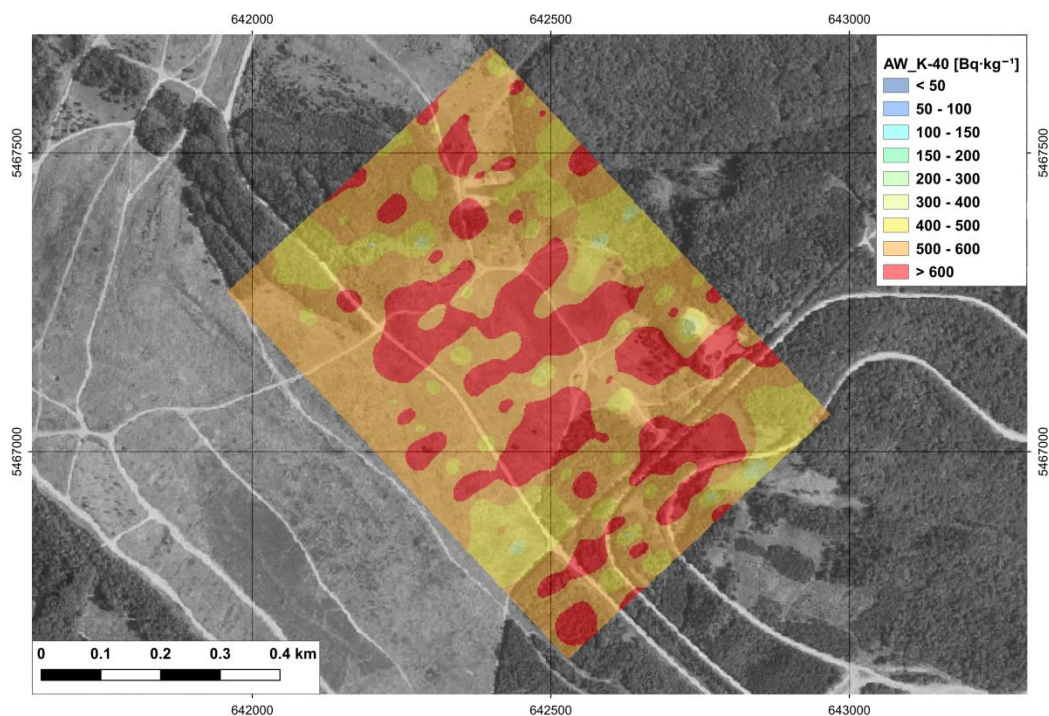


Fig. 22 Activity concentrations of  $^{40}\text{K}$  in  $\text{Bq kg}^{-1}$  from polygon survey (140 m) (Czech)

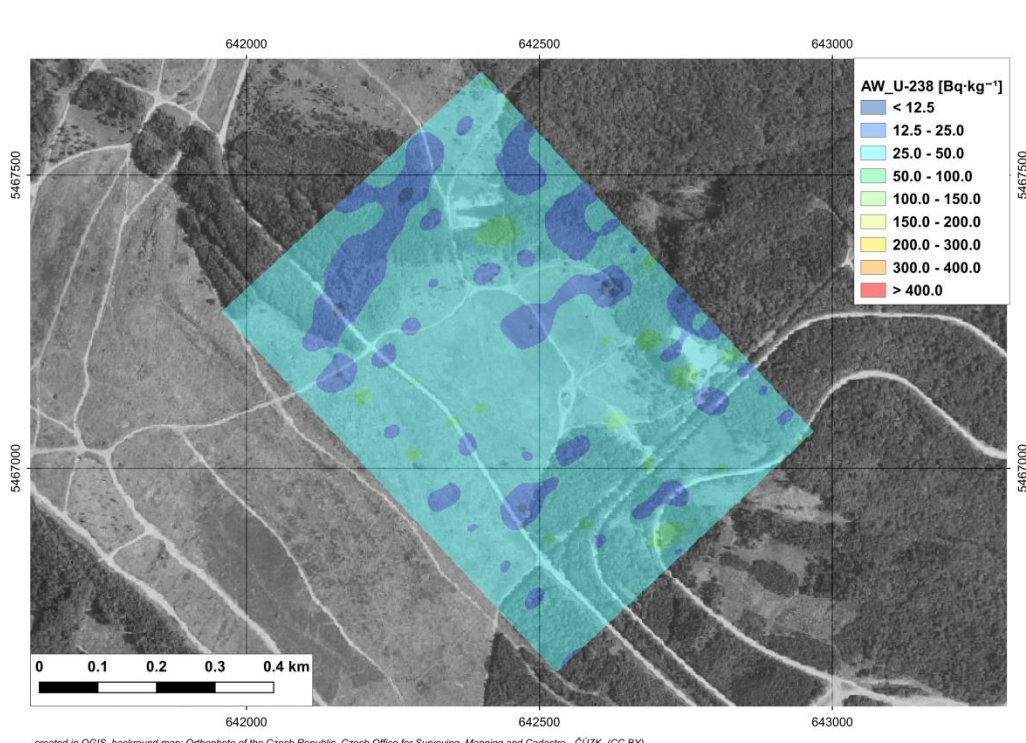


Fig. 23 Activity concentrations of  $^{238}\text{U}$  in  $\text{Bq kg}^{-1}$  from polygon survey (70 m) (Czech)

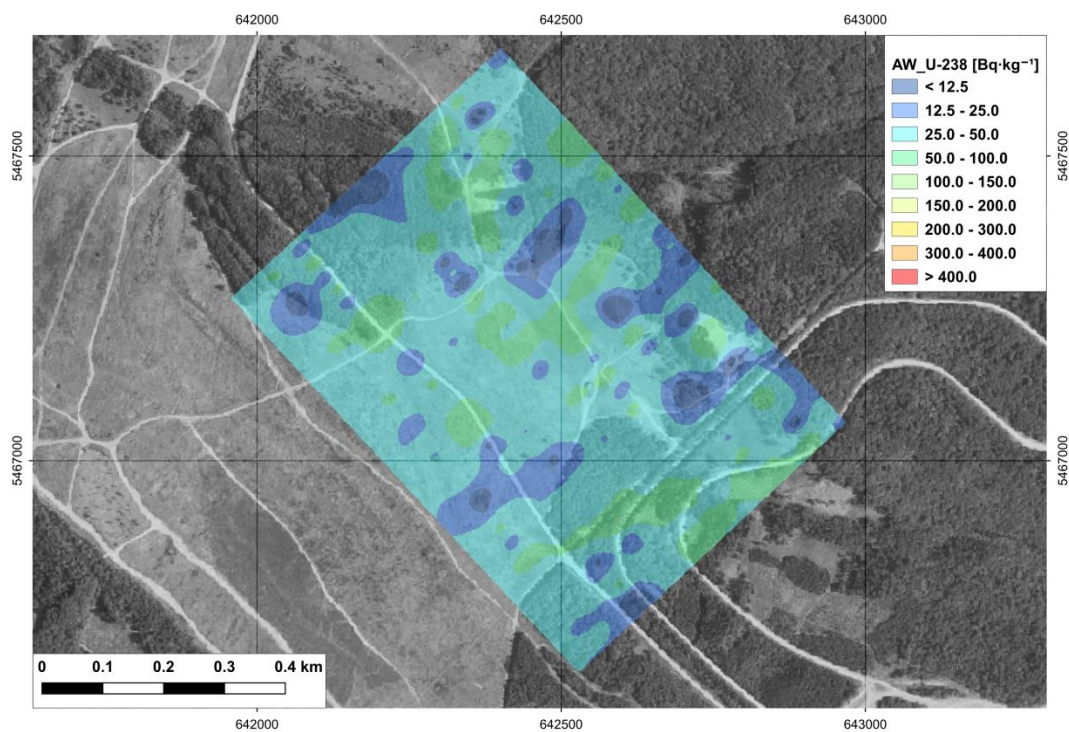


Fig. 24 Activity concentrations of  $^{238}\text{U}$  in  $\text{Bq kg}^{-1}$  from polygon survey (140 m) (Czech)

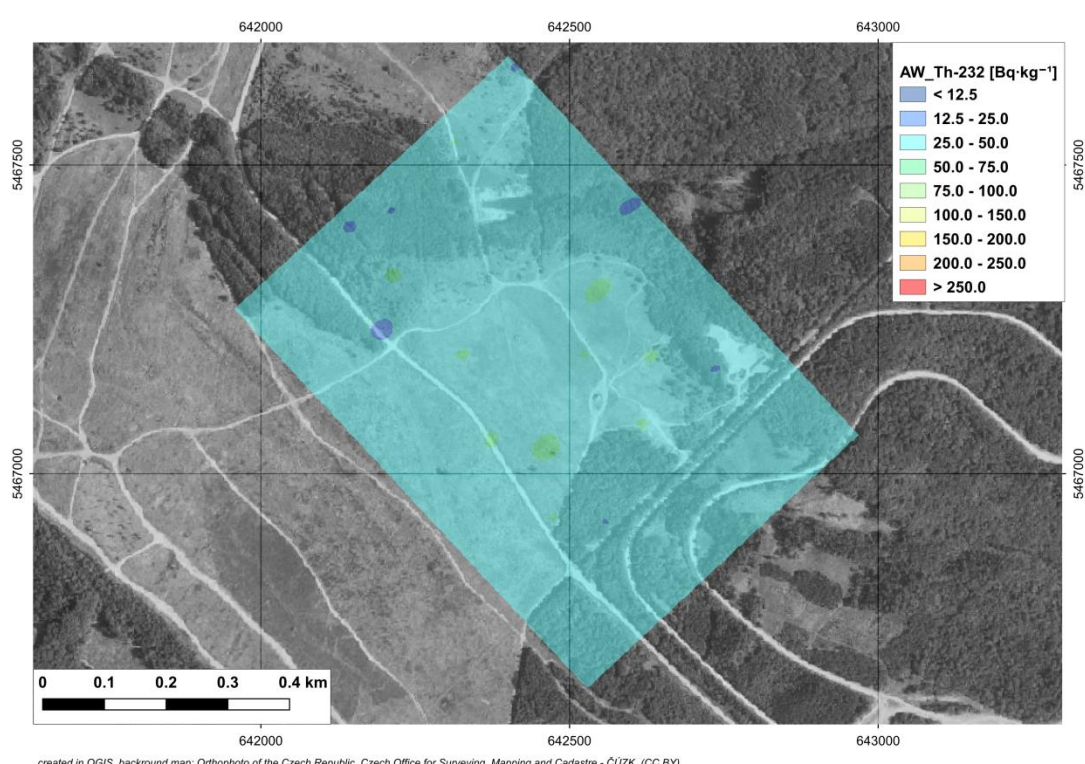
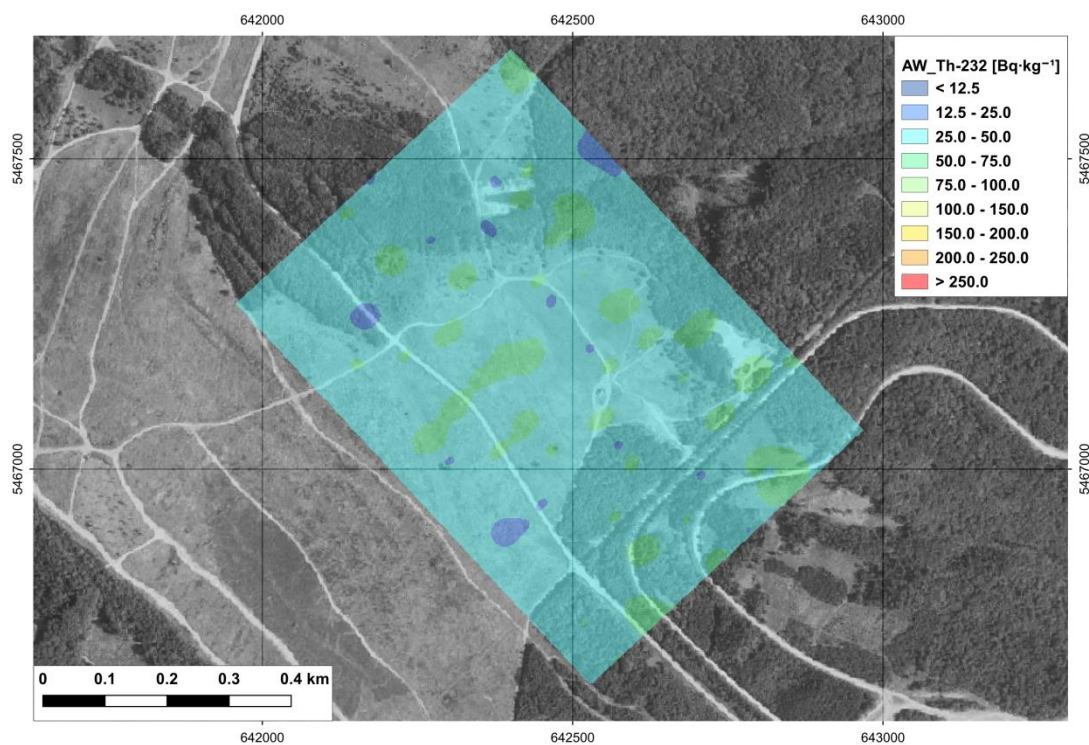
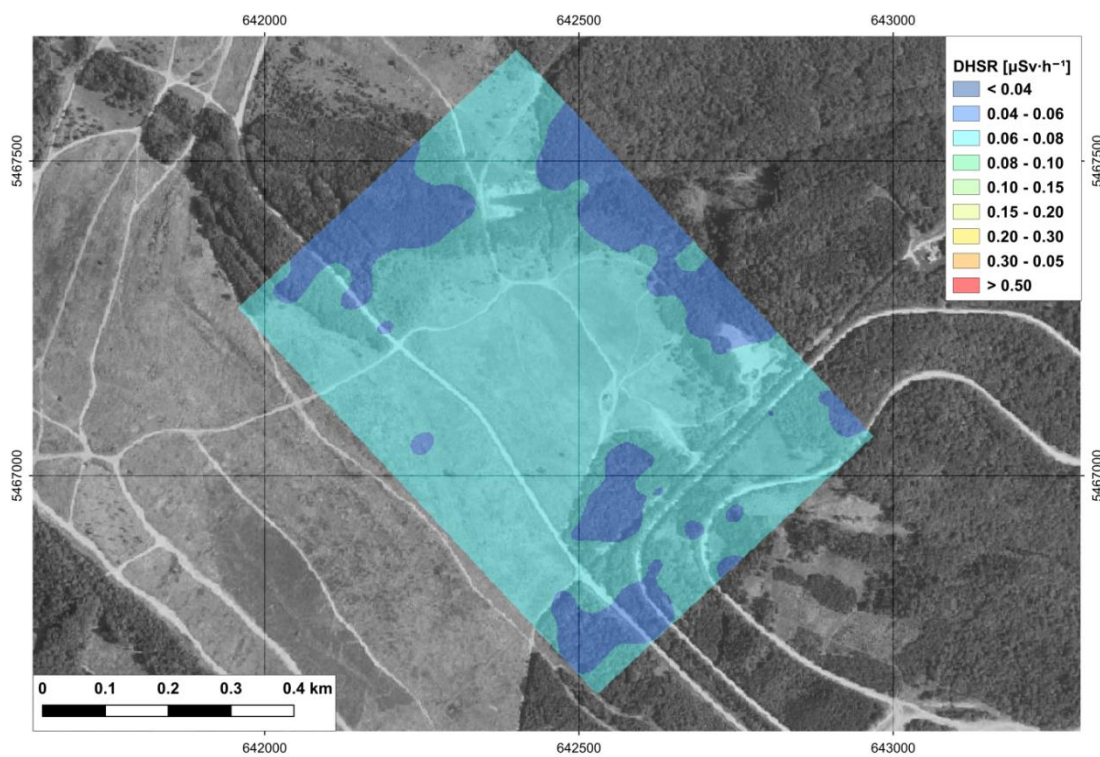


Fig. 25 Activity concentrations of  $^{232}\text{Th}$  in  $\text{Bq kg}^{-1}$  from polygon survey (70 m) (Czech)



created in QGIS, background map: Orthophoto of the Czech Republic, Czech Office for Surveying, Mapping and Cadastre - ČÚZK, (CC BY)

Fig. 26 Activity concentrations of  $^{232}\text{Th}$  in  $\text{Bq kg}^{-1}$  from polygon survey (140 m) (Czech)



created in QGIS, background map: Orthophoto of the Czech Republic, Czech Office for Surveying, Mapping and Cadastre - ČÚZK, (CC BY)

Fig. 27 Ambient dose equivalent rates in  $\mu\text{Sv h}^{-1}$  from polygon survey (70 m) (Czech)

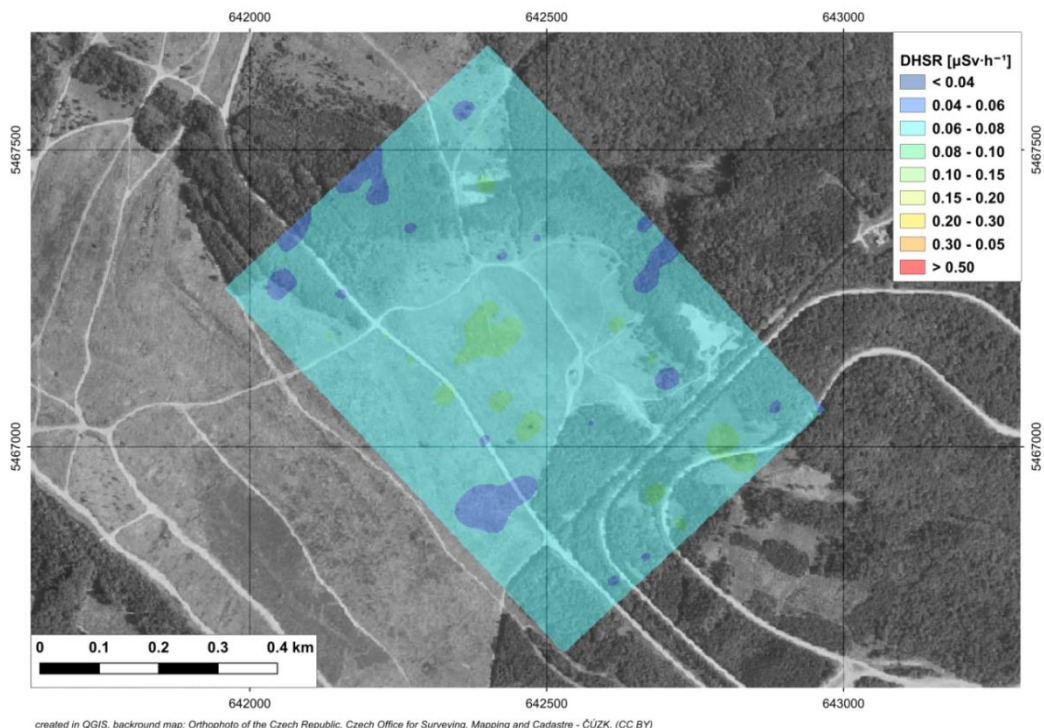


Fig. 28 Ambient dose equivalent rates in  $\mu\text{Sv}\cdot\text{h}^{-1}$  from polygon survey (140 m) (Czech)

### 7.1.2 Swiss team – polygon (70 m and 140 m)

A total of 14 flight lines were completed with a spacing of approximately 65 meters. Initially, 7 parallel lines were flown with a spacing of 125 meters. To increase measurement density, additional lines were manually inserted between the original ones. The total flight time was 15 minutes at an altitude of 70 meters, followed by 13 minutes at an altitude of 140 meters.

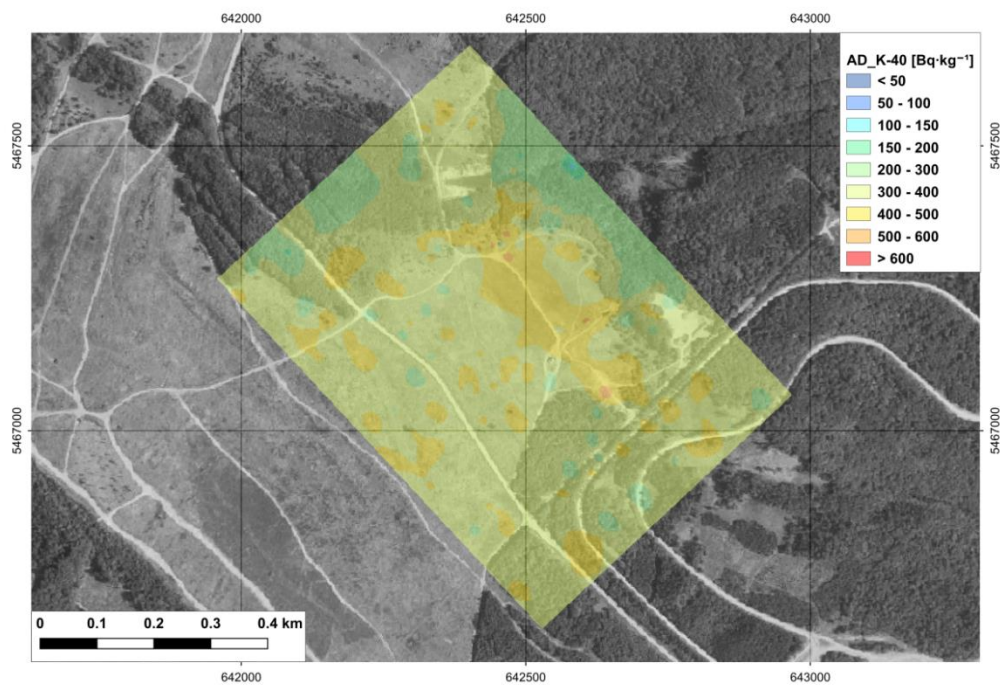


Fig. 29 Activity concentrations of  $^{40}\text{K}$  in  $\text{Bq kg}^{-1}$  from polygon survey (70 m) (Swiss)

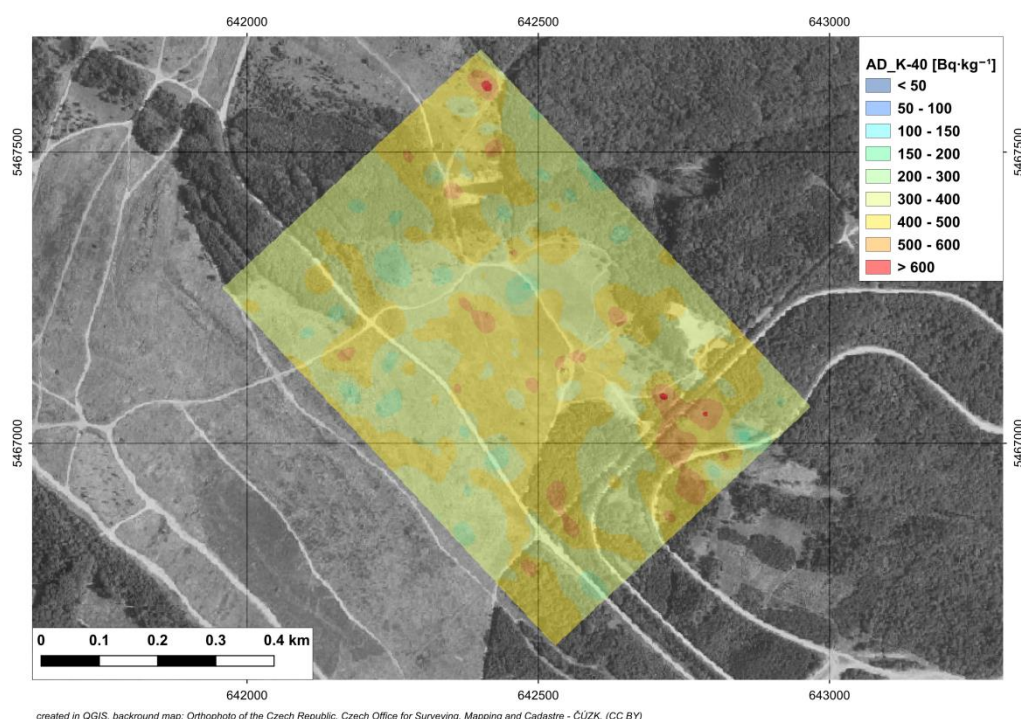
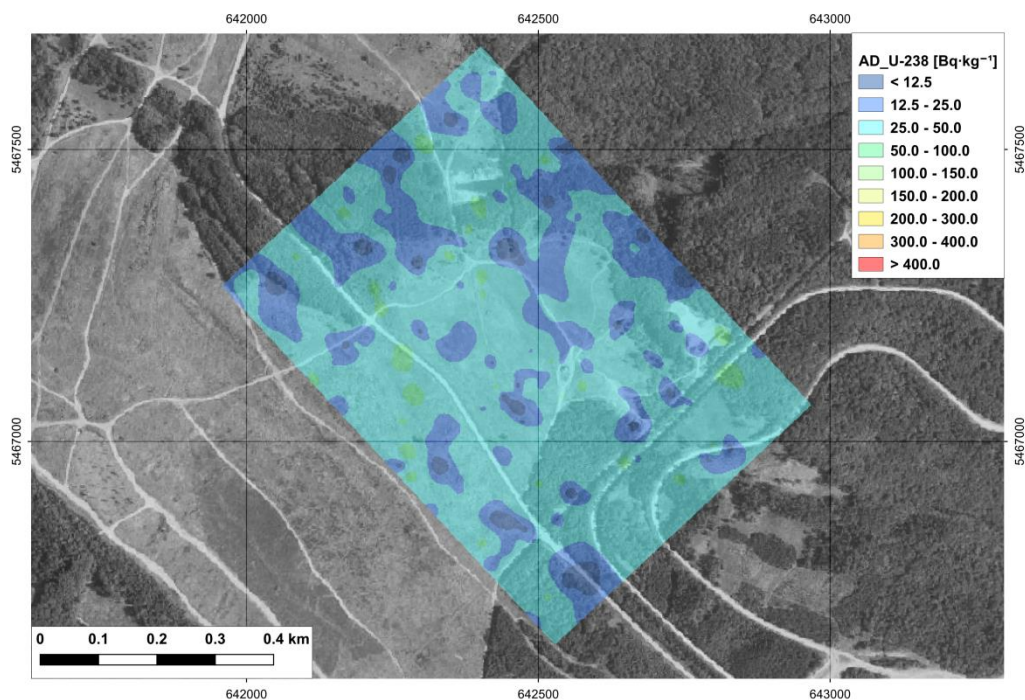
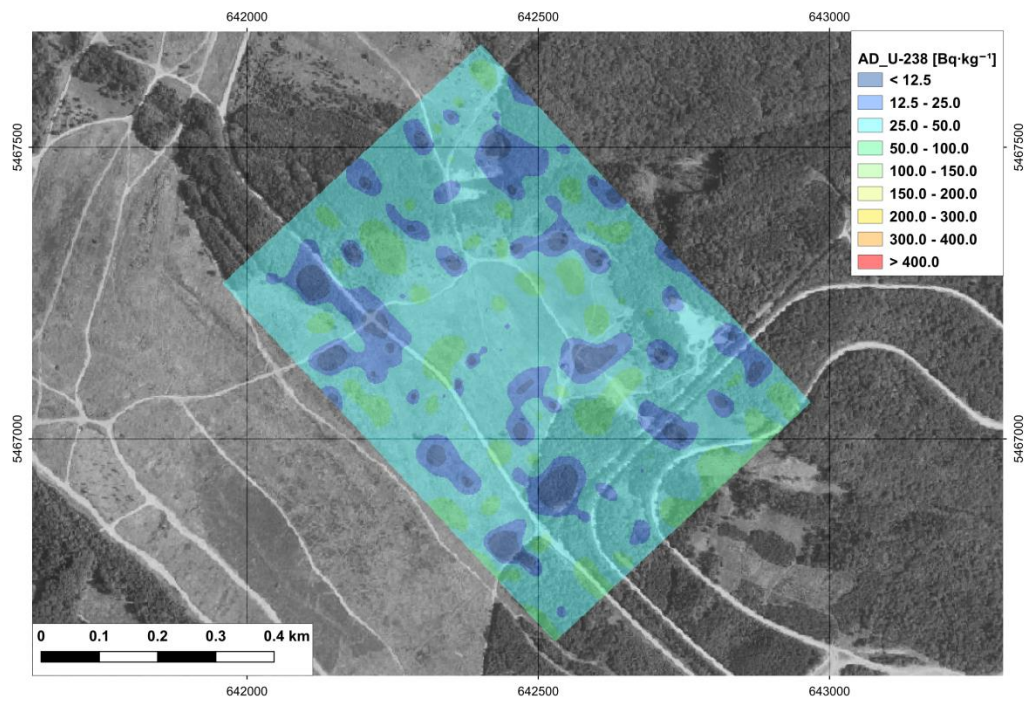


Fig. 30 Activity concentrations of  $^{40}\text{K}$  in  $\text{Bq kg}^{-1}$  from polygon survey (140 m) (Swiss)



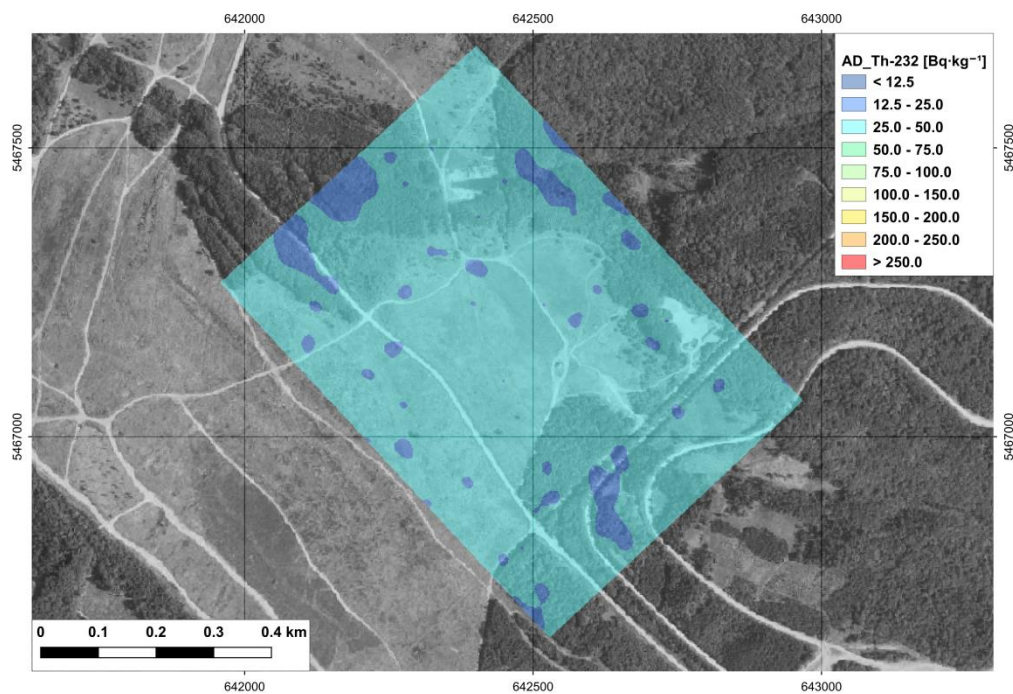
created in QGIS, background map: Orthophoto of the Czech Republic, Czech Office for Surveying, Mapping and Cadastre - ČÚZK, (CC BY)

Fig. 31 Activity concentrations of  $^{238}\text{U}$  in  $\text{Bq kg}^{-1}$  from polygon survey (70 m) (Swiss)



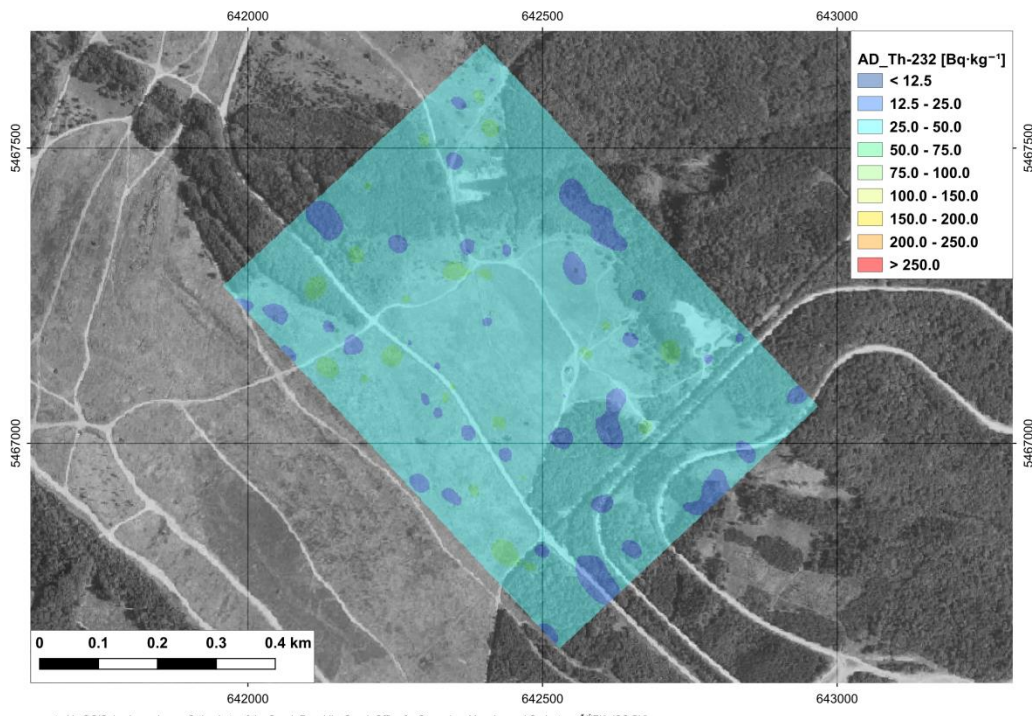
created in QGIS, background map: Orthophoto of the Czech Republic, Czech Office for Surveying, Mapping and Cadastre - ČÚZK, (CC BY)

Fig. 32 Activity concentrations of  $^{238}\text{U}$  in  $\text{Bq kg}^{-1}$  from polygon survey (140 m) (Swiss)



created in QGIS, background map: Orthophoto of the Czech Republic, Czech Office for Surveying, Mapping and Cadastre - ČÚZK, (CC BY)

Fig. 33 Activity concentrations of  $^{232}\text{Th}$  in  $\text{Bq kg}^{-1}$  from polygon survey (70 m) (Swiss)



created in QGIS, background map: Orthophoto of the Czech Republic, Czech Office for Surveying, Mapping and Cadastre - ČÚZK, (CC BY)

Fig. 34 Activity concentrations of  $^{232}\text{Th}$  in  $\text{Bq kg}^{-1}$  from polygon survey (140 m) (Swiss)

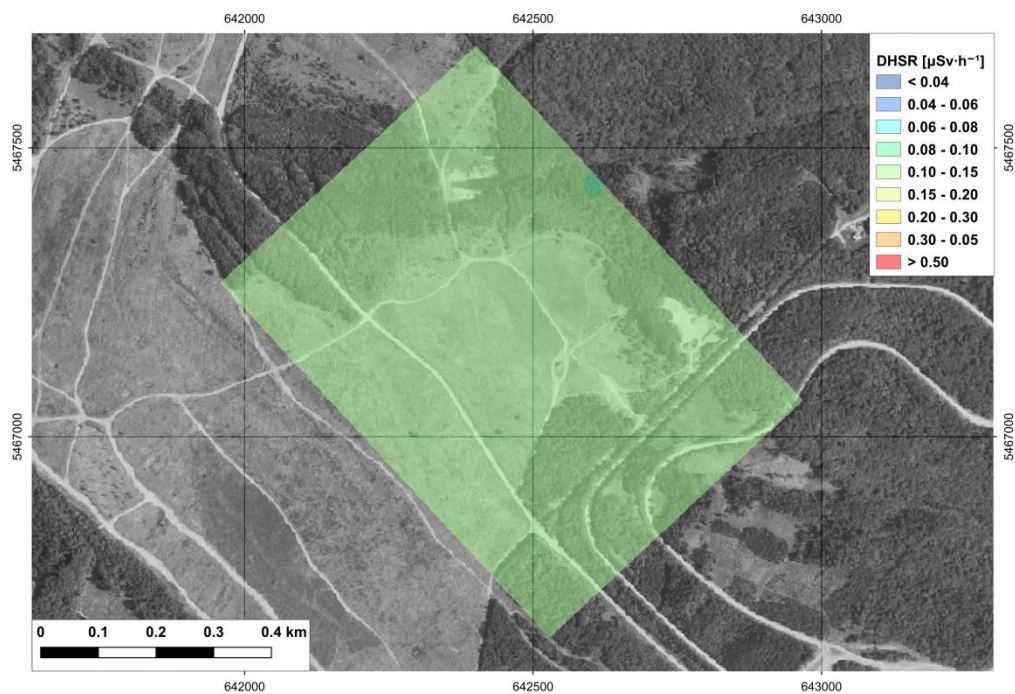


Fig. 35 Ambient dose equivalent rates in  $\mu\text{Sv}\cdot\text{h}^{-1}$  from polygon survey (70 m) (Swiss)

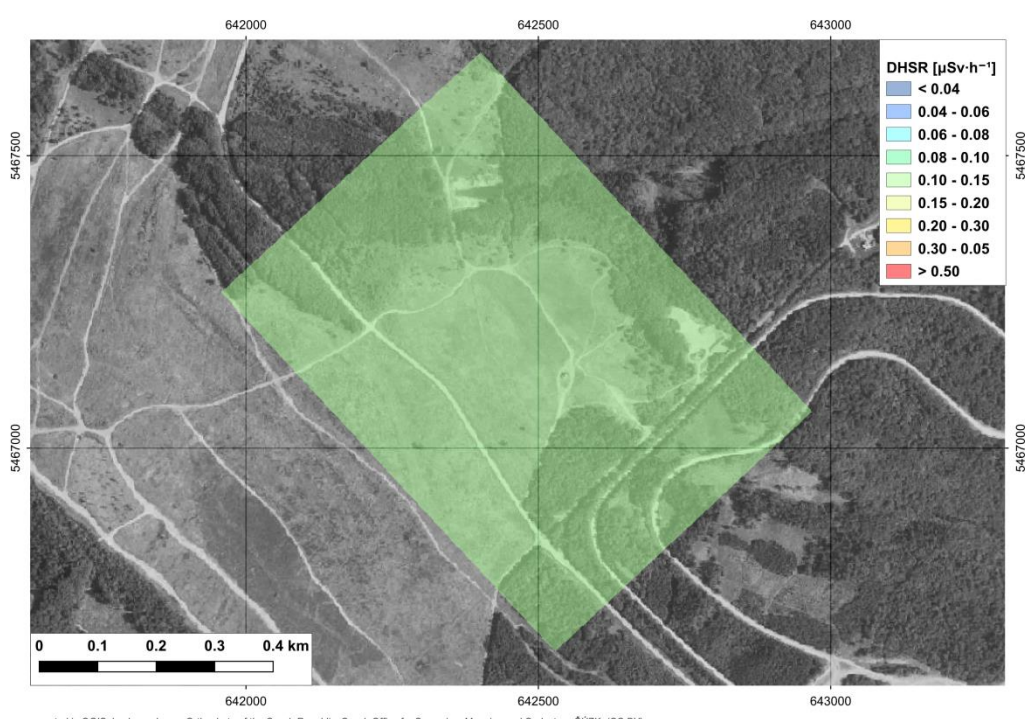


Fig. 36 Ambient dose equivalent rates in  $\mu\text{Sv}\cdot\text{h}^{-1}$  from polygon survey (140 m) (Swiss)

### 7.1.3 French team – polygon (70 m and 140 m)

Sixteen (16) flight lines were completed for both altitudes, with a spacing of approximately 40 meters at a speed of approximately 80 km/h. The duration of each flight was about 23 minutes.

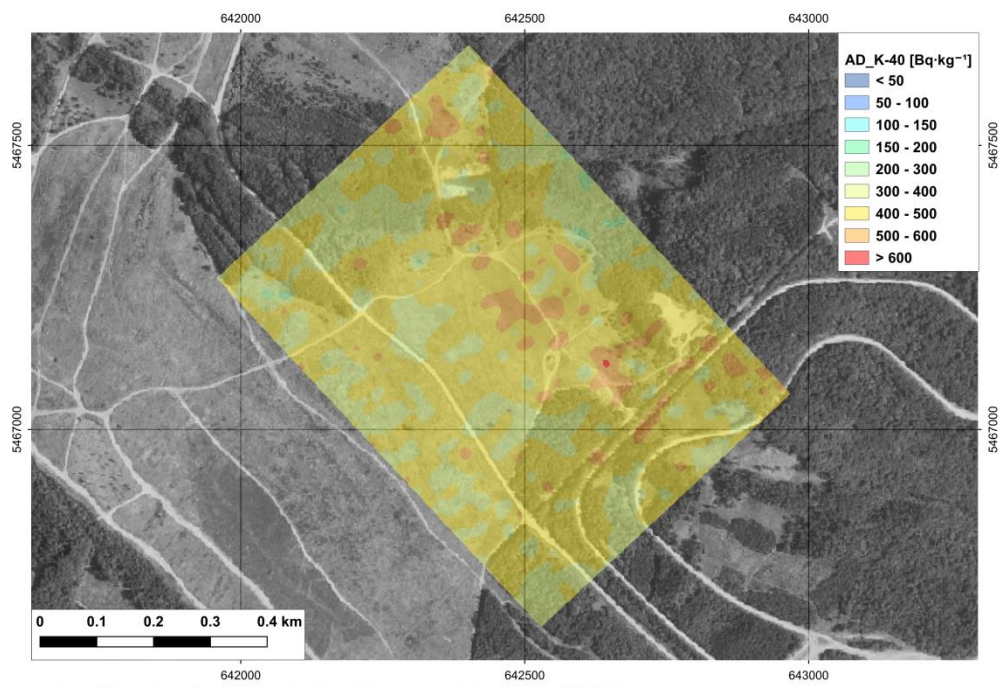


Fig. 37 Activity concentrations of  $^{40}\text{K}$  in  $\text{Bq kg}^{-1}$  from polygon survey (70 m) (French)

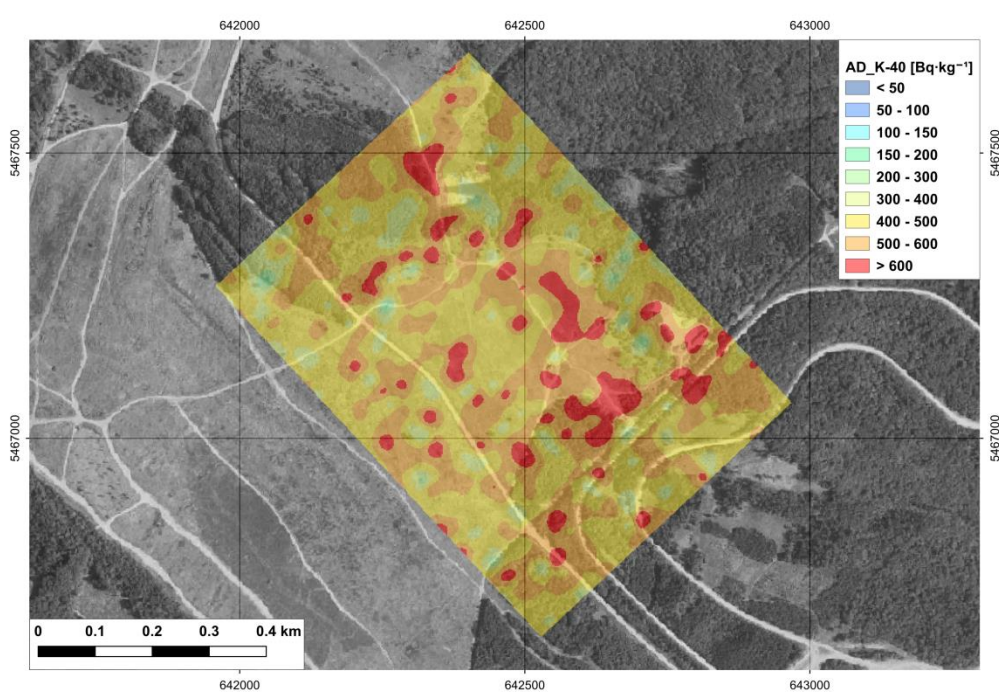
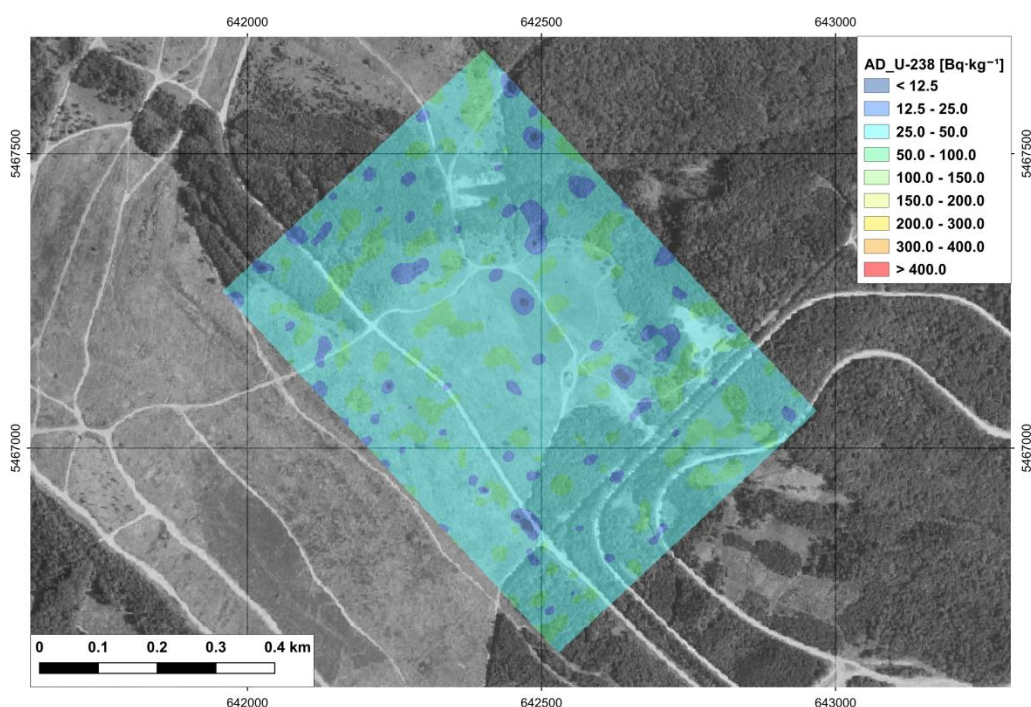
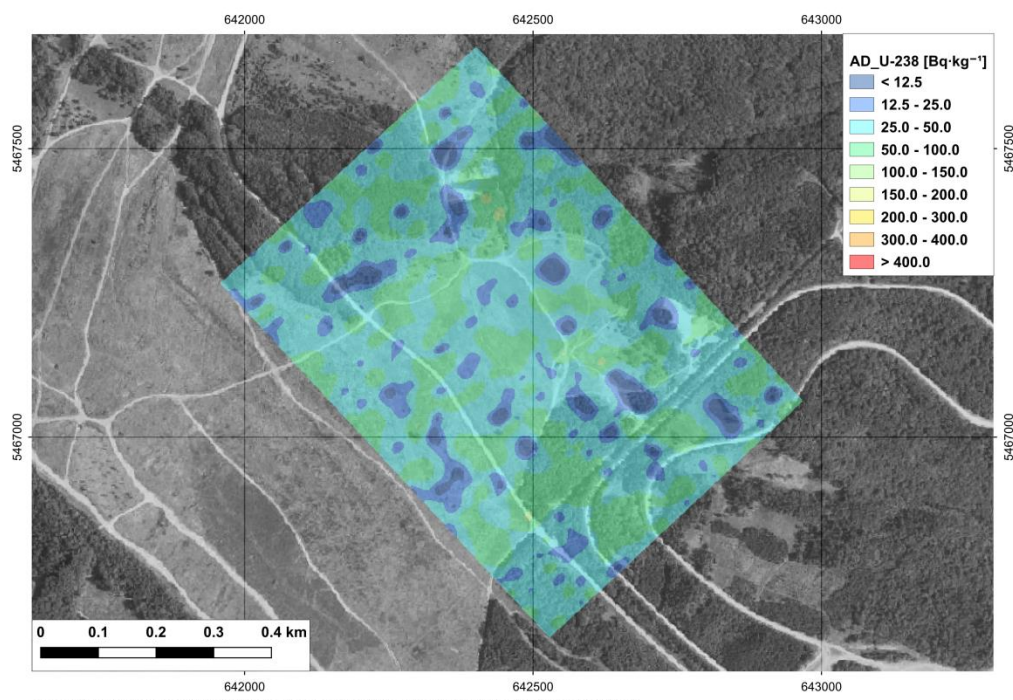


Fig. 38 Activity concentrations of  $^{40}\text{K}$  in  $\text{Bq kg}^{-1}$  from polygon survey (140 m) (French)



created in QGIS, background map: Orthophoto of the Czech Republic, Czech Office for Surveying, Mapping and Cadastre - ČÚZK, (CC BY)

Fig. 39 Activity concentrations of  $^{238}\text{U}$  in  $\text{Bq kg}^{-1}$  from polygon survey (70 m) (French)



created in QGIS, background map: Orthophoto of the Czech Republic, Czech Office for Surveying, Mapping and Cadastre - ČÚZK, (CC BY)

Fig. 40 Activity concentrations of  $^{238}\text{U}$  in  $\text{Bq kg}^{-1}$  from polygon survey (140 m) (French)

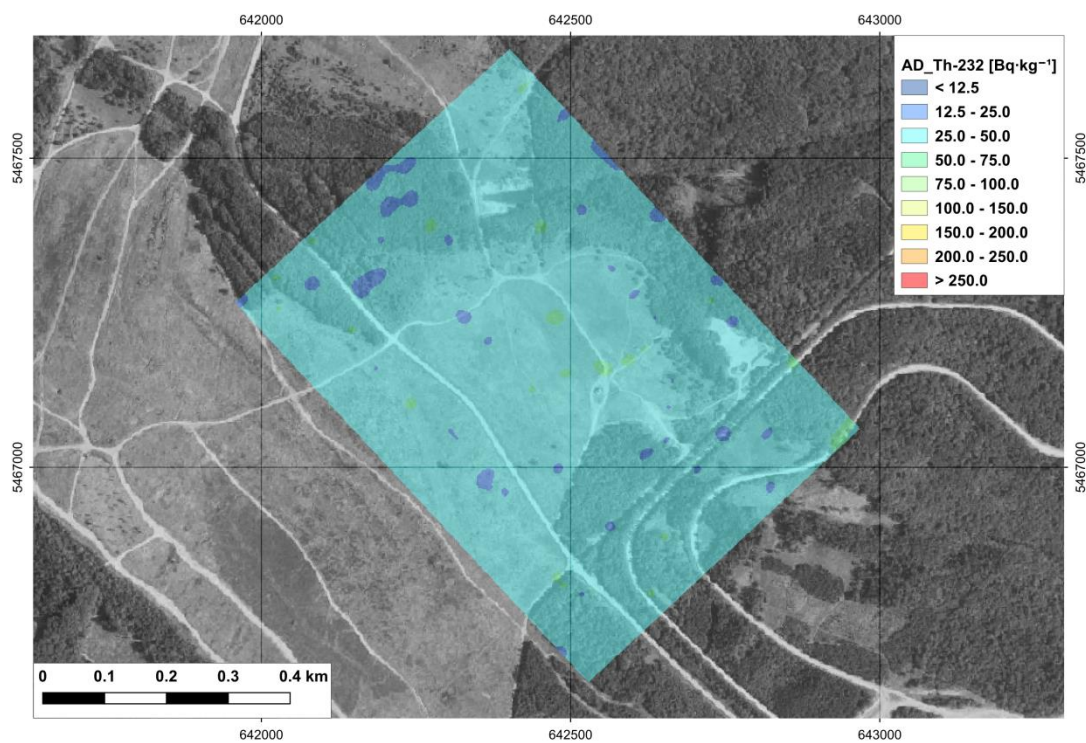


Fig. 41 Activity concentrations of  $^{232}\text{Th}$  in  $\text{Bq kg}^{-1}$  from polygon survey (70 m) (French)

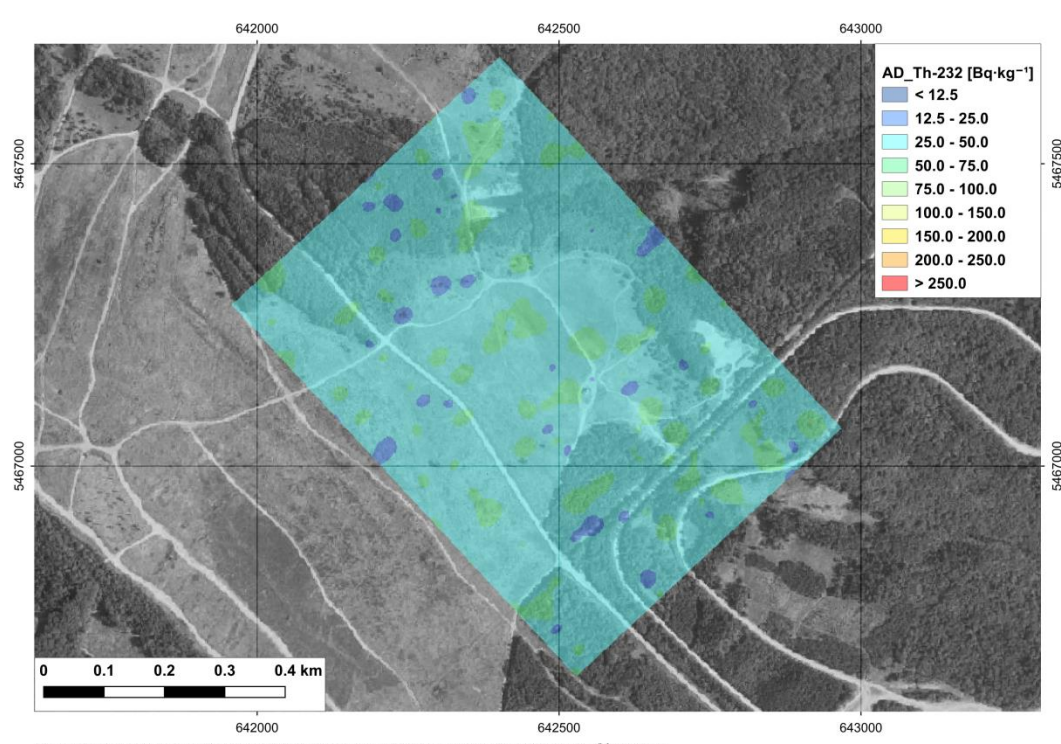


Fig. 42 Activity concentrations of  $^{232}\text{Th}$  in  $\text{Bq kg}^{-1}$  from polygon survey (140 m) (French)

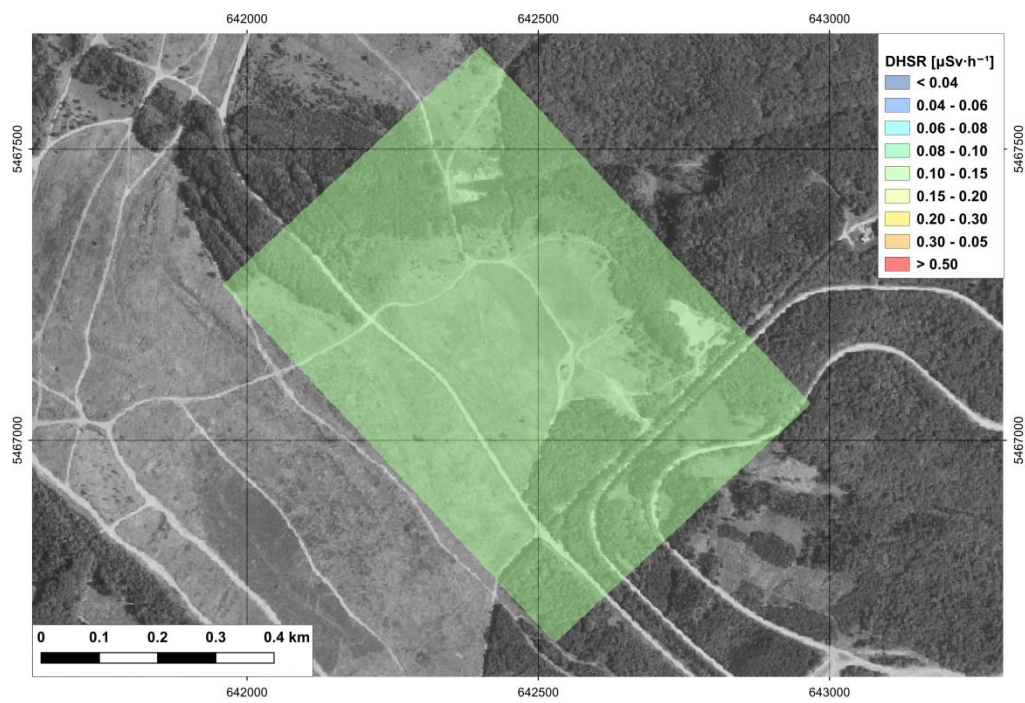


Fig. 43 Ambient dose equivalent rates in  $\mu\text{Sv}\text{ h}^{-1}$  from polygon survey (70 m) (French)

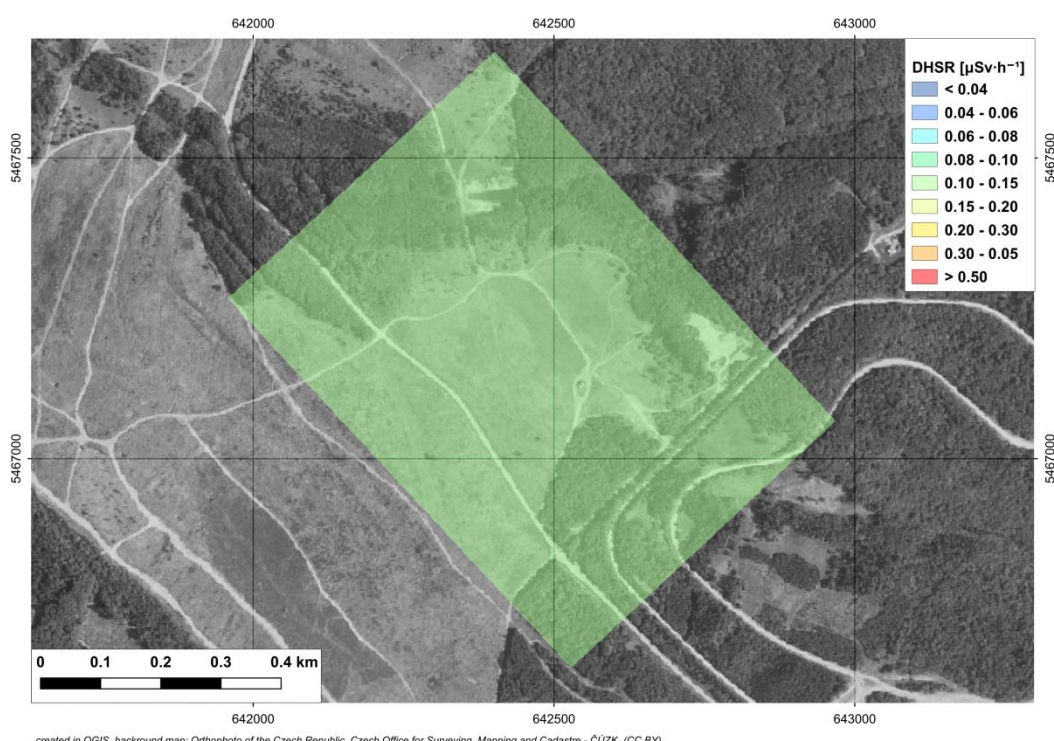


Fig. 44 Ambient dose equivalent rates in  $\mu\text{Sv}\text{ h}^{-1}$  from polygon survey (140 m) (French)

## 7.2 TASK I - B: HOVERING

This chapter presents the results of the airborne measurements over the reference area during hovering.

Tab. 6 Average values of Czech, Swiss and French team from 70 m and 140 m from hovering<sup>\*)\*\*)\*\*\*</sup>)

Qty	Unit							GROUND
		70 m	140 m	70 m	140 m	70 m	140 m	
DHSR	[ $\mu\text{Sv h}^{-1}$ ]	0.118 $\pm$ 0.005	0.124 $\pm$ 0.005	0.126 $\pm$ 0.005	0.121 $\pm$ 0.005	0.119 $\pm$ 0.001	0.120 $\pm$ 0.001	0.124 $\pm$ 0.008
$^{40}\text{K}$	[ $\text{Bq kg}^{-1}$ ]	570 $\pm$ 70	630 $\pm$ 120	380 $\pm$ 60	420 $\pm$ 80	460 $\pm$ 60	490 $\pm$ 90	599 $\pm$ 98
$^{238}\text{U}$	[ $\text{Bq kg}^{-1}$ ]	38 $\pm$ 15	39 $\pm$ 22	33 $\pm$ 15	37 $\pm$ 19	40 $\pm$ 13	47 $\pm$ 24	39 $\pm$ 7
$^{232}\text{Th}$	[ $\text{Bq kg}^{-1}$ ]	42 $\pm$ 8	44 $\pm$ 11	34 $\pm$ 7	36 $\pm$ 9	39 $\pm$ 8	44 $\pm$ 11	43 $\pm$ 7

<sup>\*)</sup> The final values including standard deviations provided by individual teams were rounded in accordance with the rules for result presentation.

<sup>\*\*) Offsets in Tab. 6 and error bars in Figs. 45 to 48 depict the standard deviations of all measurements over the reference area</sup>

<sup>\*\*\*)</sup> Bear in mind that the Swiss and French results of natural nuclides are presented as dry weight (AD<sub>—</sub>) while Czech results are given as wet weight (AW<sub>—</sub>) both in Tab. 6 and in all figures in this chapter.

The following figures show the results of the Czech, Swiss and French team for DHSR, activity concentrations of  $^{40}\text{K}$ , U-series and Th-series in  $\text{Bq kg}^{-1}$ . The surface activities of  $^{137}\text{Cs}$  are not presented because they were below minimum detectable activities (MDA).

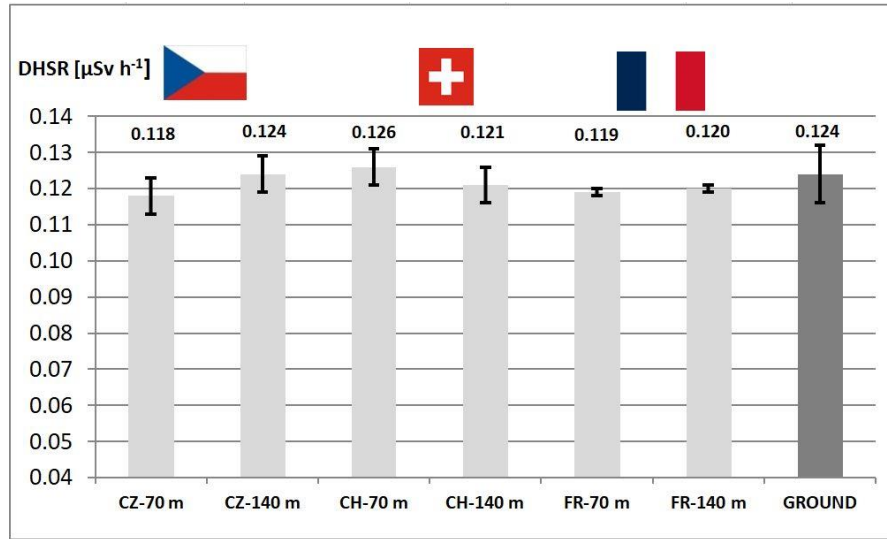


Fig. 45 Ambient dose equivalent rates in  $\mu\text{Sv h}^{-1}$  from hovering

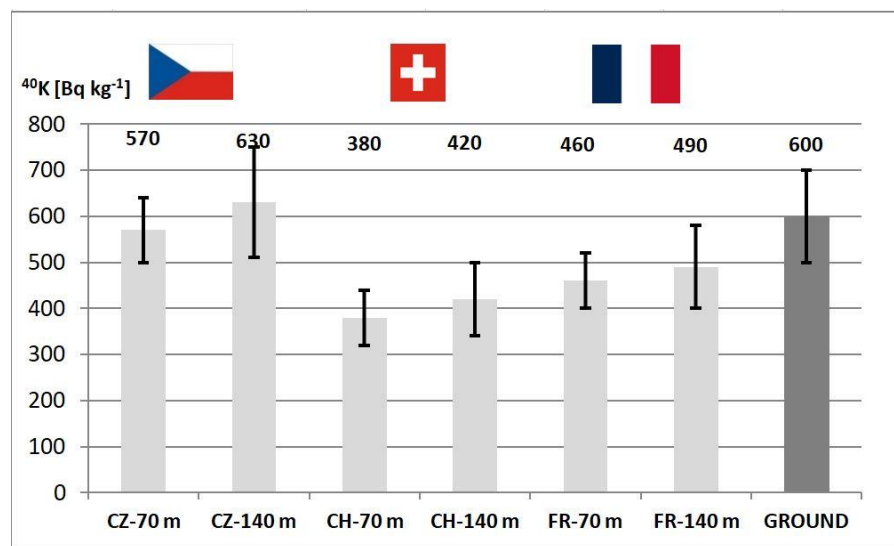


Fig. 46 Activity concentrations of  $^{40}\text{K}$  in Bq kg $^{-1}$

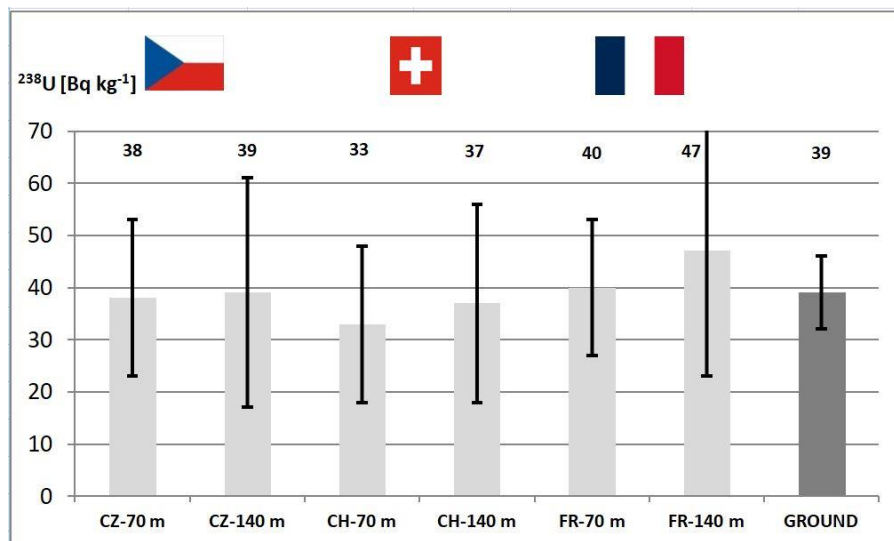


Fig. 47 Activity concentrations of  $^{238}\text{U}$  in Bq kg $^{-1}$

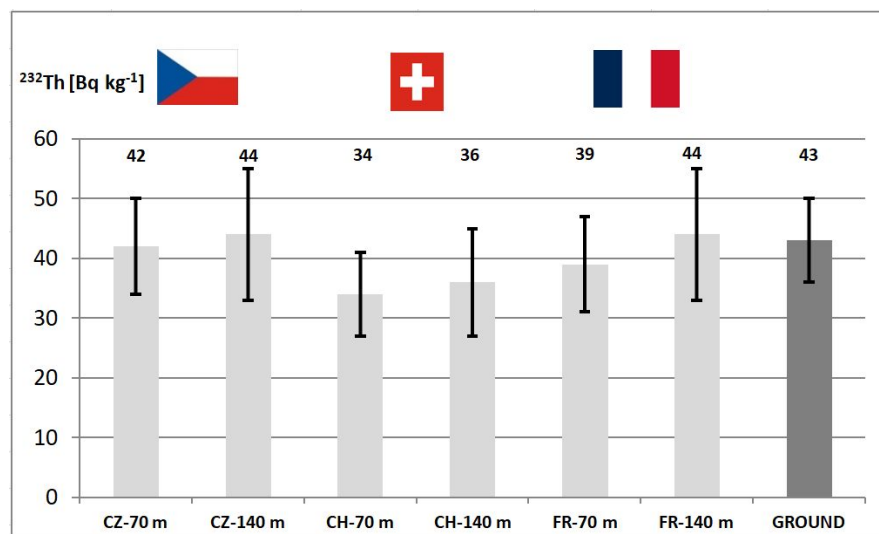


Fig. 48 Activity concentrations of  $^{232}\text{Th}$  in Bq kg $^{-1}$

## 7.3 TASK II - VYSOCINA

### 7.3.1 Czech team

To carry out the survey, a project with 16 lines was created in AGAMA, one line was approximately 7.5 km long and the total length of the flight on the polygon was 122 km. The flight speed was  $100 \text{ km.h}^{-1}$  and the flight height was 100 m above the ground. In the evaluation of  $^{137}\text{Cs}$ , a correction was made to remove the contribution of Compton radiation of  $^{238}\text{U}$  progeny in the  $^{137}\text{Cs}$  window. This method is not based on a physical principle, but only on a mathematical method assuming that there are no elevated  $^{137}\text{Cs}$  activities in the corrected region.

Because there are increased ambient dose equivalent rates at 1 m above ground in the uranium ore processing area, a plot of the  $\text{DHSR}_{\text{LOC}}$  ambient dose equivalent rate on board the helicopter versus time is also presented (Fig. 50).

Again, the Czech results are given as wet weight (AW\_) and  $^{137}\text{Cs}$  (AA\_Cs137) with model distribution according to [13].

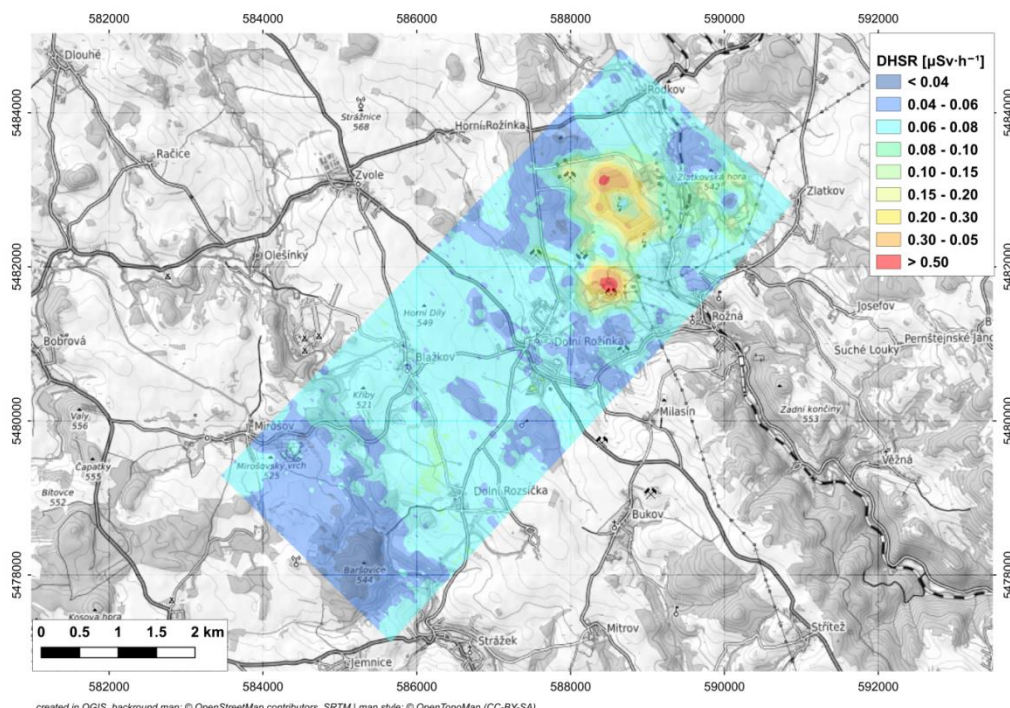
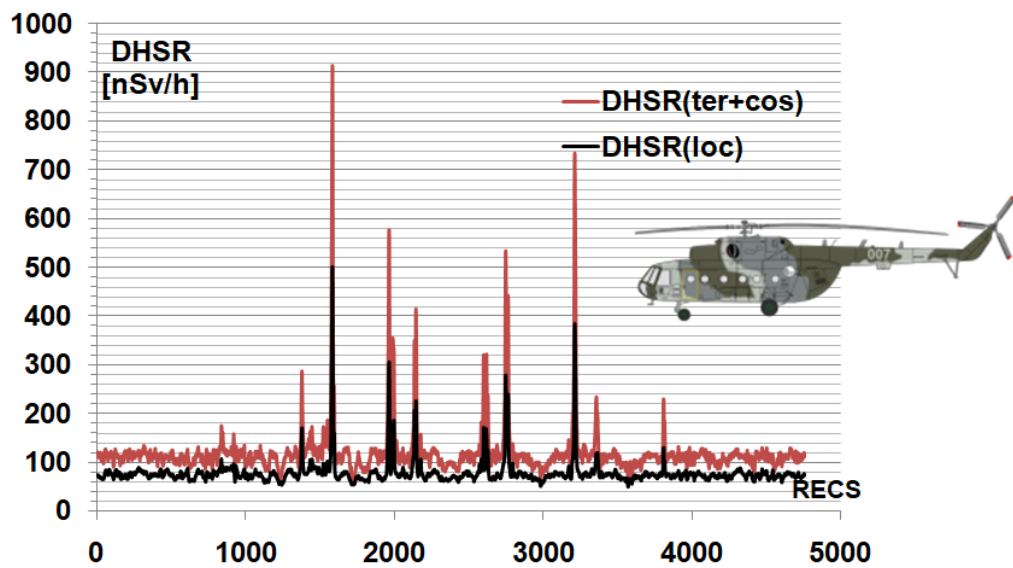


Fig. 49 Map of ambient dose equivalent rate DHSR at 1 m above ground

### DHSR on Mi-17 board + 1 m above ground



DHSR contribution from U-238 is prevailing  
DHSR contribution from Cs-137 is negligible (1 kBq/m<sup>2</sup> ~ 1 nGy/h)

Fig. 50 DHSR at 1 m above the ground and DHSR<sub>loc</sub> on board of the helicopter

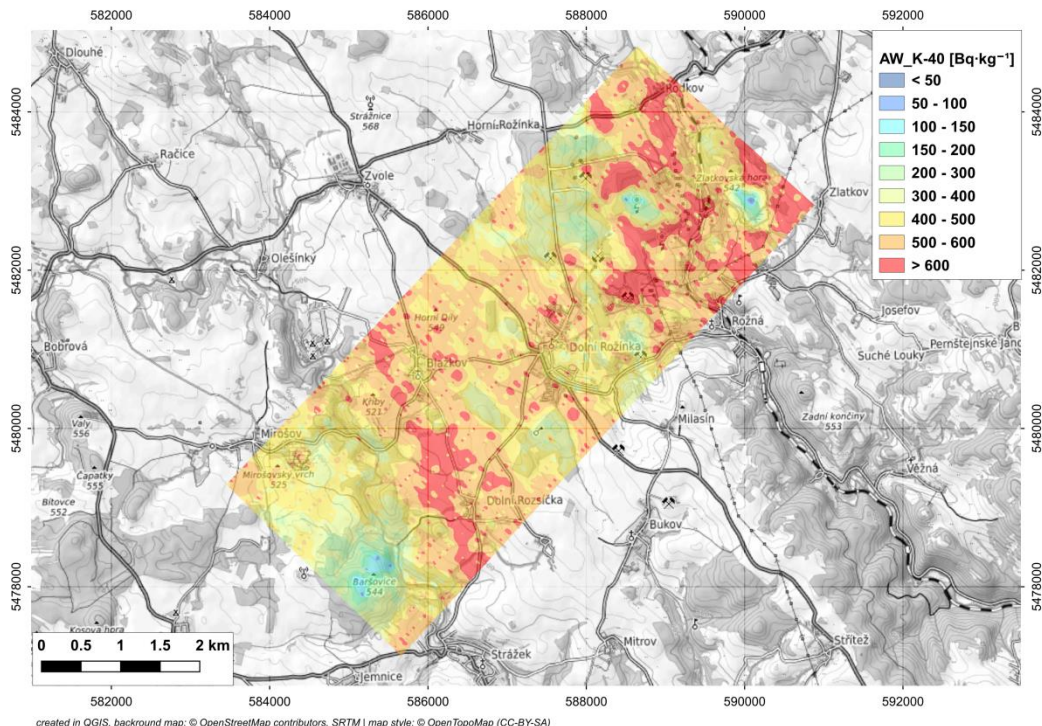


Fig. 51 Activity concentrations of  $^{40}\text{K}$  in  $\text{Bq kg}^{-1}$  from VYSOCINA polygon survey (Czech)

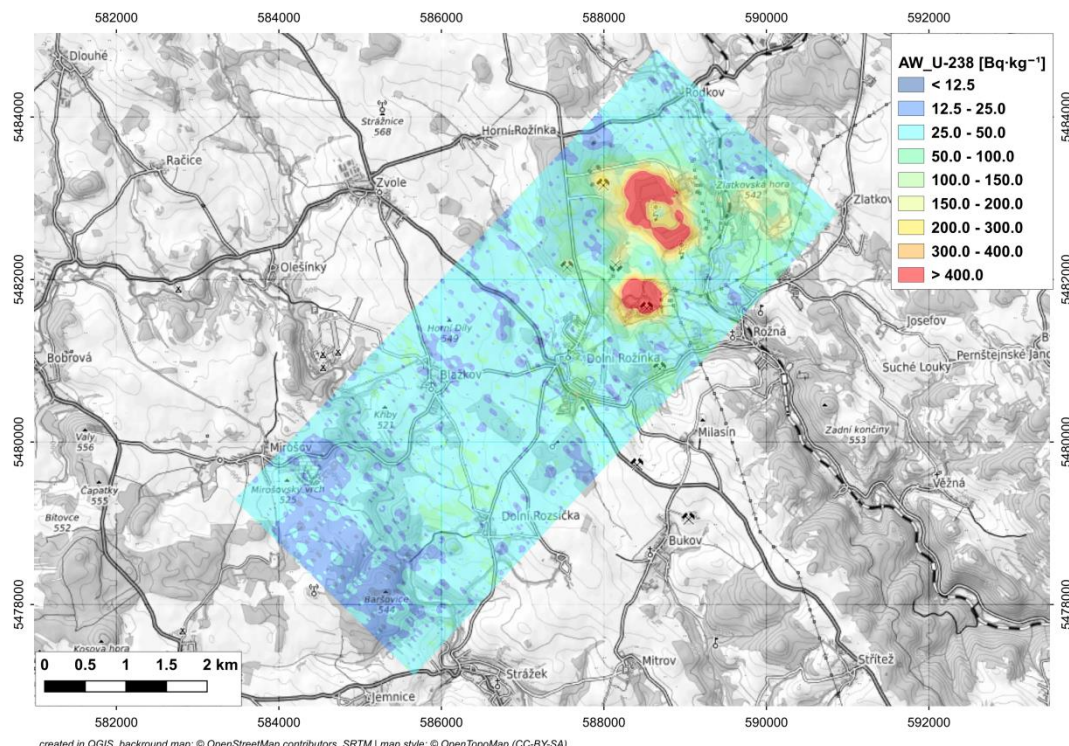


Fig. 52 Activity concentrations of  $^{238}\text{U}$  in  $\text{Bq kg}^{-1}$  from VYSOCINA polygon survey (Czech)

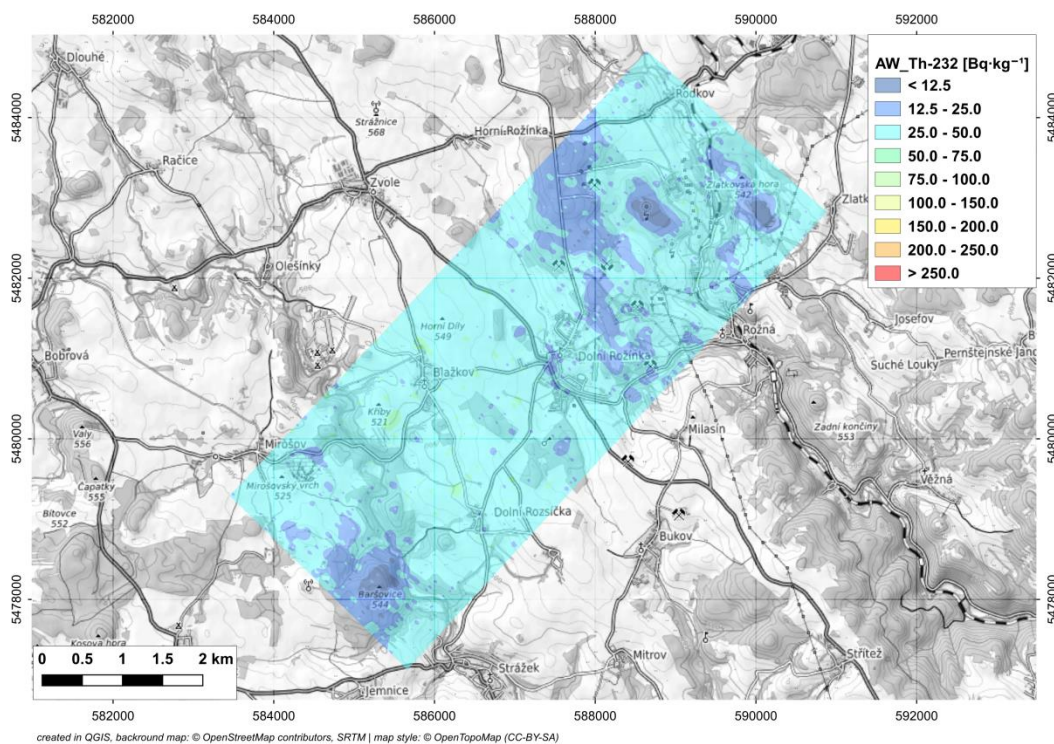


Fig. 53 Activity concentrations of  $^{232}\text{Th}$  in  $\text{Bq kg}^{-1}$  from VYSOCINA polygon survey (Czech)

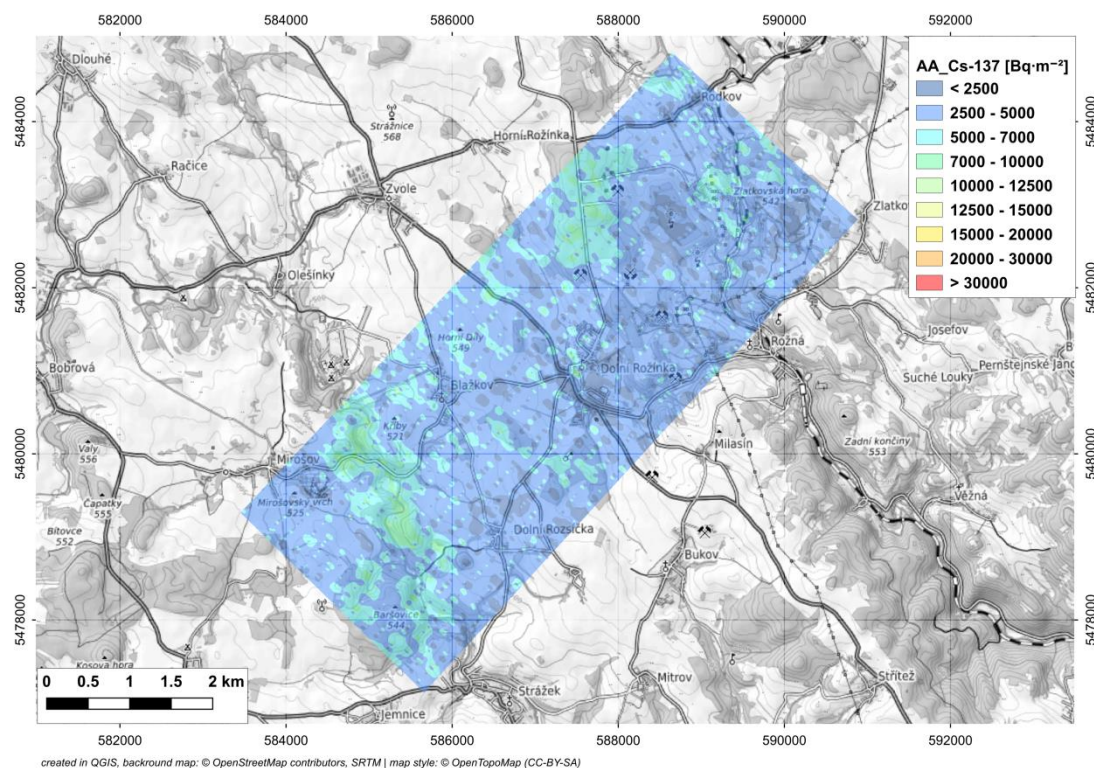


Fig. 54 Surface activity of  $^{137}\text{Cs}$  in  $\text{Bq m}^{-2}$  from VYSOCINA polygon survey (Czech)

### 7.3.2 Swiss team

The Swiss data show that, based on the measured raw data, an area of elevated uranium series activity and elevated DHSR was also detected at the uranium ore processing plant site. The Swiss team also detected an area in the vicinity of the Bobrůvka River with elevated  $^{137}\text{Cs}$ . However, the values of  $^{137}\text{Cs}$  shown in the map are higher than the ground values, this is caused by using original Swiss data with the model distribution  $\beta = 9.5 \text{ g cm}^{-2}$  [7].

It seems that there is another area with higher surface activity of  $^{137}\text{Cs}$  west of the uranium ore processing plant. An area with low content of  $^{40}\text{K}$  which is located on the Barošovice hill was also detected.

Again, the Swiss results are given as dry weight (AD\_) and  $^{137}\text{Cs}$  (AA\_Cs137) with model distribution according to [7].

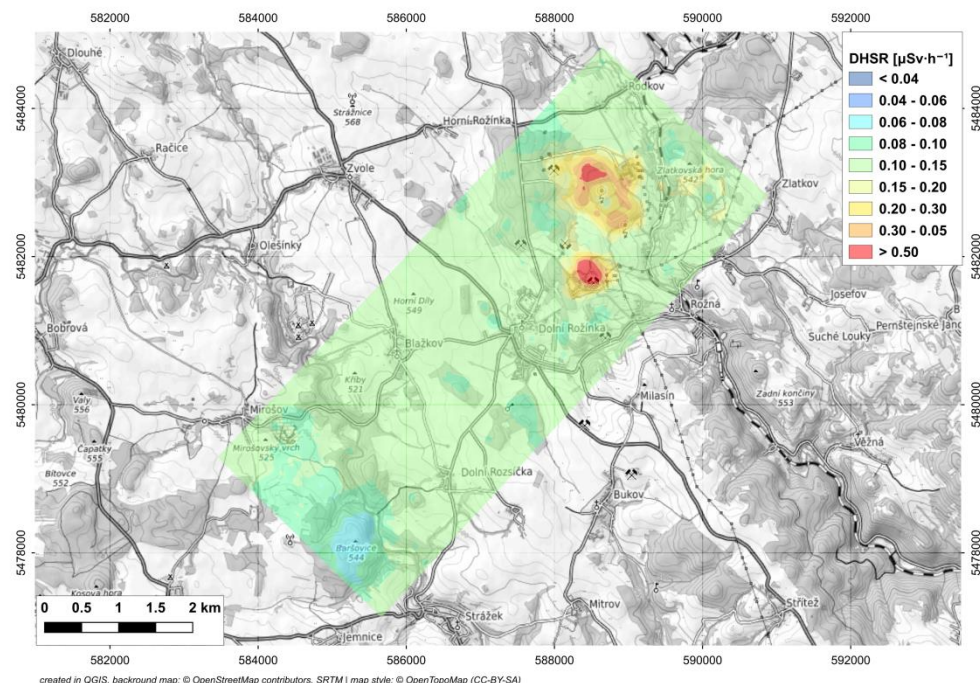


Fig. 55 Map of ambient dose equivalent rate DHSR at 1 m above ground (Swiss)

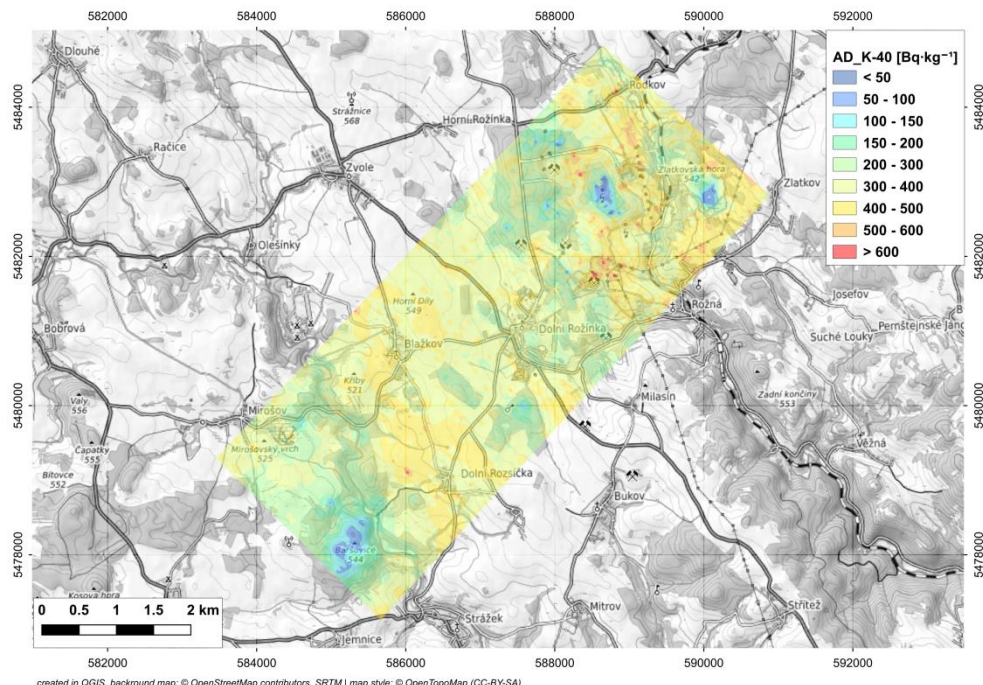


Fig. 56 Activity concentrations of  $^{40}\text{K}$  in  $\text{Bq kg}^{-1}$  from VYSOCINA polygon survey (Swiss)

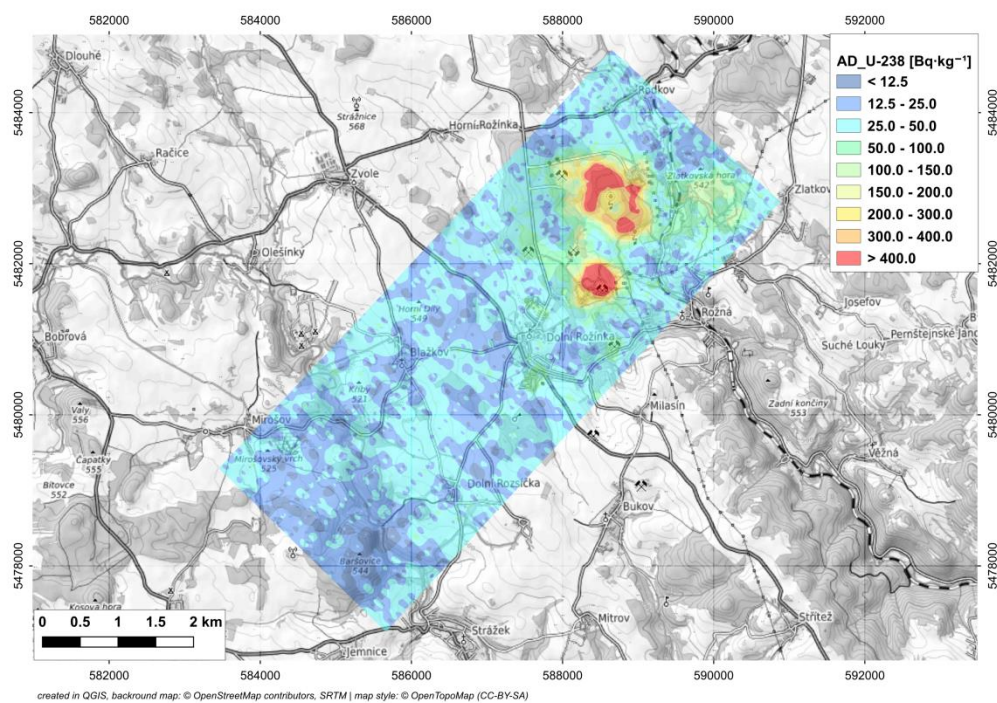


Fig. 57 Activity concentrations of  $^{238}\text{U}$  in  $\text{Bq kg}^{-1}$  from VYSOCINA polygon survey (Swiss)

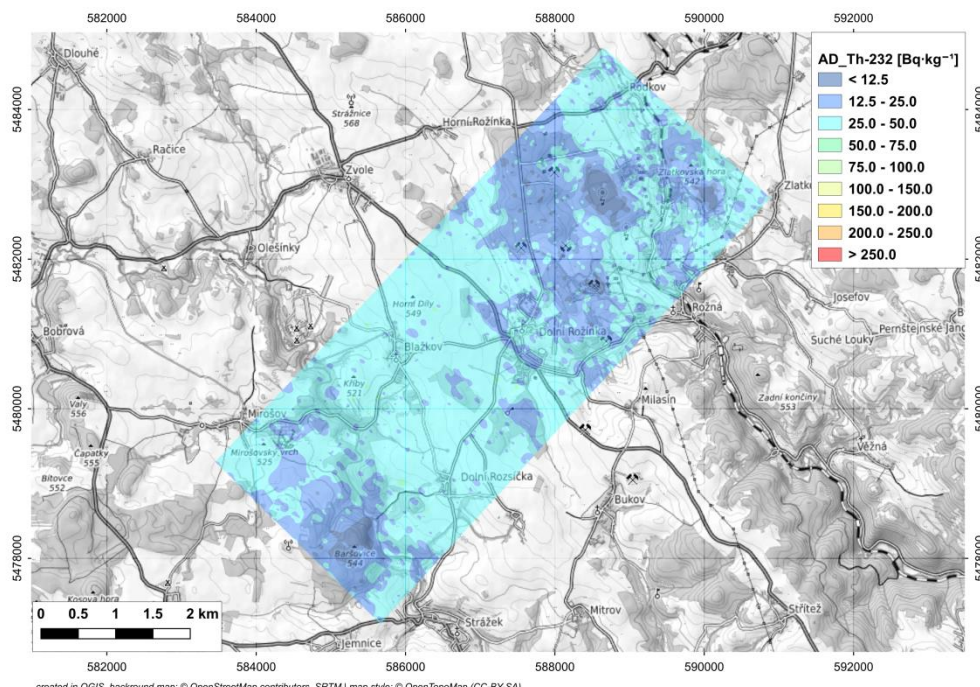


Fig. 58 Activity concentrations of  $^{232}\text{Th}$  in  $\text{Bq kg}^{-1}$  from VYSOCINA polygon survey (Swiss)

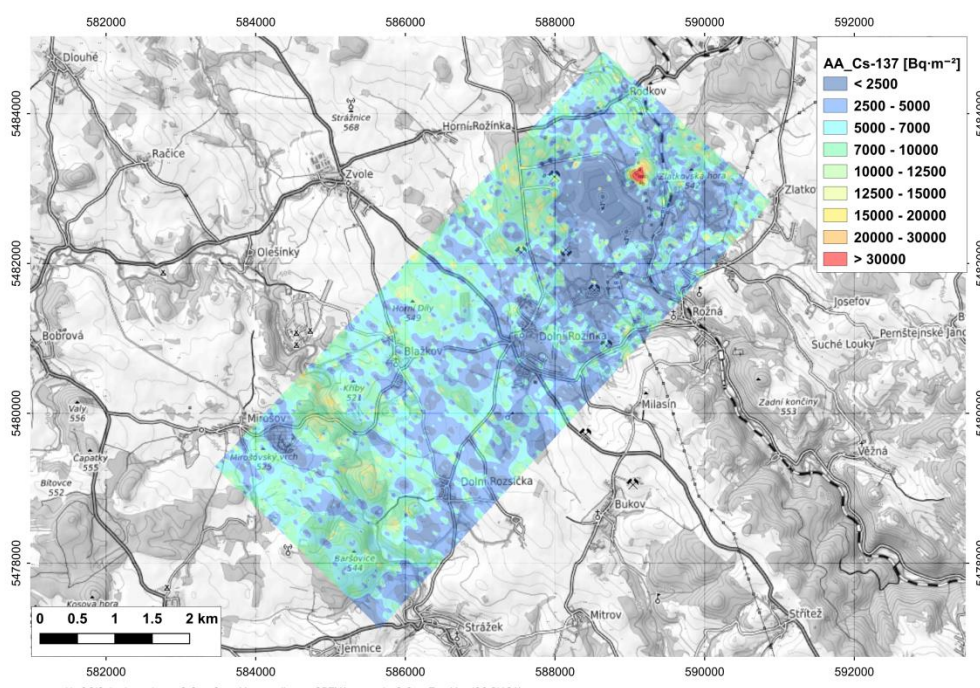


Fig. 59 Surface activity of  $^{137}\text{Cs}$  in  $\text{Bq m}^{-2}$  from VYSOCINA polygon survey (Swiss)

### 7.3.3 French team

The French data also show an area of elevated uranium series activity and elevated DHSR at the uranium ore processing plant site. The results of hot spots delineated in map are nearly identical for all three teams regarding DHSR and U-series. Again, the values of  $^{137}\text{Cs}$  of French team shown in the map are significantly higher than the ground values measured, this is again caused by using original French data with the model distribution  $\beta = 9.5 \text{ g.cm}^{-2}$  [7]. The original data were used in the  $^{137}\text{Cs}$  map as delivered by the French team with the original model distribution.

Also, a low content of  $^{40}\text{K}$  was detected on the Barošovice hill by the French team. The  $^{40}\text{K}$  values of Czech and French teams are higher than those of Swiss team. Regarding U-series and Th-series, the data in maps seem very similar.

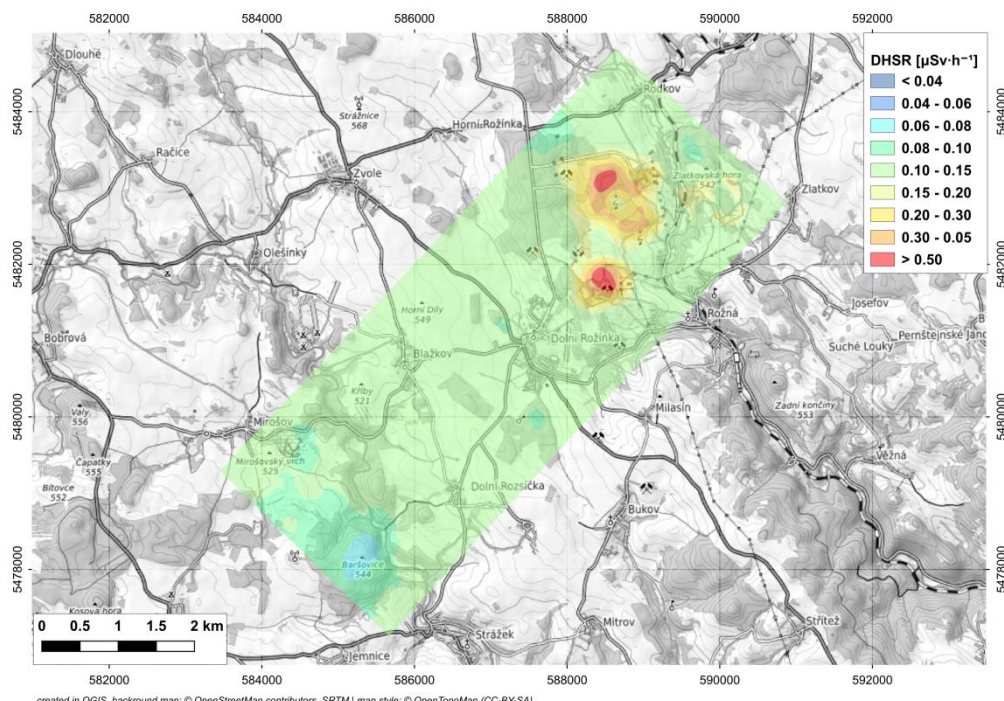


Fig. 60 Map of ambient dose equivalent rate DHSR at 1 m above ground (French)

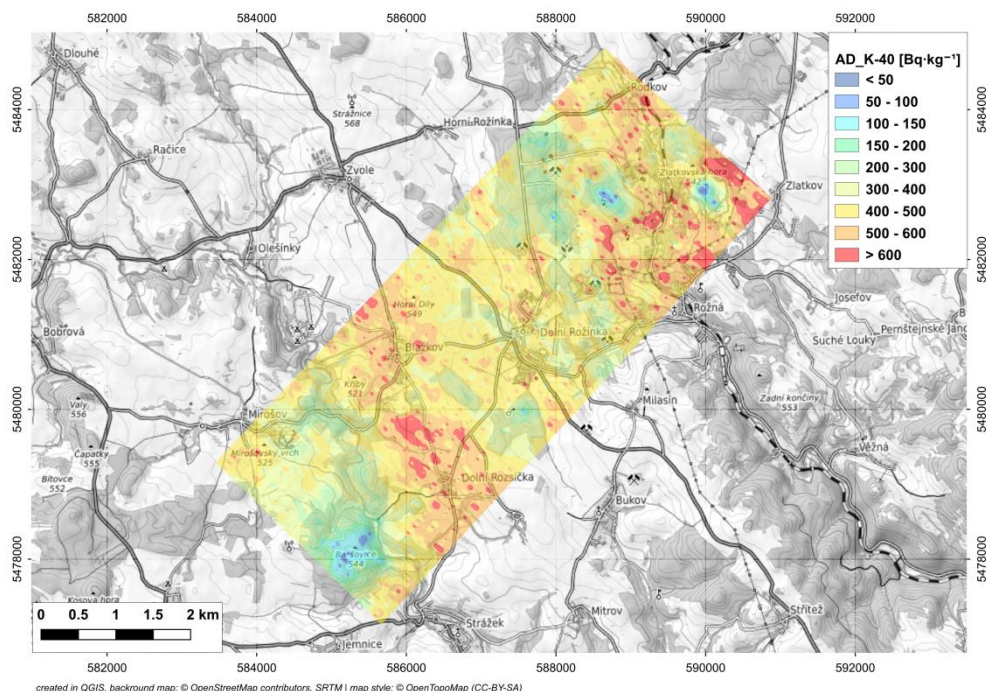


Fig. 61 Activity concentrations of  $^{40}\text{K}$  in  $\text{Bq kg}^{-1}$  from VYSOCINA polygon survey (French)

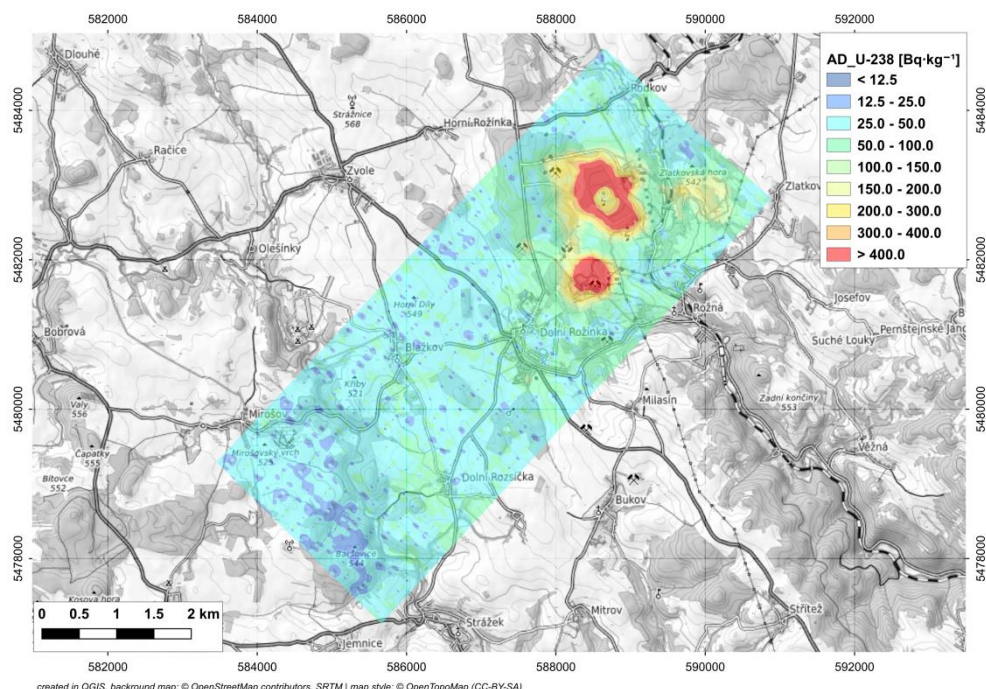


Fig. 62 Activity concentrations of  $^{238}\text{U}$  in  $\text{Bq kg}^{-1}$  from VYSOCINA polygon survey (French)

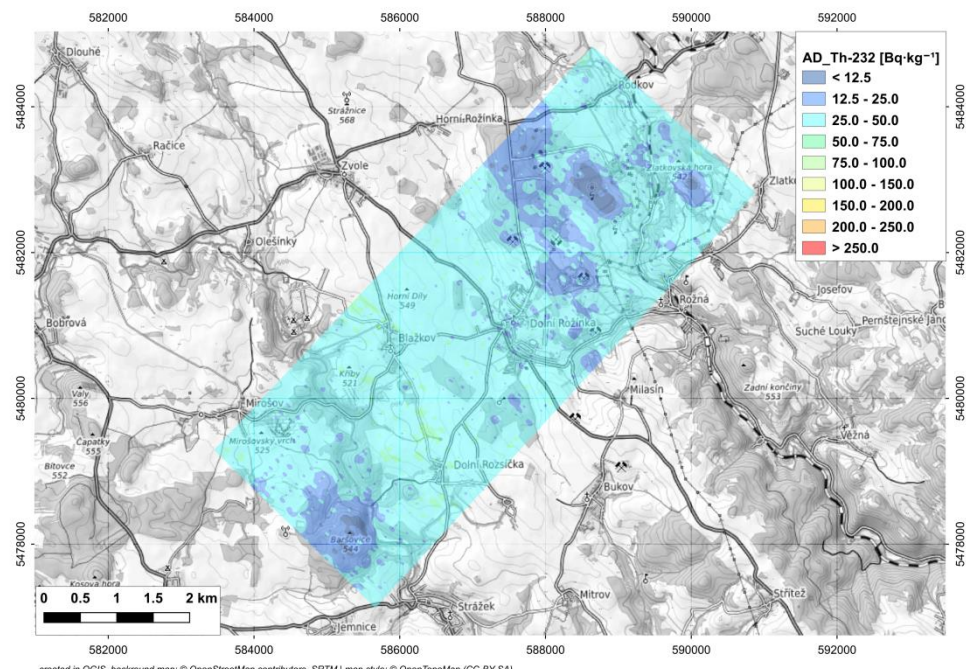


Fig. 63 Activity concentrations of  $^{232}\text{Th}$  in  $\text{Bq kg}^{-1}$  from VYSOCINA polygon survey (French)

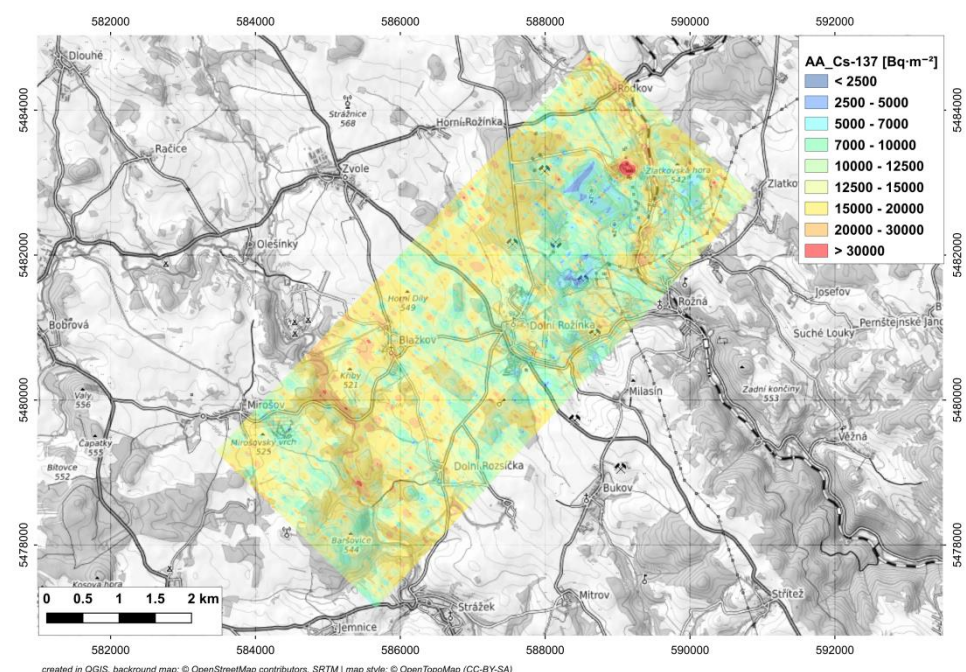


Fig. 64 Surface activity of  $^{137}\text{Cs}$  in  $\text{Bq m}^{-2}$  from VYSOCINA polygon survey (French)

## 7.4 TASK III - OPAVA REGION

Field measurements in the Czech Republic with *in-situ* gamma spectrometry have been performed since the 1980s and systematically since 1986 after the Chernobyl accident. Sampling at these sites and laboratory measurements have also been carried out. However, the results of *in-situ* measurements have always been presented as "wet" samples since we started with measurements in 1980s (AW\_ according to ERS notification). As far as  $^{137}\text{Cs}$  surface activities are concerned, we follow the  $^{137}\text{Cs}$  distribution model as published in [13]. This was used at the time of the Chernobyl accident. And we have used a model distribution of  $a/p = 0.206 \text{ cm}^2 \cdot \text{g}^{-1}$  [13] which corresponds to a relaxation length of  $r = 3 \text{ cm}$  for the model distribution of  $^{137}\text{Cs}$  [13] since late 1990s. It was also stated as such in all official reports.

The Swiss team uses, to assess the radiological situation in the helicopter as well as on the ground, the Mirion software. Based on a quick analysis done *a posteriori* by the Swiss team of the presented data compared with results from AGS\_CH software developed at PSI, they assume that all data provided during the campaign may actually be AD\_ and not AW\_. The relationship between the two quantities is:

$$AW = AD \times 0.83$$

As for  $^{137}\text{Cs}$ , the Swiss team uses a model distribution based on ICRU Report 53 [7] with a value of  $\beta = 9.5 \text{ g cm}^{-2}$ . The relation between the model distribution  $a/p=0.206 \text{ cm}^2 \text{ g}^{-1}$  and  $\beta = 9.5 \text{ g cm}^{-2}$  is given by a factor of 1.96.

The French team applied the same value for  $^{137}\text{Cs}$  model distribution as the Swiss team.

Because presented data of Czech team and Swiss and French teams somewhat differ in their meaning, we decided to present the data in the composite maps in the following way:

- To avoid any confusion, all DHSR data from all teams are presented in the composite map from the raw data without any changes.
- The Swiss data of K, U, Th activity concentration were converted from AD\_ to AW\_ values using the formula above. The surface activities of  $^{137}\text{Cs}$  of the Swiss team were converted to our model distribution and it means that the raw surface activities were divided by 1.96.
- The French raw data of natural nuclides (K, U-series and Th-series) were sent as AD\_ (dry) data and they were converted to AW\_(wet). Regarding  $^{137}\text{Cs}$ , significantly higher activities were obtained in original data. Because the original French activities of

natural nuclides converted from AD<sub>\_</sub> to AW<sub>\_</sub> were nearly similar to those of our data, we tried to apply our parameters (stripping ratios, sensitivities, etc.) for the extended window method with French raw data. We calculated <sup>137</sup>Cs surface activities for the distribution model of a/p = 0.206 cm<sup>2</sup> g<sup>-1</sup>. Finally, the original French results converted from AD<sub>\_</sub> to AW<sub>\_</sub> were used in the composite maps for natural nuclides while the results of <sup>137</sup>Cs surface activities from our extended windows method were presented in the map. In case of <sup>137</sup>Cs very good results were obtained, see Figs. 69 and 70 in comparison with the raw data in Fig. 68.

As part of this task, the three teams were provided with the GPS coordinates of the complete polygon on which the airborne radiation survey was to be carried out. Unlike the ARM17 (Switzerland) and AGC19 (France) exercises, the areas were not assigned to individual teams, but teams had to agree on logistics according to their capabilities, mainly fuel quantity and helicopter range. The result of logistic pre-flight briefing is presented in the following table, showing the number of lines, their spacing and ground speed agreed during the briefing. The allocation of the flight area is shown in the following figure. All teams selected the standard survey lines with spacing of 250 m on the individual sections of the Opava polygon.

Tab. 7 Airborne survey parameters of individual CZ, CH and FR teams

			
Number of lines	10	15	15
Spacing [m]	250	250	250
Ground speed [km h <sup>-1</sup> ]	150	150	180
Altitude AGL [m]	100	90	150

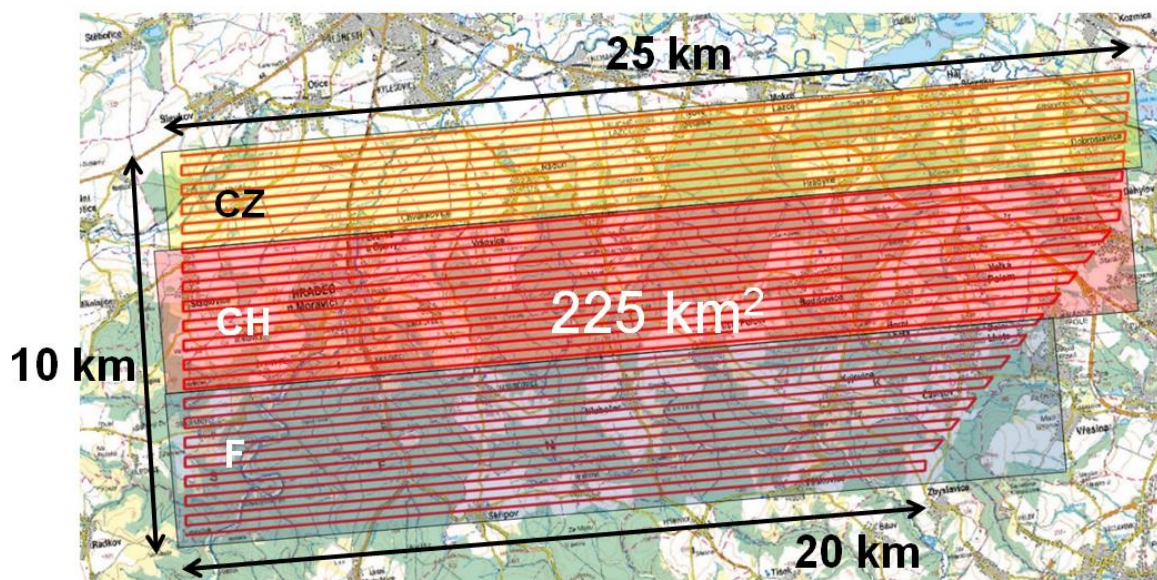


Fig. 65 Polygon distribution by individual teams CZ, CH and FR  
(total area  $225 \text{ km}^2$ ; source of map: Swiss team)

#### 7.4.1 Composite maps

As a result of the survey, the composite mapping documents showing DHSR, AW\_K40, AW\_U238, AW\_Th232 and AA\_Cs137 are available.

The first composite map shows the DHSR in  $\mu\text{Sv h}^{-1}$ . Two colour scales have been used for the display, the first corresponds to the standard requirement of Chapter 4.2. As the DHSR in this region is fairly constant, a second more detailed colour scale was also used for highlighting, Figs. 66 and 67. It can be seen in this map that the boundaries between the teams are essentially not visible and the areas relate well to each other.

#### 7.4.1.1 Ambient dose equivalent rate DHSR

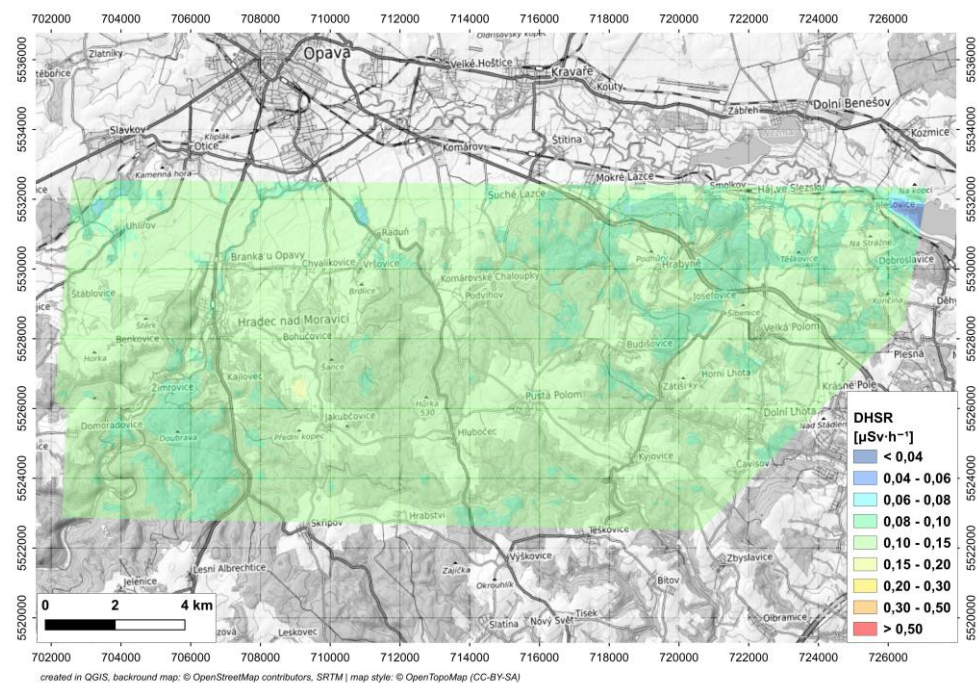


Fig. 66 DHSR ambient dose equivalent rate of CZ, CH and FR teams of complete polygon (standard colour scale)

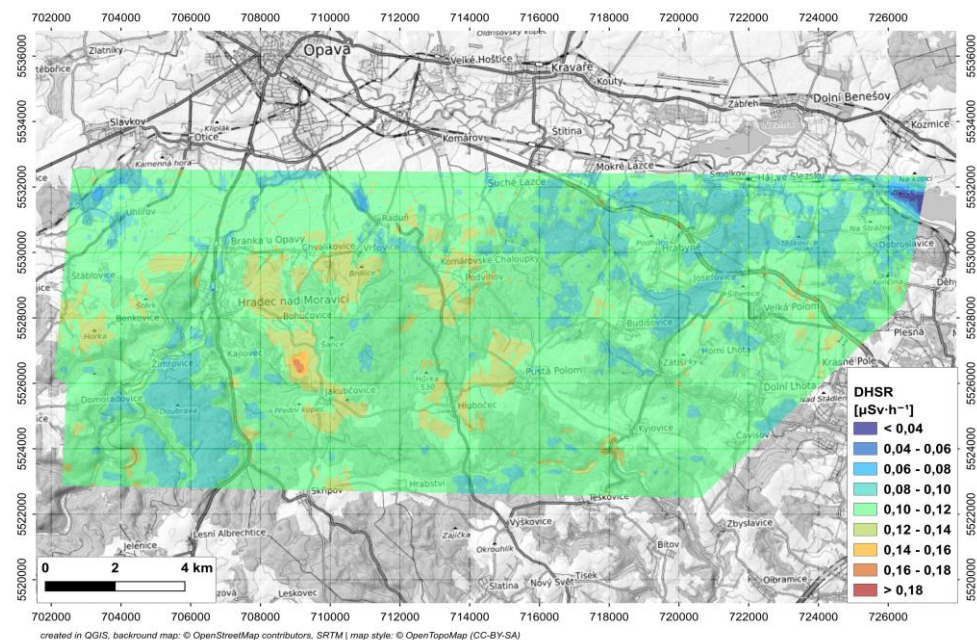


Fig. 67 DHSR - ambient dose equivalent rate of CZ, CH and FR teams of complete polygon (modified colour scale)

#### 7.4.1.2 Surface activities of $^{137}\text{Cs}$

Fig. 68 shows the original French and Swiss raw data of  $^{137}\text{Cs}$  surface activities using different model distribution in comparison with the Czech model distribution. Fig. 69 already depicts the modified data – points (see details in chapter 7.4). Fig. 70 displays the same data as in Fig. 69, but as a spline. Results of modified data seem very good.

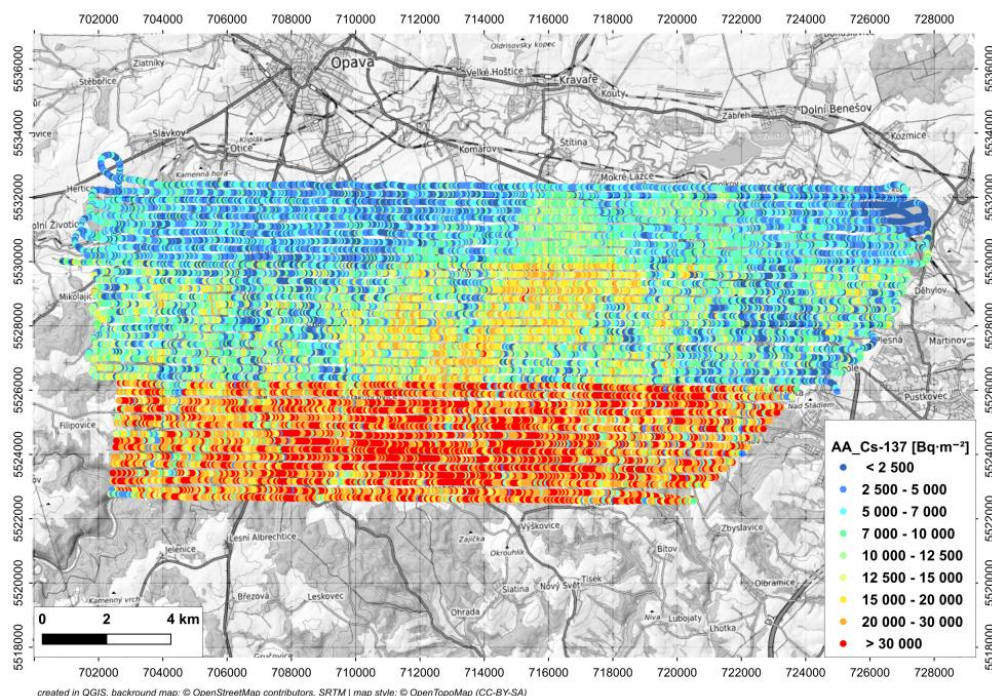


Fig. 68 Original Czech, Swiss and Swiss  $^{137}\text{Cs}$  surface activities

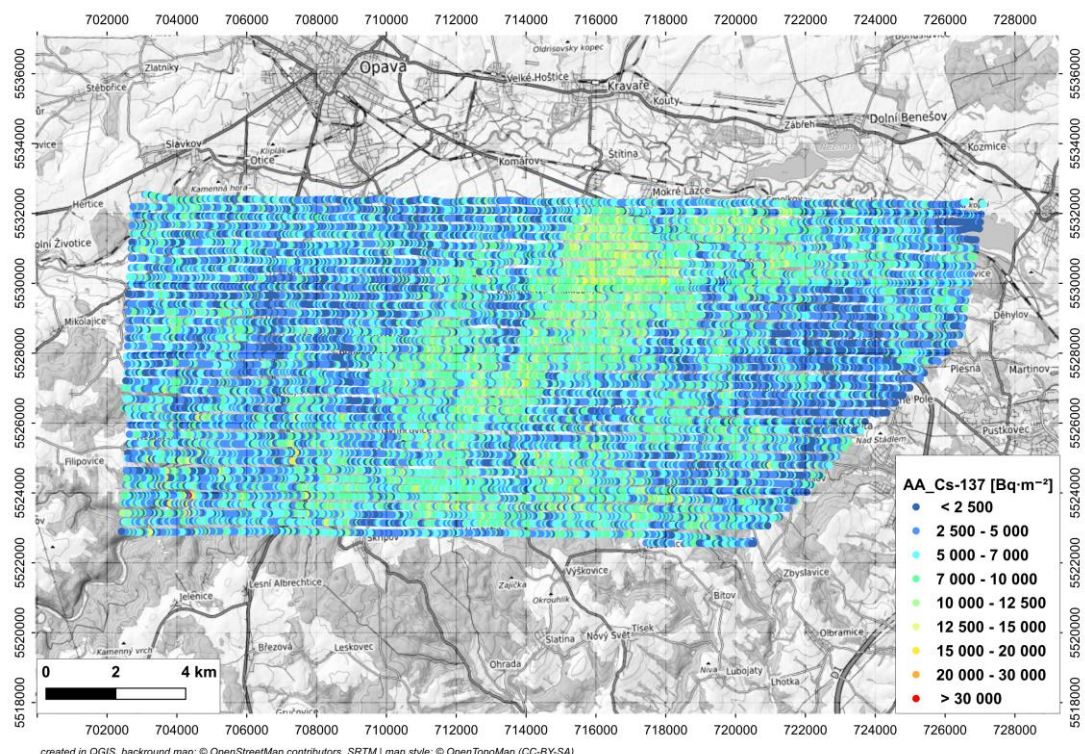


Fig. 69 Composite map from CZ, CH, FR modified data for surface activity  $^{137}\text{Cs}$  with distribution  $a/p = 0.206$  (points)

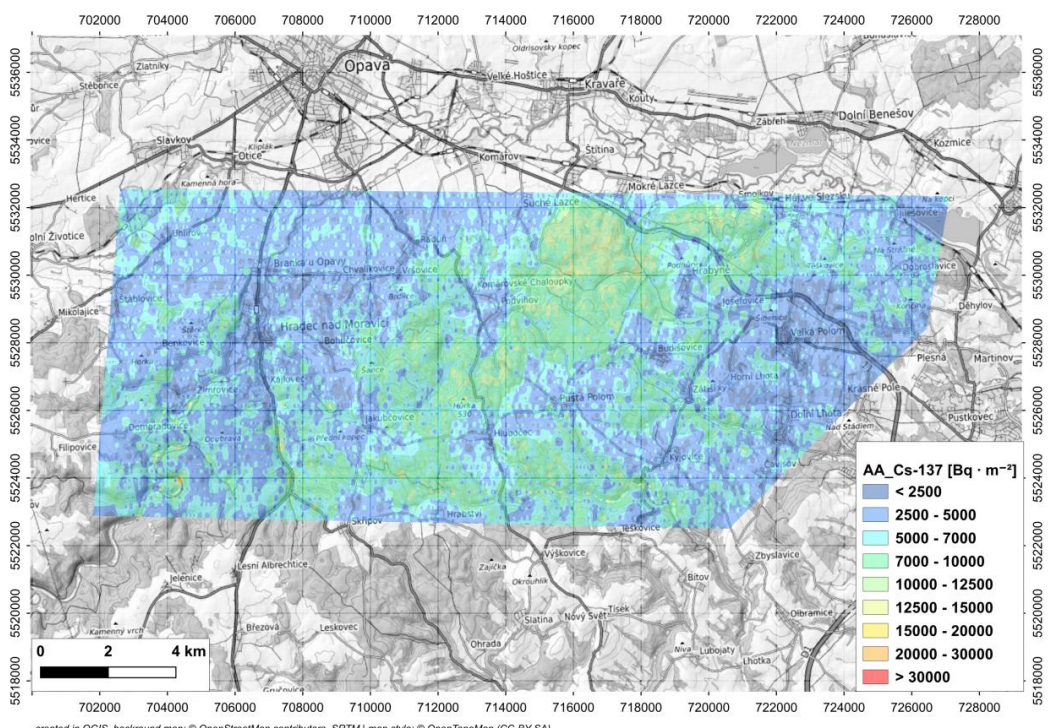


Fig. 70 Composite map for surface activity of  $^{137}\text{Cs}$  with distribution  $a/p = 0.206$  (spline)

#### 7.4.1.4 Activity concentrations of natural radionuclides

Figs. 71 to 73 show the composite spline maps of natural nuclides. The coincidence of results in the map is not so good. The differences in values between the teams are worth thinking about.

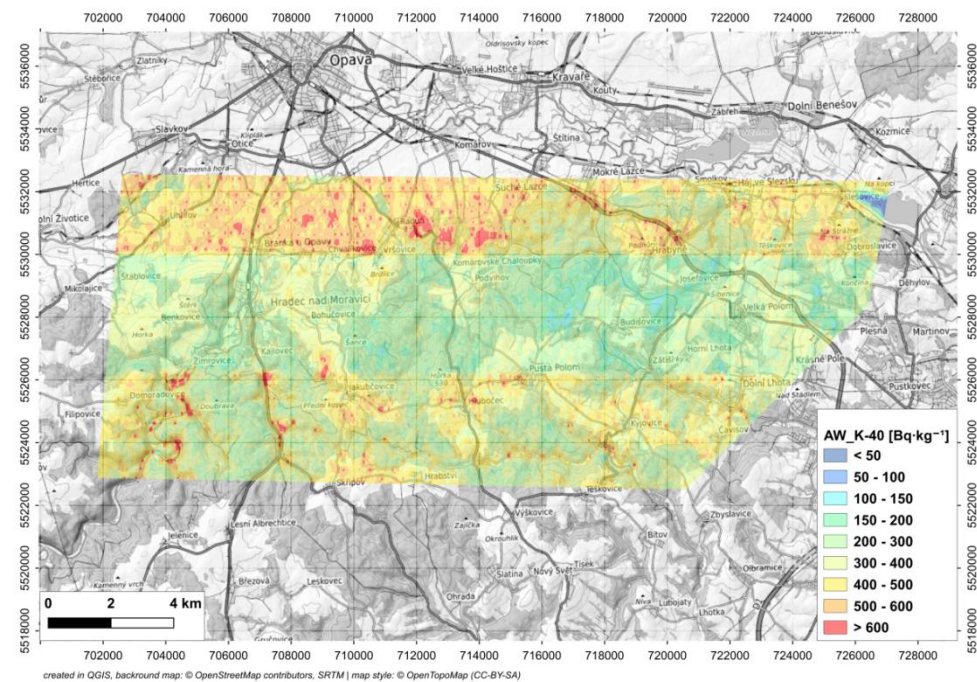


Fig. 71 Composite map for  $^{40}\text{K}$  in  $\text{Bq kg}^{-1}$  with homogeneous distribution

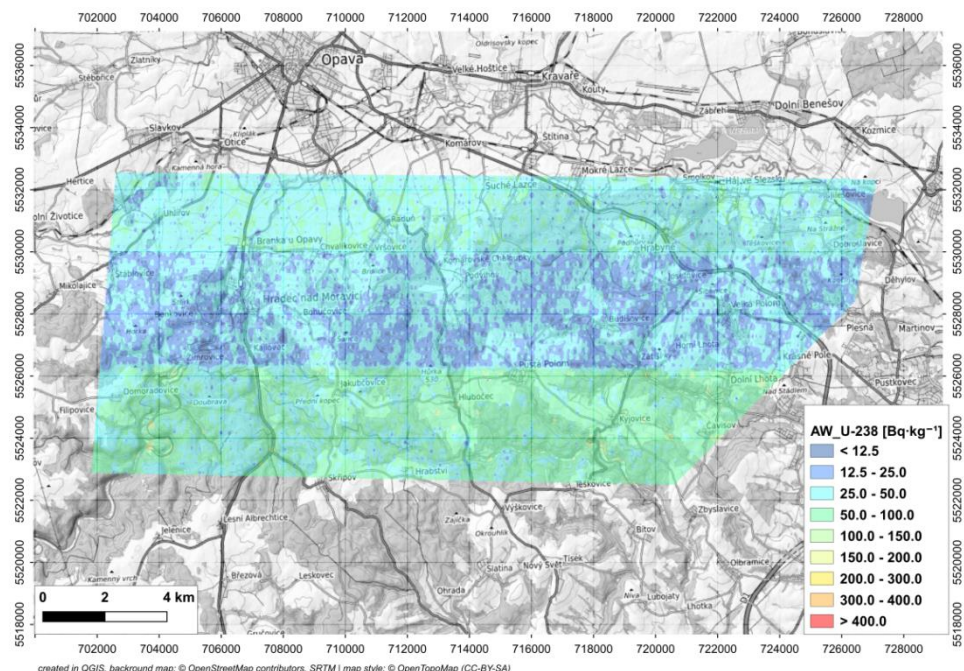


Fig. 72 Composite map for  $^{238}\text{U}$  in  $\text{Bq kg}^{-1}$  with homogeneous distribution

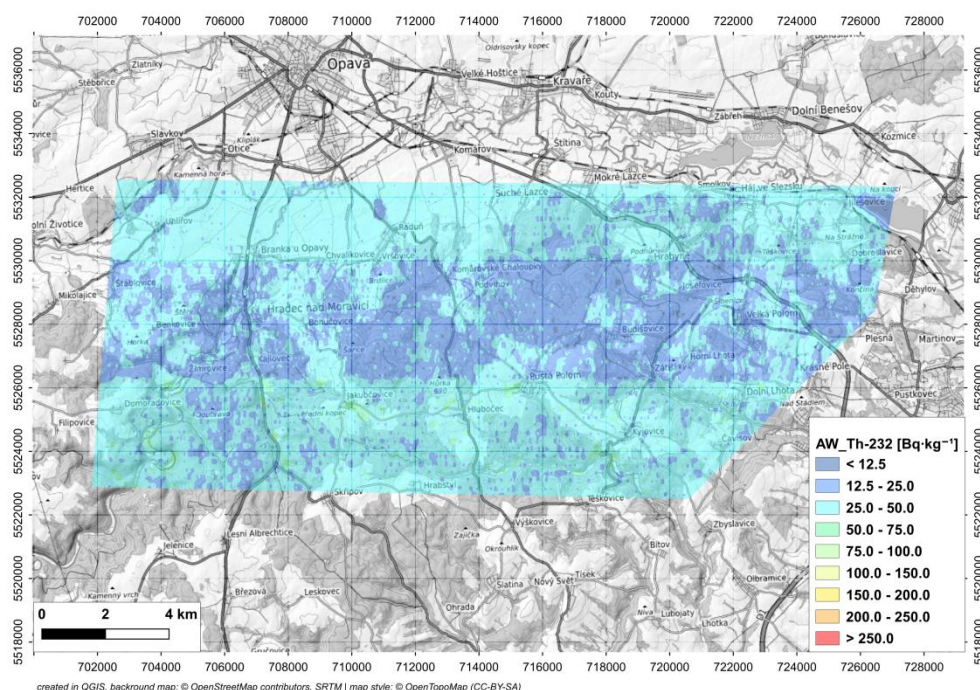


Fig. 73 Composite map for  $^{232}\text{Th}$  in  $\text{Bq kg}^{-1}$  with homogeneous distribution

## 7.5 TASK IV - LIBAVA

The following map shows the approximate locations of the sources in the Libava military training area. Sources of  $^{60}\text{Co}$ , activity of 6.2 GBq, and  $^{137}\text{Cs}$ , activity of 2.3 GBq, were located at location #1 and  $^{137}\text{Cs}$  with activity of 1.9 GBq and  $^{131}\text{I}$  with activity of 3.7 GBq were located at location #2. The precise GPS coordinates of two positions with hidden radioactive sources are given in Tab. 8. The sources were removed from the transport shielding containers and placed free a few meters apart from each other. Tab. 9 contains current rounded activities on June 5, 2024, the date of this survey.

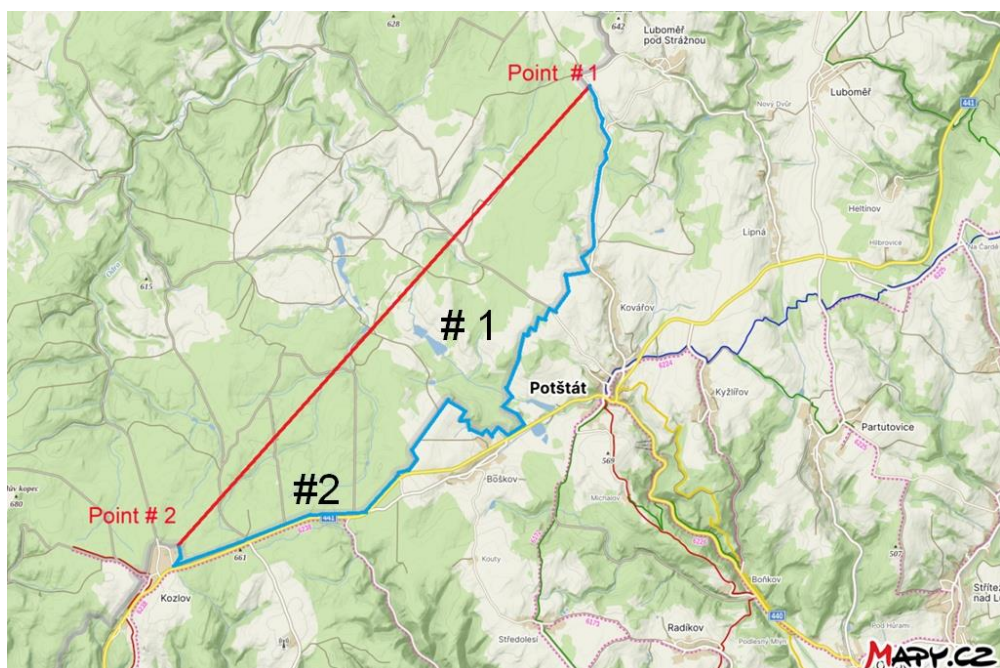


Fig. 74 Locations for the placement of sources in the military training area Libava

Tab. 8 GPS coordinates of positions #1 and #2

	Sources	Lat	Lon
Position #1	$^{60}\text{Co}$ , $^{137}\text{Cs}$	49.639651N	17.608139E
Position #2	$^{137}\text{Cs}$ , $^{131}\text{I}$	49.613586N	17.560126E

Tab. 9 Reference activities of the sources used as of 5.6.2024 at 12:00 CEST

Position #1		Position #2	
$^{60}\text{Co}$	6.2 GBq	$^{137}\text{Cs}$	1.9 GBq
$^{137}\text{Cs}$	2.3 GBq	$^{131}\text{I}$	3.7 GBq

### 7.5.1 Czech team

Both source locations were accurately determined and sources of  $^{137}\text{Cs}$  and  $^{60}\text{Co}$  were detected in position #1 and  $^{137}\text{Cs}$  and  $^{131}\text{I}$  in position #2. The following figure shows the flight lines and the flight along the boundary of the Libava VVP (Military Training Area). A point of border crossing (about 2 to 3 m) is indicated on the map. The GPS coordinates for positions #1 and #2 are shown in Tab. 10 along with the estimated activities determined by AGAMA using the NN-LSQ point source response functions. No corrections on the precise positions above the radioactive source were done, these are the raw data calculated by the AGAMA software package. Fig. 77 shows the waterfall spectra with individual nuclide detection.

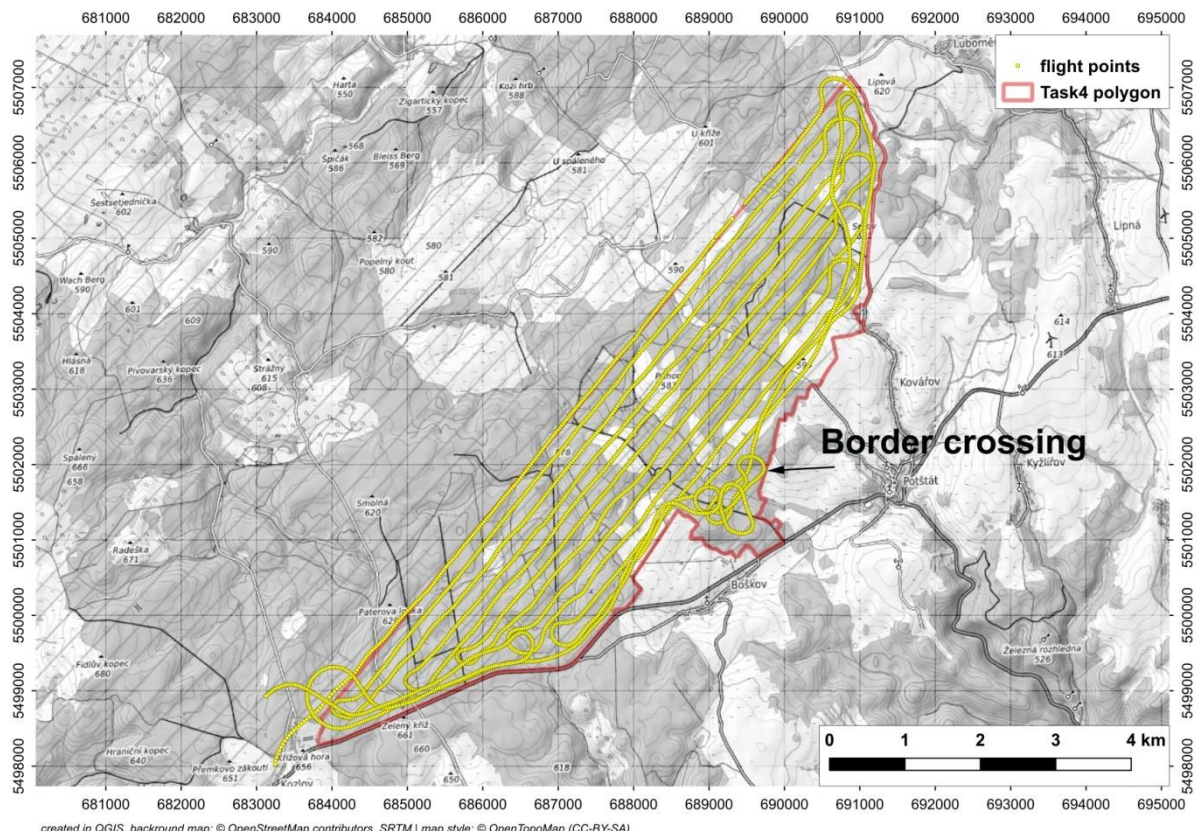


Fig. 75 Flight lines of the airborne survey of the Czech team

Tab. 10 GPS coordinates of positions #1 and #2, estimated activities of detected point sources

Position #1			Position #2		
$^{60}\text{Co}$	49.63981N	3.8 GBq	$^{137}\text{Cs}$	49.61371N	1.5 GBq
$^{137}\text{Cs}$	17.60786E	2.0 GBq	$^{131}\text{I}$	17.55995E	2.3 GBq

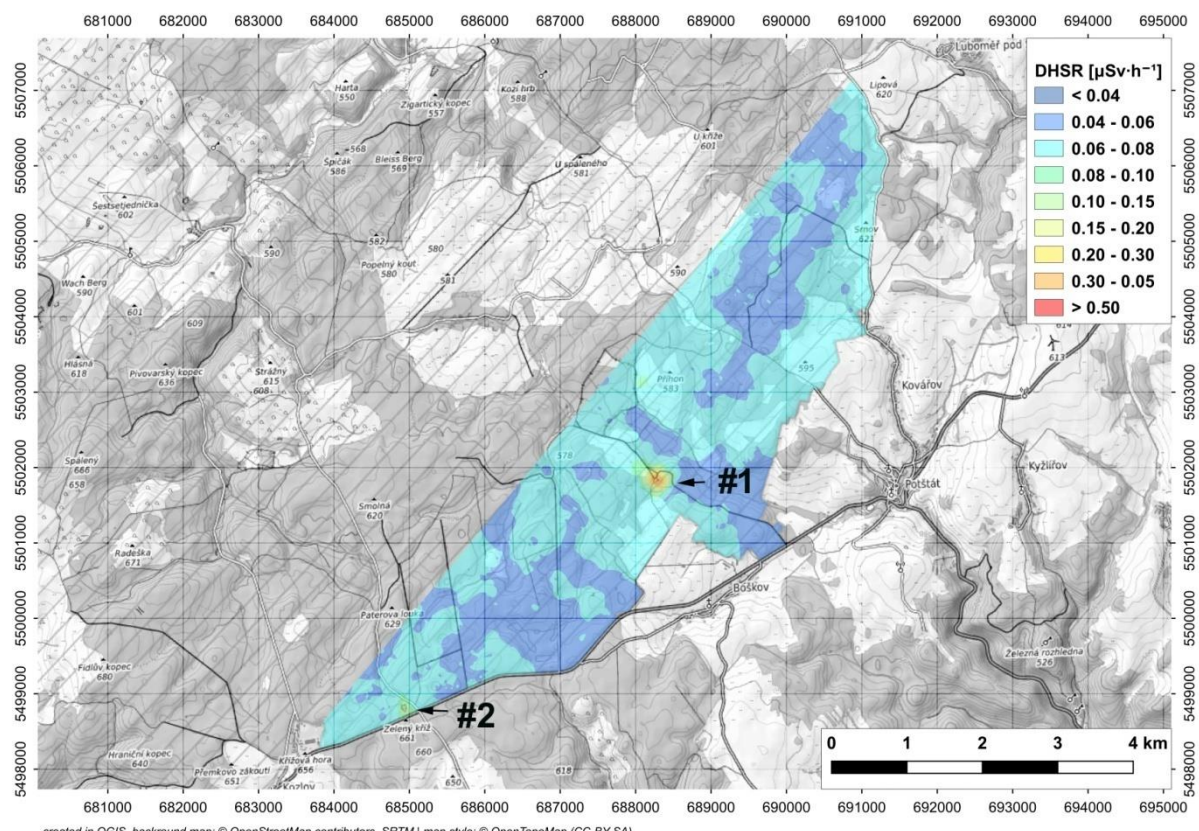


Fig. 76  $DHSR_{loc}$  on Mi-17 board

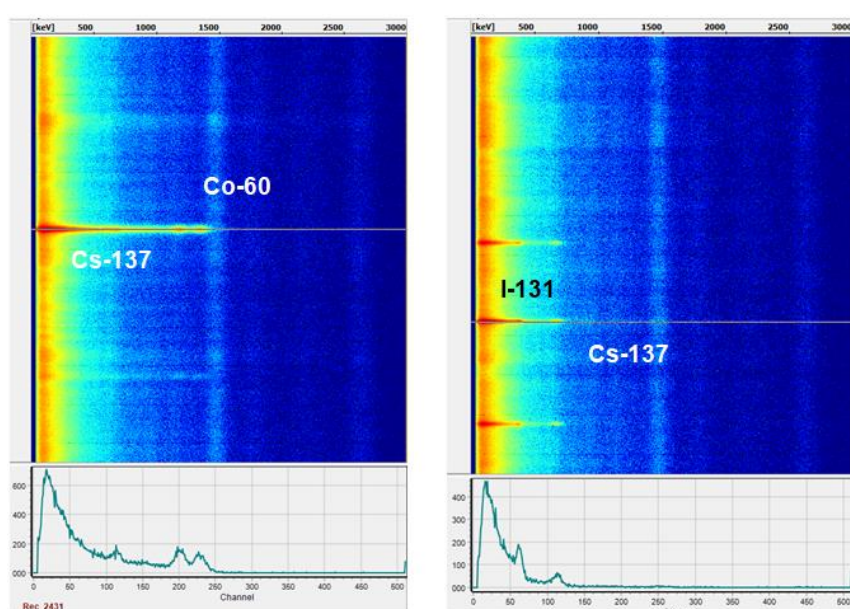


Fig. 77 Waterfall spectra showing detected nuclides  $^{60}\text{Co}$ ,  $^{137}\text{Cs}$  and  $^{131}\text{I}$

### 7.5.2 Swiss team

Both source locations were accurately determined and sources of  $^{137}\text{Cs}$  and  $^{60}\text{Co}$  were detected in position #1 and  $^{137}\text{Cs}$  and  $^{131}\text{I}$  in position #2. The following figure shows the flight lines and the flight along the boundary of the Libava VVP. The Swiss helicopter also crossed the border in a point about 2 to 3 m as indicated on the map. The GPS coordinates of positions #1 and #2 are given in Tab. 11 together with the estimated activities, the method of estimating the activities is specified in paragraph 3.2.5 of the PSI-report 18-04 [1].

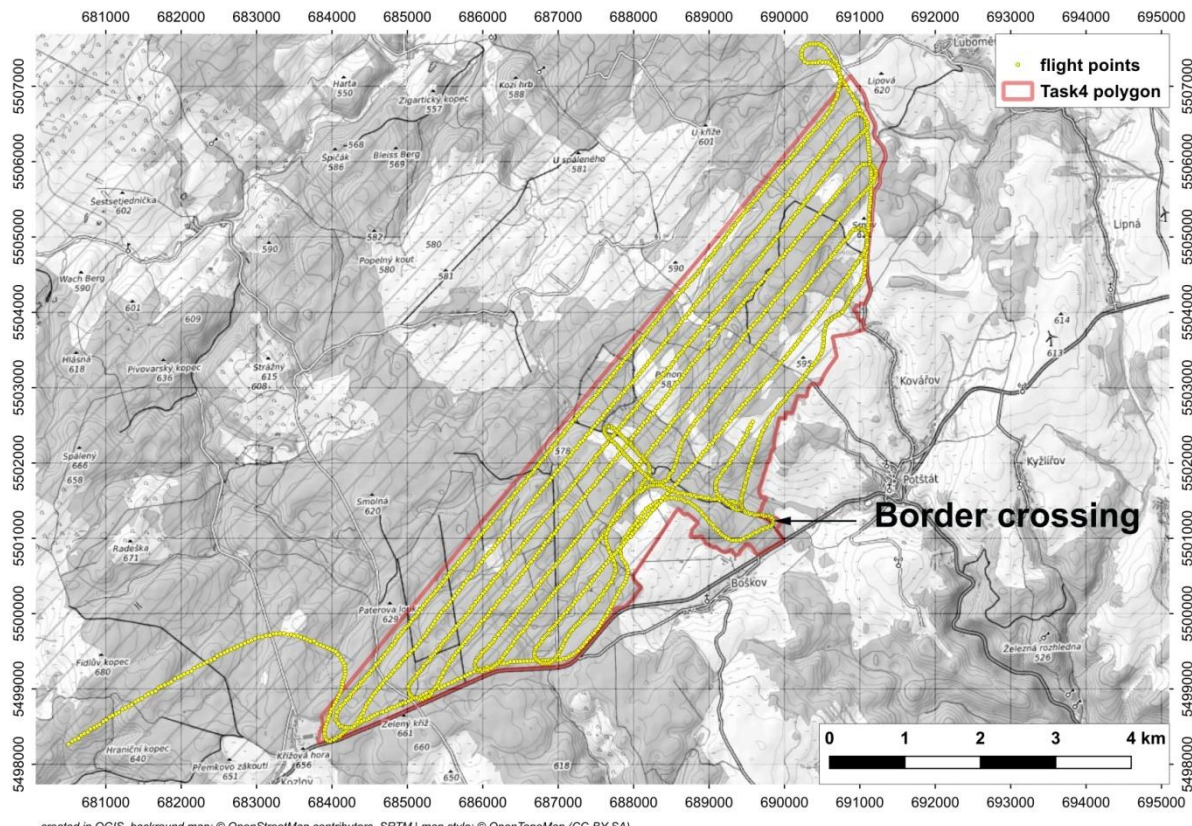


Fig. 78 Flight lines of the airborne survey of the Swiss team

Tab. 11 GPS coordinates of positions #1 and #2, estimated activities of detected point sources

Position #1			Position #2		
$^{60}\text{Co}$	49.639N	3.3 GBq	$^{137}\text{Cs}$	49.613N	2.1 GBq
$^{137}\text{Cs}$	17.607E	1.4 GBq	$^{131}\text{I}$	17.560E	0.7 GBq

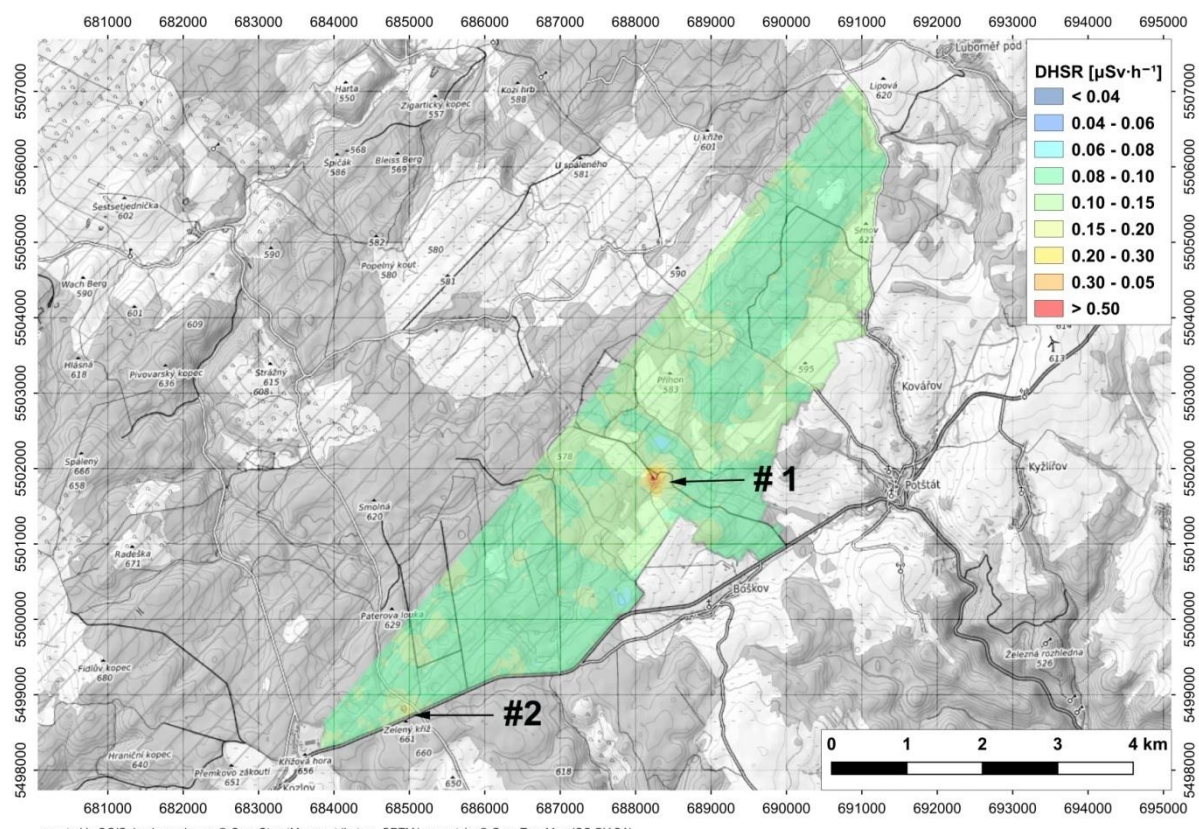


Fig. 79 DHSR measured by Swiss Team

### 7.5.3 French team

The French team also determined both source locations and detected  $^{137}\text{Cs}$  and  $^{60}\text{Co}$  sources at location #1 and  $^{137}\text{Cs}$  and  $^{131}\text{I}$  at location #2. The following figure shows the flight lines and the flight along the boundary of the Libava Military Training Area. The GPS coordinates for positions #1 and #2 are shown in Tab. 12 along with the estimated activities. The Mirion software detected the four radionuclides during the flight. Activities and accurate locations were then calculated using ASNR dedicated algorithms. The French helicopter also crossed the border.

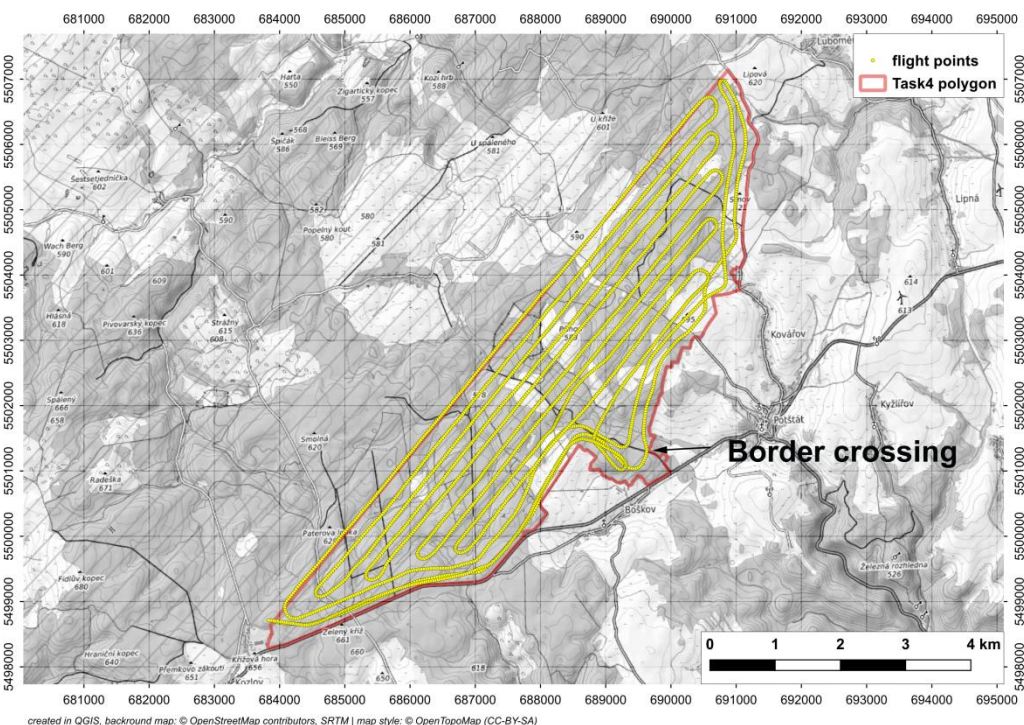


Fig. 80 Flight lines of the airborne survey of the French team

Tab. 12 GPS coordinates of positions #1 and #2, estimated activities of detected point sources

Position #1			Position #2		
$^{60}\text{Co}$	49.63981N	4.2 GBq	$^{137}\text{Cs}$	49.61371N	1.1 GBq
$^{137}\text{Cs}$	17.60786E	1.4 GBq	$^{131}\text{I}$	17.55995E	2.5 GBq

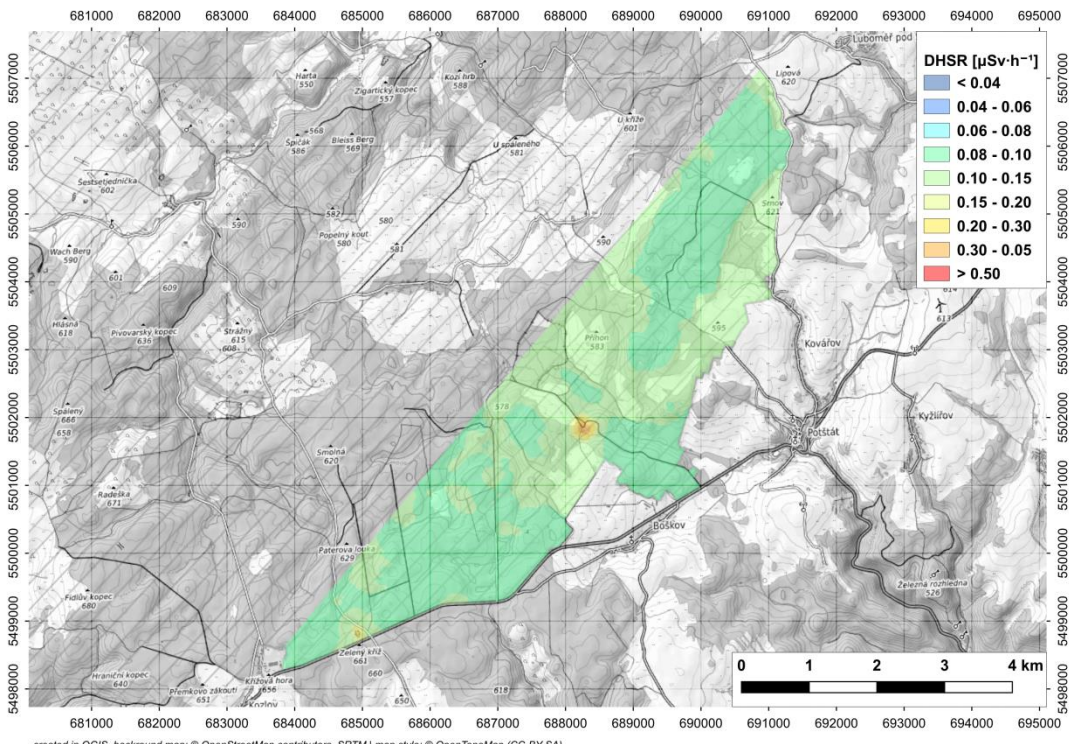


Fig. 81 DHSR measured by French team

## 7.5.4 Overview of activities of point sources

Tab. 13 Overview of estimated activities of point sources

					Reference activity
		[GBq]	[GBq]	[GBq]	[GBq]
Pos #1	Co-60	3.8	3.3	4.2	6.2
	Cs-137	2.0	1.4	1.4	2.3
Pos #2	Cs-137	1.5	2.1	1.1	1.9
	I-131	2.3	0.7	2.5	3.7

## 8 Conclusions from AGC24 international campaign

In the event of accidents at nuclear facilities, contamination with radioactive materials may cover relatively large areas. Aerial monitoring will be one of the primary methods of determining the real extent of contamination and verifying mathematical calculation models. As the movement of released radioactive material does not respect national boundaries, it may be necessary to cooperate with neighbouring countries in the field of aerial monitoring. However, such cooperation requires preparation, knowledge of the technological possibilities, logistics of cooperation, involvement of other organizations (e.g., information of municipal authorities, etc.) and mutual knowledge of the procedures for measurement and data evaluation. The AGC24 international campaign is an example of such cooperation between airborne teams. Aerial monitoring requires a certain strategy, and these exercises create scenarios that correspond to potential conditions of a real nuclear accident. The monitoring of different teams in such a situation provides training in logistics, ensuring the aircraft traffic safety during monitoring, cooperation of the different teams in providing surveys of large areas, transferring and processing data, and creating a basis for decision-makers. Exercises then provide a range of information to improve mutual cooperation. This conclusion summarises the knowledge from the AGC24 exercise. The Swiss team also analysed their results of AGC24 and presented some conclusions in [14].

### **Detailed results assessment:**

The exercise was divided into individual TASKS I - IV. All teams performed the measurements within the deadlines and the preliminary results were presented on the last day of the exercise at a joint meeting. Some remarks to individual TASKS:

**TASK I** – The values of DHSR were similar for all teams and were consistent with ground measurements. The  $^{40}\text{K}$  activity concentration values for CH and FR teams were rather lower than the ground-based values. The activity concentrations of  $^{238}\text{U}$  and  $^{232}\text{Th}$  were generally consistent with the ground-based measurements.

**TASK II** - Hot spot of  $^{238}\text{U}$  and DHSR were found in the vicinity of the uranium ore processing plant for all teams. Absolute values determined by the teams were very similar. The activity concentration values of  $^{40}\text{K}$  for FR and CZ teams ranged  $> 600 \text{ Bq kg}^{-1}$  while the values of CH team ranged between  $400 - 500 \text{ Bq kg}^{-1}$  in similar locations. Absolute  $^{238}\text{U}$  activity concentration values were roughly the same for all teams, the area of elevated values was delineated in the same way by all teams. Surprisingly, all teams found  $^{137}\text{Cs}$  contamination in

the vicinity of the Bobrůvka River which is now just above the minimum detectable activities. Also, an anomaly of  $^{40}\text{K}$  round the Barošovice Hill was found by all teams which has not been known so far.

**TASK III** - A composite map of DHSR is perfect without any modification. The same is valid for  $^{137}\text{Cs}$  composite map after modification of the data to the same model distribution. Regarding natural nuclides, the resulting data of natural nuclide activity concentrations in the composite maps partially differ between teams.

**TASK IV** - All teams found the source locations and specified their geographical coordinates and types without any problems. Regarding the estimation of absolute values of point source activities, all teams reported values lower than the conventionally true source values in the range of a factor from 2 to 10

These differences mentioned above ranging to a maximum of fifty percent were visible, but not of a magnitude where decisions based on the measuring results in a real emergency event would be influenced.

Some general comments:

During the data processing for this report, several discrepancies were identified that have not yet revealed in previous exercises and thus have not been addressed.

The first difference is presentation of the activities of natural nuclides. The Swiss and French teams presented their results as AD\_ (dry sample), while Czech teams as AW\_ (wet sample). A difference is about 17 %.

Another discrepancy concerned the  $^{137}\text{Cs}$  model distribution used to determine the surface activities of  $^{137}\text{Cs}$ . This difference is significant and it is also very visible in a composite map when is not corrected.

Both discrepancies can be eliminated by conversions. The results of natural nuclides in the report for TASK I, II and IV were presented as delivered by individual teams while the activities for the composite maps were unified and converted. In case of natural nuclides the values were converted to AW\_ (wet sample) to be comparable each other. In case of  $^{137}\text{Cs}$ , the model distribution was converted to the commonly used model distribution in the Czech Republic since the Chernobyl nuclear disaster.

The data transfer of output files using ERS 2.0 was realized well if all requirements were kept. However, only allowed standard characters must be inserted into ERS files,

otherwise problems with opening the files can occur. This happened, for example, when using "MDA < 5000".

The effect of the Compton continuum of high uranium series activities into the  $^{137}\text{Cs}$  window was manifested by the false  $^{137}\text{Cs}$  activity presence. This was related to TASK II and appeared on the maps as elevated  $^{137}\text{Cs}$  activity at the uranium ore processing plant site.

The following issues should be addressed at the next meetings in future:

- Unify how to express activity of natural nuclides, i.e., AD\_ vs. AW\_ activity
- Agree on a  $^{137}\text{Cs}$  model distribution for expression of results
- Address the issue of evaluating other man-made nuclide activities

#### **Acknowledgement:**

The Czech airborne team has been participating in such events since 2015. All participating teams, especially Swiss, German, French and now Czech teams know each other well. Their collaboration of the airborne teams was again a pleasant experience and the organisers thank all participants for their excellent work, and looking forward to the next occasion for working together.

## References

- [1] Butterweck G., et al.: International Intercomparison Exercise of Airborne Gamma-Spectrometric Systems of the Czech Republic, France, Germany and Switzerland in the Framework of the Swiss Exercise ARM17. Technical Report. October 2018.  
[https://www.researchgate.net/publication/330482739\\_International\\_Intercomparison\\_E\\_xercise\\_of\\_Airborne\\_Gamma-Spectrometric\\_Systems\\_of\\_the\\_Czech\\_Republic\\_France\\_Germany\\_and\\_Switzerland\\_in\\_the\\_Framework\\_of\\_the\\_Swiss\\_Exercise\\_ARM17](https://www.researchgate.net/publication/330482739_International_Intercomparison_E_xercise_of_Airborne_Gamma-Spectrometric_Systems_of_the_Czech_Republic_France_Germany_and_Switzerland_in_the_Framework_of_the_Swiss_Exercise_ARM17)
- [2] ERS (European Radiometric and Spectrometry format) data for software development and testing (GitHub)  
[https://github.com/juhele/opengeodata/tree/master/ERS\\_-\\_European\\_Radiometric\\_and\\_Spectrometry\\_format](https://github.com/juhele/opengeodata/tree/master/ERS_-_European_Radiometric_and_Spectrometry_format)
- [3] Recovery Management Strategy for Affected Areas after Radiation Emergency, Project of Ministry of Industry and Trade in Czech Republic, 2017-2020.
- [4] Butterweck, Gernot & Stabilini, Alberto & Bucher, Benno & Breitenmoser, David & Rybach, Ladislaus & Poretti, Cristina & Maillard, Stéphane & Hess, Adrian & Hauenstein, Fabian & Gendotti, Ulisse & Kasprzak, Małgorzata & Scharding, Gerald & Mayer, Sabine. (2024). Aeroradiometric Measurements in the Framework of the Swiss Exercise ARM23. 10.55402/psi:60054.
- [5] Kotík, L., Ohera, M., 2023. Full spectrum estimation of helicopter background and cosmic gamma-ray contribution for airborne measurements. Nucl. Eng. Technol. 55 (3), 1052–1060. <https://doi.org/10.1016/j.net.2022.11.024>
- [6] Basic principles of AGAMA software package. Internal Report SÚRO No. 6/2023 (in Czech)
- [7] ICRU, 1994. Report 53. Gamma-Ray Spectrometry in the Environment. International Commission on Radiation Units and Measurements, Washington, DC.

- [8] Ohera, M., Sas, D., Sladek, P., 2020. Calibration of spectrometric detectors for air kerma rates in environmental monitoring. *Nucl. Technol. Radiat. Protect.* 35 (4), 323–330. <https://doi.org/10.2298/NTRP2004323O>.
- [9] Currie L.A.: Limits for Quantitative Detection and Qualitative Determination, *Analytical Chemistry*, 40, pp. 586 – 593
- [10] ISO, 2010. ISO 11929. Determination of the characteristic limits (decision threshold, detection limit and limits of the confidence interval) for measurements of ionizing radiation. Fundamentals and Application. International Organization for Standardization, Geneva
- [11] In-situ gamma-spectrometry on reference area. Ministry of Defence, Czech Republic. Order. No. 18325/2018-SE. 2018
- [12] Rulík P., Helebrant J.: Mapa kontaminace půdy České republiky  $^{137}\text{Cs}$  po havárii JE Černobyl. Zpráva SÚRO č. 22/2011 (in Czech)
- [13] Beck, H. L., De Campo, J., Gogolak, C., 1972. In situ Ge(Li) and NaI(Tl) gamma-ray spectrometry. Report No. HASL-258. Health and Safety Laboratory. <https://doi.org/10.2172/4599415>. US Atomic Commission, New York. Briechle, S., Molitor, N., Krzystek, P., Vosselman, G., 2020.
- [14] Stabilini, A. et. al.: Aeroradiometric Measurements in the Framework of the Swiss ARM24 and international AGC24 exercises. Technical Report, Paul Scherrer Institute, 2025. <https://doi.org/10.55402/psi:68900>